DEVELOPMENT OF AN IN VITRO SYSTEM TO ASSESS THE ORAL BIOAVAILABILITY OF HYDROPHOBIC CONTAMINANTS

by

Luba Vasiluk

M.Sc. Ben Gurion University of the Negev, Israel, 2001
B.Sc. Ben Gurion University of the Negev, Israel, 1998

THESIS SUBMITTED IN PARTIAL FULFILLMENT OF
THE REQUIREMENTS FOR THE DEGREE OF

DOCTOR OF PHILOSOPHY

In the
Department
of
Biological Sciences

SIMON FRASER UNIVERSITY

Spring 2006

APPROVAL

Name: Luba Vasiluk

Degree: Doctor of Philosophy

Title of Thesis:

Development of an in vitro system to assess the oral bioavailability of hydrophobic contaminants

Examining Committee:

Chair: Dr. D. Green, Assistant Professor

Dr. M. Moore, Professor, Senior Supervisor
Department of Biological Sciences, S.F.U.

Dr. R. Cornell, Professor
Department of Molecular Biology and Biochemistry, S.F.U.

Dr. F. Gobas, Professor
School of Resource and Environmental Management, S.F.U.

Dr. C. Eickhoff, Director of Toxicology
Vizon SciTec Inc.

Dr. C. Kennedy, Associate Professor
Department of Biological Sciences, S.F.U.
Public Examiner

Dr. R. Lanno, Associate Professor
Department of Entomology, Ohio State University
External Examiner

Jan. 20/06
Date Approved

ABSTRACT

Thousands of chemicals are currently awaiting categorization for their bioaccumulation potential. Animal testing is impractical for this purpose, therefore accurate and inexpensive in vitro screening models are urgently needed. The aim of this research was to develop an in vitro screening tool for estimating the oral bioavailability of hydrophobic organic contaminants (HOCs) from a solid matrix (soil, sediment, food). The bioavailability of two HOCs with high log K_{ow} values (chrysene (CHR) and benzo[a]pyrene (BaP)) was studied. For comparison, the bioavailability of a hydrophilic herbicide (glyphosate) was also examined. The model included a simulated gastrointestinal digestion and exposure to intestinal epithelium or its surrogate, ethylene vinyl acetate (EVA).

We analyzed the transport kinetics of [^{14}C]-glyphosate in two cell lines: the human intestinal epithelial cell line, Caco-2, and the rat small intestinal crypt-derived cell line, IEC-18. At glyphosate concentrations below 10mg/ml, >90% remained in the apical ('lumenal') compartment. Exposure to glyphosate concentrations >10 mg/ml increased paracellular permeability and disrupted the barrier properties of cells. Binding of glyphosate to cells was saturable, but negligible.

The bioavailability of [^{14}C]-CHR and [^{14}C]-BaP bound to digestible (skim milk powder) or indigestible matrices (sediment or soil) was monitored using Caco-2 cells or a surrogate epithelium, EVA. The kinetics of partitioning from the aqueous phase was similar for both CHR and BaP, and for both EVA and Caco-2 cells, and best fit a one-compartment model. pH shift (from gastric to intestinal fluids) had the greatest effect on the amount of HOC detected in the aqueous compartment. The lipid-normalized fugacity capacity of Caco-2 cells was higher than EVA for both HOCs. Nevertheless, Caco-2 cells and EVA demonstrated similar desorption kinetics. The amount of HOC in the aqueous phase (bioaccessible fraction) did not always parallel the amount in the sorptive epithelium (bioavailable fraction); sorbed concentrations were up to 2000-fold higher

than the aqueous fraction for both matrix types. These results provide further evidence that the transport of hydrophobic chemicals between tissues or "compartments" of the body is fugacity-driven. The EVA and Caco-2 models provide complementary information that could be used to predict the relative oral bioavailabilities of HOCs.

Keywords: Benzo[a]pyrene; Chrysene; Ethylene vinyl acetate (EVA); Caco-2 cells; Mobilization; Bioaccessibility; Bioavailability.

DEDICATION

To the memory of my father, Vadim Trampolsky, the most loving and unselfish man, I have ever known.

Those, who were blessed to know him, knew he was one of a kind.

I love you Dad, and miss you very much. I wish you could be here so we could celebrate and enjoy together the achievement that this thesis represents.

The following is for you.

ACKNOWLEDGEMENTS

First and foremost I would like to sincerely acknowledge the valuable guidance, support and mentoring provided to me over the last few years by my senior supervisor, Margo Moore. I am very grateful to have had such a brilliant and supportive teacher. I have been privileged to have an opportunity to work in your lab, Margo. You are one of the finest mentors I have ever known.

I would like to thank the members of my supervisory committee, Rosemary Cornell, Frank Gobas and Curtis Eickhoff for their assistance with my project, insightful comments and helpful discussions, and their encouragement of my development as an environmental toxicologist. In particular, I thank Frank Gobas for introducing me to the world of chemical partitioning and fugacity and all the "chitchats" along the way. I also thank my public examiner Chris Kennedy, my chair David Green and my external examiner Roman Lanno for participating in my thesis defence.

To the members of The Moore Lab, past and present, I owe my sincerest gratitude. I would like to say to Linda Pinto, Julie Wasylnka, Anna Hissen, Alison Hadwin, Luis del Rio, Jas Minhas, Mark Warwas, Jason Catterson, as well as all of the numerous other wonderful people that have passed through The Moore Lab in the last four and a half years, "It was great to have a tea-pot-membership with all of you." I also wish to thank a few undergrad students who helped me along the way: Sandy Tsang, Zahra Walji and Sheila Smith. My special thanks to Linda Pinto for her endless scientific and emotional support and advice, for enriching my English from day one and most importantly, for always putting things in perspective. There are no words to express my gratitude for you, Linda.

I would like to acknowledge the members of the Tox Lab for helping me wrap my head around difficulties with fugacity theory: Victoria Otton, Cheryl Mackintosh, Lizanne Meloche, Adrian deBruyn. To the many other people in SFU that helped me all along: Sharon Hope, Kate Scheel, Teresa Kitos, to name just a few – thank you.

I would like to thank UBC BioImaging Facilities: Dr. Elaine Humphrey, Derrick Horne and Garnet Martens for helping me to obtain such an amazing images of Caco-2 cell.

For funding my project, I would like to thank Vizon SciTec Inc. (formerly BC Research); particularly Curtis Eickhoff and Ann Eastman, for a successful collaboration process that has prompted my interest in environmental consulting and helped me appreciate the challenges of the "real-world" application of science. Financial support from National Sciences and Engineering Research Council of Canada is greatly appreciated.

I would like to thank my family and friends for their love and support over the course of my degree. To my parents Vadim and Galina Trampolsky, thank you for supporting me emotionally and financially, and making it possible for me to have a child and pursue my dream at the same time. To my sister Natasha, her husband Dmitri and their two sons Daniel and Nikita, thanks for always being there for David and me, and for babysitting David on many occasions when I needed it.

Lastly, I thank my son David for being with me from the beginning of this journey, for his love, support and encouragement to finish it, so our dreams can come true sooner.

TABLE OF CONTENTS

LIST OF FIGURES

LIST OF TABLES

GLOSSARY

BSA	Bovine Serum Albumin
CEPA	Canadian Environmental Protection Agency
DPM	Disintegrations Per Minute
EPA	Environmental Protection Agency
EVA	Ethylene Vinyl Acetate
GI	Gastrointestinal
GIF	Gastrointestinal Fluid
GIT	Gastrointestinal Tract
HBSS	Hank's Balanced Salt Solution
HOC	Hydrophobic Organic Contaminants
PAH	Polycyclic Organic Hydrocarbons
PBET	Physiologically-Based Extraction Test
PBS	Phosphate-Buffered Saline
PCB	Polychlorinated Biphenyl
SOM	Soil Organic Matter
WHO	World Health Organization

CHAPTER 1: GENERAL INTRODUCTION

1.1 Introduction to the problem

Environmental contaminants are substances present in the environment as a result of intentional or unintentional human action. They may be natural or anthropogenic in origin, and organic or inorganic [1]. The definition covers over 100,000 industrial substances that are currently used worldwide, and many preparations and mixtures, amounting altogether to several hundred million tonnes being emitted into the environment each year [1, 2]. Several hundred substances are added annually.

Because of the large number of chemicals released into the environment annually, it is not feasible to complete an assessment of human exposure and possible associated health effects for all "new" and "existing" chemicals. In most cases, reliable data on the hazards of these chemicals to human health are lacking and does not even begin to address the hazards of exposure to mixtures of chemicals.

1.1.1 Canadian environmental protection act regulations

In 2001, the Canadian Environmental Protection Act (CEPA), 1999 [3] required the Ministry of the Environment and the Ministry of Health to conduct screening assessments of substances that meet the categorization criteria set out in the Act and Regulations. The purpose was to determine whether substances present a risk to the environment and/or to human health. A screening assessment involves the analysis of a substance using conservative assumptions to determine whether the substance is "toxic" or capable of becoming "toxic" as defined in CEPA 1999 [3]. Based on the results of a screening assessment, the Ministry can propose: (1) taking no further action with respect to the substance, (2) adding the substance to the Priority Substances List (PSL) for further assessment, or (3) recommending that the substance be added to the List of Toxic Substances and, where applicable, the implementation of virtual elimination.

Canada has adopted a Toxic Substances Management Policy under the CEPA, that considers virtual elimination of chemicals that meet criteria for Persistent, Bioaccumulative, Toxic substance (PBT) (see 3 above). This classification would place thousands of commercial substances within PBT. In theory, this requires that they undergo a screening level risk assessment in Canada that is to be completed and publicly posted by September 2006. Currently, bioaccumulation criteria are based on the K_{ow} model developed for aquatic organisms. This model is also considered to be appropriate for assessing bioaccumulation in numerous other organisms, including birds, reptiles, mammals, and humans. Although the deadline for the screening assessment was set for 2006, there are still ~23,000 chemicals awaiting categorization. Due to existence of thousands of untested toxic chemicals as well as new compounds being isolated or developed at ever-increasing rates, simple, accurate, reproducible and inexpensive models are needed urgently to screen compounds for their potential risk to the environment or human health. Procter and Gamble (P&G) estimated, based on Canada's recent experience (2002 Canadian Pilot Exercise for Categorization and Screening of Domestic Substances List), that to collect and submit data would require an average of 50 hours per chemical. Furthermore, they calculated that using current methods, screening level assessments for 1000 PBT category chemicals would require 961 man-years to complete, and costs for bioaccumulation tests on fish could exceed $80 million. This estimate does not include time spent by regulatory agencies in reviewing data and developing risk assessments (Weisbrod, AV, personal communications).

1.2 Current methods for estimating bioavailability

1.2.1 Current screening assessment of bioavailability

There are several routes of exposure to xenobiotics including inhalation, dermal and ingestion. Ingestion of contaminated soil or food can be a major route of chemical exposure [4]. At present, the amount of contaminant that is extractable by chemical solvents is considered the exposure dose [5-7]. However, the fraction of contaminants that are accessible for intestinal absorption, can be affected by sorption to its solid matrix (e.g., soil, food, sediments, etc.). In recent years, hydrophobic partitioning (octanol-water

partition coefficient, K_{ow}) has been used as a predictor of bioavailability in studies of the environmental fate of hydrophobic organic chemicals (discussed in detail below). Because of their high K_{ow} values, hydrophobic chemicals partition to tissue more than polar compounds [8]. However, these high K_{ow} compounds (also known as hydrophobic organic compounds, or HOCs) also bind more strongly to matrices [9], which can reduce their oral bioavailability. At the present, these factors are not taken into account in risk assessment procedures. For example, the absorption of nutrients takes place mainly (>90%) in the small intestine [10], and hydrophobic compounds with high K_{ow} values will be ingested primarily bound to soil or food particles. Because absorption of soil particles in the gastrointestinal tract is thought to be negligible, the fraction of HOCs that is sorbed to soil particles is considered unavailable for absorption [6, 11, 12]. However, intestinal secretions such as bile salts or hydrolytic enzymes could mobilize a proportion of the sorbed fraction during digestion. The fraction that is mobilized into intestinal fluid would now be available for sorption into the intestinal tissue.

1.2.2 Octanol-water partitioning coefficient

Due to the lack of empirical data for many organic contaminants, K_{ow} is used as a surrogate for bioaccumulation potential [13]. This useful measurement is generally easy to obtain and is usually expressed as log K_{ow} or log P. Many of the principles in pharmacology, environmental toxicology and chemistry are expressed in terms of log K_{ow}. Estimates of soil sorption [14], animal bioconcentrations [15-17], water solubility [17, 18], and membrane permeability [19, 20] of organic molecules have all been based on the log K_{ow}.

However, log K_{ow} does not appear to be a sensitive measurement for predicting the intestinal absorption efficiency of dietary toxicants in mammals. Biological lipid contains a number of distinct hydrophobic domains, i.e. triacylglycerol droplets, membranes, and hydrophobic pockets in proteins, each of which interact with organic molecules with varying degrees of specificity and with varying solvent capacities [21]. Octanol provides only a simplified surrogate of biological lipid. According to Chiou et al [22], octanol can dissolve substantial water (2-3 M) and is also somewhat soluble in

water (4.5×10^{-3} M). In addition, for some high melting point chemicals, it is possible to have molecules with high log K_{ow} that are actually less fat soluble and less absorbable at environmental temperatures than some chemicals with low log K_{ow} [13, 23, 24]. Thus, the use of octanol to represent biological lipids and log K_{ow} as a measurement of lipophilicity may be less than ideal.

1.2.3 Chemical approaches for estimating bioavailability

A number of chemical and physical procedures have also been proposed to assess the bioavailability of organic compounds, mainly in soil. One of the chemical methods involves the analysis of dissolved pore-water concentrations of sequestered HOCs from sediment [25]. The authors found that the pore-water concentrations of HOCs (log K_{ow} between 4.5 and 7.5) are established by equilibrium partitioning between the rapidly desorbing HOC fraction in the sediment and the pore-water. Kraaij et al [25] suggested that that HOC residues in sediment-dwelling organisms can be estimated on the basis of concentrations in pore-water and bioconcentration factors.

Solid phase extraction with C-18 membranes has been used to assess the bioavailability of several different polycyclic aromatic hydrocarbons (PAHs), and this method showed a very good correlation to in vivo results with earth worms [26].

Similarly, desorption of organic compounds from contaminated sediment or soil has been studied using the solid-phase sorbent, Tenax beads (poly (2,6-diphenyl-p-phenylene oxide) – a lightweight, hydrophobic, porous polymer with an extremely high affinity and sorption capacity for HOCs, since they provide a theoretically infinite sink for sorbates [27]. The authors compared the rapidly-extracted fraction of 10 PAHs, 4 polychlorinated biphenyls (PCBs) and 9 chlorobenzenes from six sediments in 6 h to a slowly desorbing fraction in 30 h of extraction and concluded that extraction by Tenax provides an easy way of measuring the rapidly desorbing fraction of HOCs that pose actual risks for transport to (ground) water, and determines the amount available for uptake by organisms. Sodergren and Sabaliunas [28] used membrane-based passive samplers to study the uptake of organochlorine pesticides (lindane, aldrin, dieldrin, and chlorpyriphos) in a continuous-flow system. The membranes were filled with

cyclohexane and a mixture of cyclohexane and triolein to mimic membranes. Uptake of the chemicals was 24-84 times faster in polyethylene membranes compared to cellulose membranes. The diffusion rate of chemicals through polyethylene membranes was dependent not only on their lipophilicity but also on their molecular mass [28]. Other artificial lipophilic materials (lipid containing semi-permeable membrane devices or solvent filled dialysis membranes) have also been studied as a means for estimating bioaccumulation and bioavailability of HOC in natural waters [29].

Mayer et al [14] used solid-phase microextraction with poly(dimethylsiloxane) (PDMS)-coated glass fibers for the extraction and analysis of hydrophobic organic analytes. The researchers applied this method to the PDMS water partition coefficients of 17 hydrophobic analytes including chlorinated benzenes, PCBs, PAHs, and p,p'-DDE and found that the partition coefficients were proportional to their K_{ow} values.

1.2.4 Physiologically based extraction tests (PBETs)

There are several routes by which hydrophobic contaminants enter biological organisms, but for humans, ingestion is recognized as the main route of exposure [4]. In most cases, the bioavailability of a contaminant is assumed to be 100% of that which is extractable by chemical solvents [5, 6]. For oral bioavailability research, the most widely used matrices are food and water. Unfortunately, estimations of bioavailability from one matrix may not be sufficient to generalize for other matrices. Soil-borne HOCs have been tested mainly in vivo, and the data suggests that their bioavailability may be reduced due to a limited mobilization of the chemical from the solid matrix, when compared to food matrices [30]. As a result of these matrix-related differences, there is a possibility of overestimating the health risk posed by xenobiotics in soil. In the past, much work concentrated on soil extraction techniques in order to determine the "total" concentration of contaminants in the soil environment. Currently, there is a new emphasis on the development of methods that will assess the actual human exposure to HOCs.

At present, there is no universally accepted definition of bioavailability. From a classical pharmacological perspective, the bioavailability of a toxicant can be defined as the fraction of the administered dose reaching the blood or systemic circulation [31]. In

pharmacokinetic studies, oral bioavailability is calculated from the ratio of areas under the blood concentration-time curves (AUCs) of orally and intravenously administered doses of a drug.

In environmental toxicology and for the purpose of this research, the term '**bioavailable fraction**' refers to the fraction of a chemical that is sorbed by cells or transformed by living organisms. Only the freely-soluble fraction of a pollutant is available for absorption in the digestive tract, while the remaining fraction, which is still fixed to indigestible particles, leaves the body without effect. The fraction that is mobilized from a matrix into digestive juices and now is available for absorption during the transport through the intestine has been defined by Ruby [12] as the '**bioaccessible fraction**'.

To account for the effect of matrix in risk assessment, researchers have developed in vitro models that simulate human physiological gastrointestinal digestion. To determine the factors that affect the mobilization of polycyclic aromatic HOCs (PAHs and PCBs), Hack and Selenka used in vitro models [32, 33] that simulate the conditions within the gastrointestinal tract, i.e. gastric followed by intestinal digestion [32]. They found that intestinal juice mobilized contaminants more effectively than gastric juice which they attributed to the emulsifying and solubilizing action of bile micelles. Another model established by Holman [33] explored the reduced bioavailability of petroleum hydrocarbon residues in weathered soils collected from diesel- and crude oil-contaminated sites. The authors studied the fate of HOC in the fasting and fat-digesting conditions using a synthetic upper small intestinal digestive fluid that included bile salts and intestinal lipids, but did not include a transition from stomach to intestine. The gastrointestinal solubility of hydrocarbons increased from the fasting phase to the fat-digesting phase. This model identified five-steps in the solubilization of HOC: (1) diffusion of bile salts to the soil surface, (2) absorption onto the surface (3) reaction with hydrocarbons to form micelles and (4) desorption of hydrocarbons from the soil, followed by (5) diffusion into the fluid of the lumen. Holman et al [33] assumed that a three-step absorption mechanism subsequently followed solubilization: (1) the micelles penetrate the unstirred layer; (2) hydrocarbons sorb to the microvilli of enterocytes, diffuse across the cells and (3) enter the systemic circulation.

Given the criticisms that can be leveled at current in vitro systems, it is tempting to look at animal testing as the only method which produces reliable data. However, apart from the obvious 'drawbacks' of animal studies (expense, time and personnel requirements, and ethical concerns in the wider community as well as the scientific community), in vitro systems can provide useful data which cannot be gathered by in vivo testing. For example, it is extremely difficult to follow the kinetics of chemical transport within an organ system, such as the gastrointestinal tract in an intact animal. The various factors which may influence bioaccessibility and bioavailability can be manipulated and measured using in vitro models. In vitro models have been in use for over 50 years to estimate the bioavailability of polar compounds such as pharmaceuticals and metals. At this time, there is a PBET for lead that correlates well with results obtained in animal models. This PBET model has been used routinely to develop relative bioavailability estimates for human health risk assessment for metals [34]. The PBETs that are in development for HOC reflect the greater complexity of HOC uptake and will require conducting in vivo studies to establish the oral bioavailability of those chemicals, especially from soil. Only then will there be success in developing in vitro models that capture the critical mechanisms by which hydrophobics become bioavailable by the oral route. At present, there are no published studies with use of PBETs for hydrophobic compounds bound to solid matrices evaluated in vivo. The processes that control the transport of hydrophobic compounds from solid matrices, such as soil, sediment or food into biological tissues, are chemically quite distinct from those that allow the transport of polar compounds, and must therefore lead to the design of different models. Hence, there is a need for an in vitro digestion model based on PBET, which is simple and inexpensive and will provide a reproducible tool to estimate the relative bioavailability of hydrophobic organic contaminants.

1.3 Hydrophobic organic contaminants (HOCs)

The term "hydrophobic organic contaminant" (HOC) is a generic term covering a wide range of organic xenobiotics that have found their way into the environment, and that are characteristically poorly soluble in water, are relatively resistant to biological, chemical and photolytic breakdown [35]. They include the simple aromatic compounds,

polycyclic aromatic hydrocarbons (PAHs), including naphthalene, phenanthrene and benzo[a]pyrene, and polychlorinated biphenyls (PCBs). There is concern about the occurrence and concentrations of HOCs in the environment because some of these compounds have been shown to be potentially toxic, and/or have endocrine-disrupting activity.

1.3.1 Polycyclic aromatic hydrocarbons (PAHs)

PAHs are HOCs containing two or more fused benzene rings and consist of a group of over 100 different chemicals. PAH are formed during the incomplete combustion of coal, oil and gas, garbage, wood, or other organic substances such as tobacco or grilled foods, and are usually found as a mixture containing two or more of these compounds. It has been acknowledged for over half century that emissions from incomplete combustion contain compounds such as PAHs. The US Environmental Protection Agency has determined that several PAHs, including benzo[a]pyrene (BaP), are probable carcinogens. BaP has been the most studied PAHs and has shown carcinogenicity after oral administration, intraperitoneal injection, subcutaneous injection, and inhalation or after direct application into the lungs or skin of experimental animals [36]. Generally, the aqueous solubility and volatility decreases and hydrophobicity increases with the increase in the number of rings. Due to their high hydrophobicity, PAH tend to partition into hydrophobic adsorbents, especially organic matter [8].

1.3.2 Structure, and physico-chemical properties of PAHs

The rings in most PAHs are six-membered and contain only carbon and hydrogen atoms. The structure of PAHs, especially the number of rings and arrangement of rings determines a PAH's biological activity. The structure of a representative PAH molecule, benzo[a]pyrene, showing the regions denoted K and Bay, is shown in Fig. 1-1.

The metabolic activation at the K region mainly results in non-toxic and non-carcinogenic metabolites and hence rather plays a role in detoxification [37]. The bay-

region activation has been favoured to explain the carcinogenic potency of PAH, e.g. bay-region-derived metabolites tend to be most reactive [37].

PAHs have high heats of combustion and low water solubility [36]. The greater the number of aromatic rings in a molecule of PAH, the higher the molecular weight, and thus the greater the resonance energy and stability of the PAH molecule. The higher stability renders these molecules resistant to both abiotic and biotic degradation; therefore, PAHs with more than three benzene rings can persist for years in contaminated soil and other areas in the environment [36].

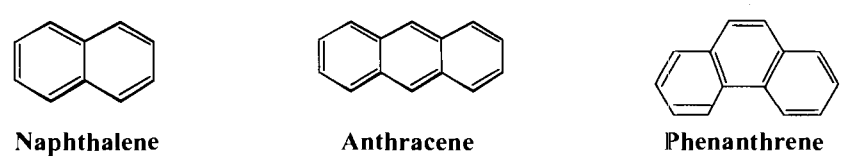

Naphthalene **Anthracene** **Phenanthrene**

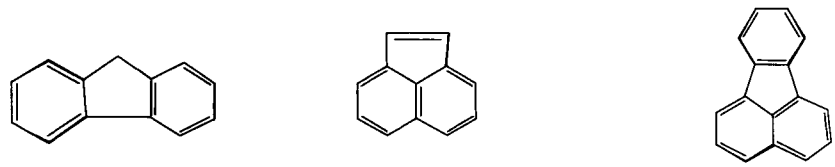

Fluorene **Acenaphthylene** **Fluoranthene**

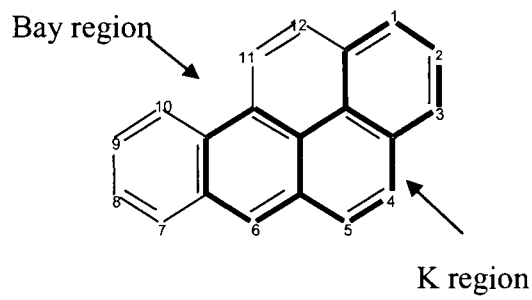

Benzo[a]pyrene

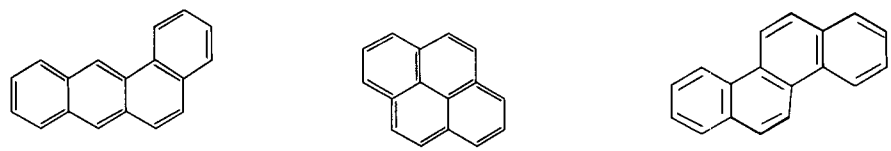

Benz[a]anthracene **Pyrene** **Chrysene**

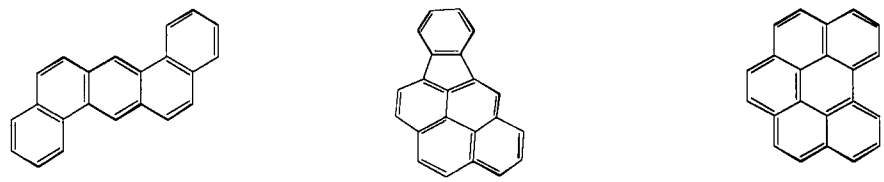

Dibenz[a,h]anthracene **Indeno[1,2,3-c,d]pyrene** **Benzo[g,h,i]perylene**

Figure 1-1. Representative polycyclic aromatic hydrocarbons

Regions related to biological activity in benzo[a]pyrene: the 'K' region is identified as the external corner of a phenanthrene moiety (bold), the 'Bay' region is identified as an open inner corner of this moiety [36].

1.3.3 Toxicity of PAHs

PAHs have been reported to cause a wide range of toxicities encompassing different organ systems. The toxicity of PAHs is related to both their structure and molecular weight. Acute toxic effects are mainly associated with the low molecular weight PAHs, such as naphthalene. Low molecular weight PAH typically have a log K_{ow} values of 2-3. These molecules are mobile, highly bioavailable, and can cause narcosis, a non-specific toxic condition resulting from accumulated concentrations in the cell membranes, which affects membrane permeability and enzymatic activities in the cell, thereby altering cell growth and development [36]. PAHs can also cause teratogenicity, osmoregulatory and respiratory impairment, and altered behaviour [38]. The persistence of low molecular weight PAHs in the environment is generally from days to weeks, since they are relatively volatile and readily degraded by numerous microorganisms [39].

High molecular weight PAHs are relatively more persistent in the environment than low molecular weight PAHs, due to their reduced water solubility (typically less than 0.0001mg/l) and very high lipophilicity (log K_{ow} greater than 4) [8]. PAHs lack polar and ionizable functional groups and therefore readily dissolve in, and cross lipoprotein biological membranes. The adverse health effects of short-term (acute) exposure to high molecular weight PAHs are minimal. Instead, via their oxidized metabolites, they exert chronic effects in cellular physiology by disrupting genetic expression in cells, macromolecular adduct formation, altered biochemical functions, and oxidative stress [40]. Some PAHs are suspected to have estrogenic effects, and are believed to play a role in the etiology of human breast cancer [41]. In general, genotoxicity, mutagenicity, carcinogenicity, teratogenicity, immunological effects as well as damage to specific tissues such as the haematopoietic system, are caused by PAH metabolites and not by the parental PAH *per se*. A description of the metabolic pathways that transform PAH and other HOCs follows.

1.3.4 Metabolism

1.3.4.1 Overview of xenobiotic-metabolizing enzymes

Within biological organisms, the fate and the effect of many xenobiotics are controlled by the ability of various oxidative and conjugative enzyme systems to metabolize these compounds into more water-soluble and less toxic metabolites. Oxidative metabolism of foreign compounds is catalyzed primarily by the cytochrome P450-mediated monooxygenase system (CYPs), located in the endoplasmic reticulum (microsomes) of many tissues [42]. The major system consists of NADPH-cytochrome P450 reductase and the terminal oxygenase cytochrome P450. The substrate specificities of monooxygenase-catalyzed reactions are controlled by distinct isozymes of the latter protein [42]. Although the monooxygenase system is generally considered to be a detoxification system, in some cases the metabolites produced are more toxic/carcinogenic than the parent compounds [43].

Cytochrome P450s are heme-containing isozymes that demonstrate a characteristic absorption peak at 450 nm upon reduction with carbon monoxide [44]. P450s can catalyze a wide range of reactions, mainly by the insertion of oxygen into substrate:

$$\mathbf{R\text{-}H + NAD(P)H + H^{+} + O_2 \rightarrow R\text{-}OH + NAD(P)^{+} + H_2O}$$

Various conjugating enzymes present in the cell almost exclusively enhance detoxification and elimination of metabolites produced by the monooxygenase system. Hydroxylated metabolites may be conjugated with glucuronic acid or sulphate via the activities of UDP-glucuronosyltransferases (UDP-GT) and sulfotransferases, respectively. Epoxides can be enzymatically conjugated to the tripeptide glutathione by glutathione transferases (GSH-T) or hydrolyzed to diols by epoxide hydrolase (EH) [42, 43].

In general, non-metabolizable hydrophobic chemicals tend to accumulate in tissue with high lipid content and have relatively long biological half-lives. Other chemicals, such as PAH, are readily metabolized and excreted by the organism.

1.3.4.2 Benzo[a]pyrene as a model of PAH biotransformation

Most of PAHs undergo metabolic transformation in the organism, resulting in polar products that are destined for excretion. Some PAH may form reactive metabolites that can form covalent adducts with DNA. In fact, the formation of PAH:DNA adducts is considered the beginning of the three-stage model of chemical carcinogenesis. Therefore understanding the development of reactive PAH metabolites is very important in order to understand the carcinogenicity of these compounds [4]. As an example of metabolic transformation of PAHs, the metabolic fate of benzo[a]pyrene, including both activation and detoxification routes are shown in Fig.1-2.

Using a mutagenicity assay such as the Ames test and various carcinogenicity models, it has been determined that the metabolic activation in the bay region of BaP results in the formation of the ultimate carcinogen benzo[a]pyrene±7,8-diol-9,10-epoxide [36]. There are four stereo isomers of this compound and while each is considered toxic, the (+)-7b,8a-dihydroxy-9a,10a-epoxy-7,8,9,10-tetrahydrobenzo[a]pyrene ((+)-diol epoxide-2) is considered the most carcinogenic (Fig.1-2, with asterisk) [45].

Conjugation of hydroxylated PAH metabolites with glucuronides, sulphate or glutathione is generally considered a detoxification process as it facilitates their elimination from the organism [46]. However, in higher eukaryotes, conjugation of some xenobiotics with glutathione can actually enhance their toxicity by mobilization to specific receptors. Thus, Koob and DeKant demonstrated that glutathione conjugates of menadione caused nephrotoxicity in rat kidneys [47].

In mammals, high molecular weight PAHs can exert toxicity through diverse mechanisms, all dependent on metabolic activation to reactive metabolites. It is important to note that the metabolism of PAHs that are not considered genotoxic (such as pyrene) can still lead to the production of very mutagenic metabolites, as well as to enhanced mutagenicity of other compounds such as BaP [48].

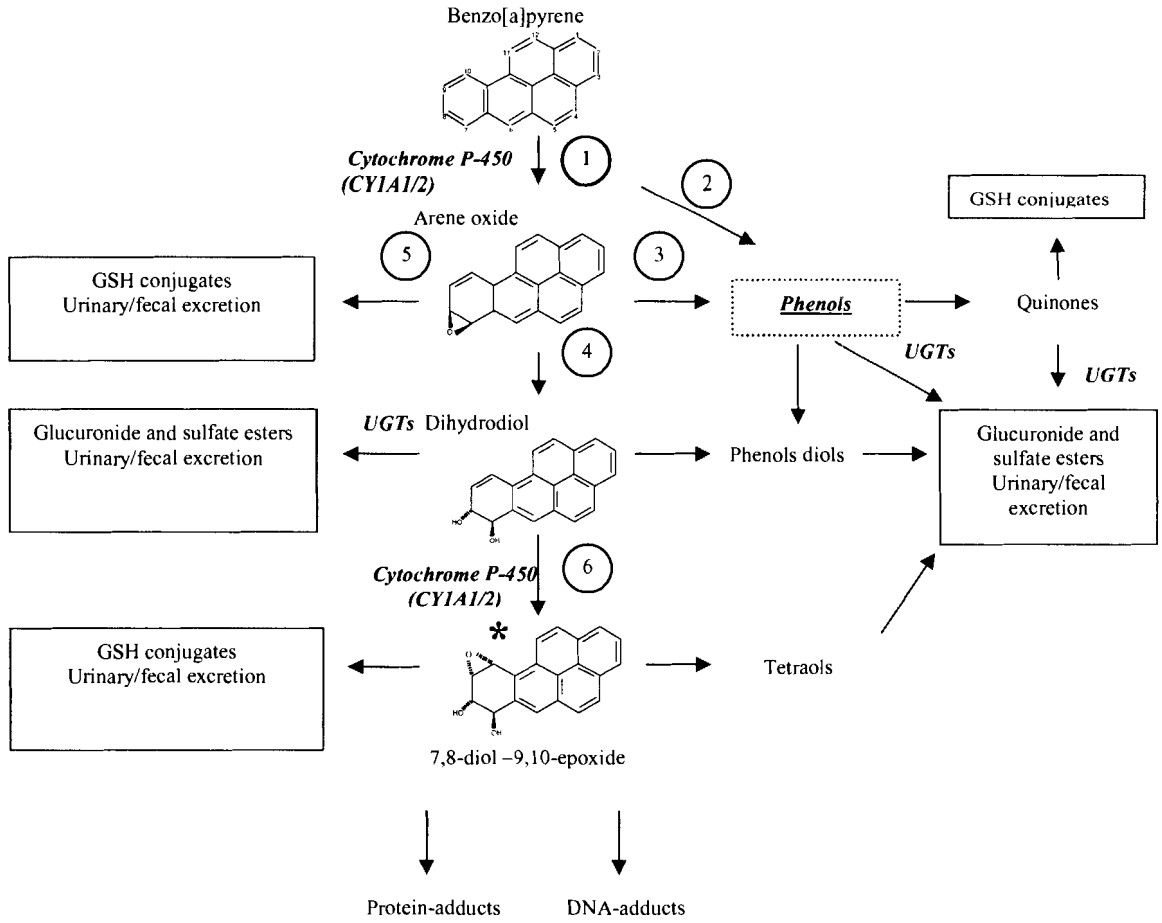

Figure 1-2. Metabolic fate of benzo[a]pyrene.

Benzo[a]pyrene is metabolized initially by the microsomal cytochrome P-450 monooxygenase system to several arene oxides (reaction 1). Once formed, these may rearrange spontaneously to phenols (reaction 3), undergo hydration (reaction 4), or react covalently with glutathione (spontaneously or catalysed by UGTs) (reaction 5). Phenols may also be formed by cytochrome P-450 directly (reaction 2). The phenols, quinines and dihydrodiols can all form conjugates. In addition to being conjugated, the dihydrodiols may undergo further oxidative metabolism by cytochrome p450 (reaction 6), creating primarily a single diol epoxide isomer, (+)-7b,8a-dihydroxy-9a,10a-epoxy-7,8,9,10-tetrahydrobenzo[a]pyrene ((+)-diol epoxide-2). * This isomer is also the only isomer with high tumorogenic activity, found covalently bound to DNA in a variety of mammalian cells and organs, exposed to benzo[a]pyrene [36].

1.3.4.3 Cytochrome P-450-monooxygenase-mediated BaP metabolism in different tissues

The cytochrome P-450-dependent monooxygenase (CYPs) system plays the central role in xenobiotic metabolism in all vertebrates, from fish to mammals [42]. The liver is generally the organ with the highest concentration and amount of CYPs [43]. Monooxygenase activity occurs in other tissues as well, including those that are directly exposed to environmental agents (such as the lungs and gastrointestinal tract of mammals

[43]). In mammals, the importance of intestinal metabolism of orally-administered drugs and carcinogens has been recognised for years [49, 50]. The monooxygenase system of mammalian intestine is very sensitive to inducing agents present in the diet. Exposure to dietary PAHs, for example, results in a large and rapid increase in the levels of intestinal CYPs [42]. Moreover, in vivo studies indicate that considerable metabolic activity occurs during the passage of many dietary xenobiotics, including BaP, through the intestinal mucosa [51, 52].

1.4 PAHs and food

Food ingestion is the major route of general population exposure to PAHs [53]. Studies conducted on human exposure to BaP revealed that the range and magnitude of dietary exposure (2-500 ng/day) was greater than that for inhalation (10-50 ng/day) [54] or occupational exposure [55]. Among PAHs, fluoranthene and BaP are two compounds that have been detected in high levels in grilled food [56].

1.4.1 Food contamination

PAH contamination of food can come from two sources: the environment and food-processing techniques [36, 57]. Unprocessed food such as vegetables, fruits, grains, vegetable oils, dairy products and seafood are subject to deposition of PAH from atmospheric airborne particles containing PAHs [58]) and soil. In addition, from contaminated pastures and vegetation, PAHs enter livestock (i.e. food of animal origin) [59, 60]. Fish and shellfish PAH contamination is due to contamination of the fresh and coastal waters. Cooking methods (i.e. grilling, smoking), cooking temperature, time, amount of fat, and oil can contribute substantially to the formation of PAHs in food products such as meat, fish, cheeses, even vegetables [61-63]. Some drying techniques used for cereal preservation and refining processes for oils can also contribute to the increase in PAH in these foods [64]. Table 1-1 lists the ranges of concentrations of fluoranthene, benzo[a]pyrene, chrysene and pyrene found in various types of food products.

Table 1-1. PAH concentrations in various food products

Concentrations are given in μg/kg dry weight for grains, flours, breads, coffee, fish; μg/kg of wet weight in vegetables and fruits; μg/kg in oils. References are given in square brackets.

Compound	*Vegetables and fruits*	*Grains, flour and breads*	*Dairy products*	*Refined oils*	*Raw meat or fish*	*Cooked fish or meat*	*Coffee*
Fluoranthene	0.037-1.3 [57]	0.2-0.7 [66]	1.2-3.4 [63, 68]	4.2-18 [4, 64]	1.8-1800 [73, 74]	11-120 [56]	8.0 [4, 77]
Benzo[a]pyrene	0.014-30 [4, 65]	0.19-4.13 [4, 36]	1.5-7.5 [59, 68]	0.2-88 [64, 69]	0.7-31 [75]	0.04-78 [36]	0.5-15.8 [36]
Chrysene	0.025-28 [36]	0.1-0.8 [66, 67]	5.6-8.6 [59, 63]	0.5-200 [69, 70]	2.1-260 [68, 76]	1.5-290 [56, 62]	0.6-19.1 [77, 78]
Pyrene	0.034-0.3 [4, 57]	0.1-0.5 [4]	5.5-36 [68]	2.6-20 [71, 72]	5-1500 [36]	2.3-127 [4, 61]	8.1 [4]

Fruits and vegetables can accumulate contaminants if they are grown in contaminated soils or in proximity to highways [79, 80]. Jones et al [66] demonstrated that often cereal and bean crops are contaminated by the aerial deposition of PAHs. The high PAH concentrations are a matter of concern because ingredients such vegetable oils and fats are common in a variety of manufactured or cooked foods.

Cooking techniques and the presence of vegetable oils as an ingredient also appeared to increase PAH levels even in infant formulae in which the mean BaP content (0.49 μg/kg) was four times higher than that found in skimmed milk [81].

Products of animal origin such milk, butter, eggs and cheese normally have considerably low concentrations of PAHs; however, additional cooking and heat sources contribute to high PAH contamination in those foods [63]. High PAH levels (0.04-290 μg/kg) were found in the edible portion of all barbequed or grilled meats and fish [36].

PAHs are present not only in broiled and smoked fish or meat and roasted coffee [61, 62, 77, 78], but also in fresh meats and seafood (Table.1-1) [55, 75]. The amount of PAHs found in aquatic organisms depends on the level of contamination of their habitat and the ability of those organisms to metabolize PAHs. For example, sediment-feeding shellfish accumulate a large amount of PAHs from contaminated sediments due to their high lipid content tissues, limited motility and low metabolic capacity [75].

In 2001, Kazerouni et al [82] measured the quantities of BaP in more than 220 food items in USA and reported a daily BaP intake from 40 to 60 ng in the general population. In this study, the bread/cereal/grain, and grilled/barbecued meat, respectively, contributed 29 and 21 percent to the mean daily intake of BaP. Another study from Spain [83] covered more than 100 food items and showed that by food group, the highest levels of total PAHs were detected in cereals (14.5 μg/kg) and in meat and meat products (13.4 μg/kg). They reported that most subjects who participated in the study had BaP uptake of 20ng/day, when the total amount of PAH intake ranged between 100 and 150 ng [83]. This study found significant differences in average dietary intake of PAHs for different age groups with the highest intake for children (0.307 μg/kg/day), followed by adolescents (0.150 μg/kg/day), and senior citizens and women (0.102 μg/kg/day).

1.5 Fate of PAH in soil

Soil plays an important role in the fate of PAH in the environment. PAHs mostly exist at contaminated sites either in non-aqueous phase liquid (NAPL) or sorbed onto soil [11]. Contaminants enter the soil mainly by deliberate application, by spills and leakage, and by atmospheric deposition. As a result, the soil is a sink for PAHs. While PAHs may be lost from the soil via various processes (Fig.1-3), significant amounts may be retained within soils.

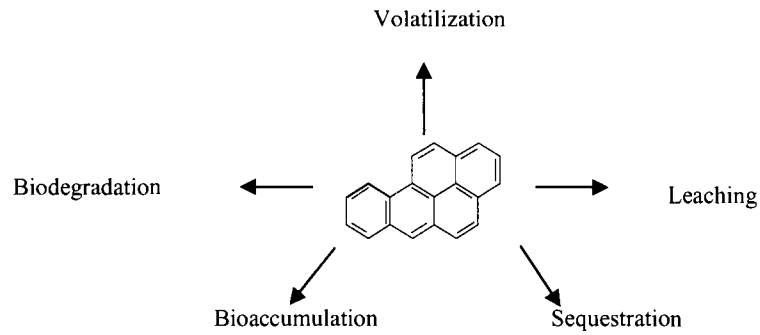

Figure 1-3. Fate of benzo[a]pyrene in soil

1.5.1 Soil contamination

The fate and behavior of organic contaminants in soil has been the subject of intensive research, with particular interest directed at the bioavailability of contaminants in the soil.

Most of the current research on HOCs in soil is focused on the characterization of the carbonaceous phases in soil, because carbonaceous materials are considered to be the primary sites of HOC sorption. This work includes separation of humic, fulvic and humin fractions of soil organic matter, because each of these fractions has a different affinity for HOCs, and the use of petrography and elemental analysis to evaluate the degree of condensation and polarity of carbonaceous materials in soil. More condensed forms of carbonaceous materials (chars, soots, coals, and kerogens) are considered to be important sorption sites for HOCs, and their presence may result in reduced bioavailability [34].

1.5.2 PAH in soil

PAHs have received more attention since Blumer [84] found them in soils for the first time in 1961. Almost twenty years later, in the early eighties, several research groups presented the first reviews on the fate of PAHs in soil-plant systems [85]. Individual PAH concentrations in soil produced by natural processes like vegetation fires and volcanic exhalation have been estimated to be in the range of 1-10 μg/kg [85]. Even in the most remote areas such as the arctic, BaP concentrations range between 0.8 and 4.3 μg/kg and those are still considered to be preindustrial levels [86]. Generally, PAH concentrations in soils increase with increasing impact of industry, traffic, and domestic heating. Most PAHs reach the soil via deposition from the atmosphere [87]. Sorption and desorption are crucial processes for PAH bioavailability and PAH transport in soil. As with other HOC, soil organic matter is the most important sorbent for PAHs [87]. Sorption of PAHs to soil has been shown to resemble the partitioning of PAHs among water and organic matter. PAH sorption is rapid and indicating that it is an entropy-driven process [88]. As noted above, there are indications that soil organic matter type influences PAH sorption [89].

1.5.3 Ageing of PAHs onto soil

Normally, as the time of contact between the contaminant and soil increases there is a decrease in chemical and biological availability, a process called "ageing" [90]. Over time, the readily extractable fraction diminishes, as some fraction is degraded or lost from the soil and an increasingly recalcitrant fraction becomes unavailable for extraction. At first, this fraction can be accessed only by specific and sometimes aggressive solvent extraction techniques, but eventually the recalcitrant fraction is converted into a non-extractable fraction. The mechanism of ageing has been investigated [30]. As a result, it is known that interactions between soil and PAHs are affected by both the amount and nature of the soil organic matter [89, 90], by the pore size and structure of the inorganic components [91], and by the microbial population and the amount of contamination [35].

It has also been established that aged organic contaminants in soil demonstrate reduced bioavailability, which results in a non-degraded residue in the soil. Aged contaminants in soil are not available for degradation even though freshly added

compounds are still degradable [11]. Bosma et al [92] have suggested that sorption is the major factor preventing complete bioremediation of hydrocarbon contamination.

The main mechanisms required for ageing are sorption and diffusion (generally referred to as sequestration). These mechanisms involved interactions between the contaminant and the solid fractions, such as minerals and organic matter [5]. Together with the physico-chemical characteristics of the contaminant, these soil fractions determine the rate and extent of ageing in soil [30].

In general, sorption of organic contaminants exhibits bimodal kinetics [5]. The first phase is fast, where a portion of the contaminant is sorbed quickly by creating hydrogen bonds and van der Waal's forces [93]. This phase can take minutes to a few hours. The remaining fraction is sorbed more slowly, occurring over weeks or months [5]. During this stage, the contaminant creates additional non-covalent bonds with organic matter, which results in a stable irreversible incorporation into soil [93].

Currently, two general models are proposed to explain the effect of ageing in soils. The first model is "organic matter diffusion". Diffusion is random movement under the influence of a concentration gradient [94]. Proponents of this model postulate that diffusion through natural organic matter, which can be classified as rubbery, glassy or adsorptive is the rate-limiting step. Rubbery and glassy phases contain dissolution sites; the latter having more rigid cavities for the interaction of contaminant with the organic matter. For example, soil humic acid has condensed polyaromatic regions (glassy structure), even after extraction and reconstitution to a particulate form; it has been suggested that these polyaromatic structures provide adsorption sites [5].

The second model is the "sorption-retarded pore diffusion" model in which it is postulated that the rate-limiting process is molecular diffusion in pore water. This type of diffusion is retarded by rapid-reversible local sorption on pore walls, which may or may not contain organic matter [30]. According to this model, the rates are dependent on the radii of soil particles, on the tortuosity of pores (bending and twisting interconnectivity, presence of dead-end pores) and on the constrictivity (steric hindrance) in the pores [5].

It is likely that both scenarios exist in the environment, often even in the same particle. Organic matter diffusion may be dominant in soils with high organic matter, while sorption-retarded diffusion may predominate in soils with higher aggregation.

As mentioned above, the rate of sorption and desorption control the physical availability of the organic pollutants. However, when ingested, the oral bioavailability of the soil contaminants primarily depends upon the ability of the gastrointestinal tract to dissolve the contaminant and absorb it through the gastrointestinal membrane.

1.5.4 Oral exposure to PAH-contaminated soils

Soil ingestion is a major route of exposure to PAHs in children [95]. Ingestion is often unintentional, for example, the consumption of unwashed fruit or vegetables grown on contaminated land or the hand-to-mouth contact of children playing on a polluted playground [96].

The oral bioavailability of the soil contaminants primarily depends upon the ability of the stomach and small intestine to dissolve the contaminant and absorption of the contaminant through the intestinal membrane. Absorption requires that the HOCs be dissolved in a carrier, e.g. bile [97]. It is generally accepted that most of the uptake takes place in the small intestine [98]. In the stomach, the acid may dissolve adsorbed contaminants while in the intestine the soil organic matter is dissolved and the more sequestered contaminants are released [99]. This fraction is then available for entry to the systemic circulation via translocation across intestinal cell membrane.

1.6 The gastrointestinal tract

1.6.1 Overview of ingestion and absorption

The movement of the food/soil through the gastrointestinal tract (GIT) begins with oral ingestion. The GIT involves a number of organs and processes that convert food into a form that can be absorbed and utilized by the rest of the body and non-absorbed material eliminated as waste material. Once food has been savored, it is mixed with saliva, and reduced in particle size through the process of chewing. Saliva contains two

enzymes: α-amylase, which initiates the degradation of starch, and lingual lipase, which plays an important role in the hydrolysis of dietary lipid. The resulting bolus of food is swallowed, passes into the esophagus and is carried by peristalsis to the stomach. The wall of the stomach is lined with the various cells of the gastric mucosa that secrete a highly acidic gastric juice, resulting in gastric juice with a pH < 1 in adults, and approximately 2-2.5 in children [98]. A high concentration of hydrochloric acid is required for the conversion of inactive pepsinogen to the proteolytic enzyme pepsin, which is responsible for the dissolution of ingested protein into soluble chyme. Relative to the intestine, little absorption occurs in the stomach. However, some water, certain ions, and some drugs such as aspirin and ethanol are absorbed from the stomach into the blood. As the contents of the stomach become thoroughly liquefied, they pass into the duodenum, the first segment (about 10 inches long) of the small intestine. Two ducts enter the duodenum: one draining the gall bladder and the other draining the exocrine portion of the pancreas. The exocrine cells (duct cells) of the pancreas produce a large amount of aqueous bicarbonate that neutralizes the acidity of the fluid arriving from the stomach, raising its pH to about 8 in adults, and to 7-7.4 in children [98]. The endocrine cells of the pancreas (the islets of Langerhans) synthesize and secrete major enzymes for digestion: pepsin, amylases, lipases, nucleases and "zymogens" — proteins that are precursors to active proteases. Pancreatic lipases hydrolyse triglycerides to free fatty acids, monoglycerides and glycerol. This action is enhanced by the detergent effect of bile salts, which emulsify the fat droplets into smaller particles, forming micelles with a greater total surface area. The zymogens are rapidly converted into active proteolytic enzymes such as trypsin, which cleaves the peptide bonds of arginine and lysine; chymotrypsin, which cuts tyrosine, phenylalanine, and tryptophan residues; and carboxypeptidase, which removes, one by one, the amino acids at the C-terminus of peptides [100].

When food, especially fatty food, enters the duodenum, the release of the hormone cholecystokinin (CCK) stimulates the gall bladder to contract and discharge stored bile into the duodenum. Bile contains bile acids (amphipathic steroids) that emulsify ingested fat; the hydrophobic portion of the bile acids dissolves the fat while the negatively-charged side chain interacts with water molecules. The mutual repulsion of

these negatively-charged droplets keeps them from coalescing. Thus, large drops of fat (liquid at body temperature) are emulsified into tiny droplets (about 1 μm in diameter) that can be more easily digested and absorbed [101].

The result of the combined actions described above is the production of simpler molecules that can be absorbed and transported from the lumen of the small intestine into the systemic circulation (discussed below). The small intestine merges with the large intestine (colon), for which the principal function is re-absorption of water [98]. Approximately 9 litres of water enters the gastro-intestinal tract every day: 2 litres are ingested and 7 litres are secreted into the stomach and small intestine via the various digestive glands; the same amount of water must be reclaimed to avoid dehydration [102]. The additional role of the colon is to store unabsorbed material until elimination. During this further time, metabolism of the remaining food materials by colonic bacteria can take place.

1.6.2 Physiology of the small intestine

The major roles of the small intestine are the selective absorption of major nutrients such as sugars and amino acids, finishing digestion, and serving as a barrier to digestive enzymes, ingested compounds, and bacteria [103]. These multifunctional characteristics make the small intestinal epithelium structurally complex. The luminal mucosa is composed of a monolayer of epithelial cells, the connective tissue scaffold (*lamina propria*), and a thin layer of smooth muscle (*muscularis mucosa*). The *lamina propria* provides a structural support for the monolayer of epithelial cells and has anatomical modifications that increase the luminal surface area – Kerkring's fold, villi, and microvilli (Fig.1-4). The microvilli are prominent on the apical surface of columnar epithelial cells or enterocytes and goblet cells, and collectively comprise the brush border region. Enterocytes function in digestion, absorption, and secretion, whereas goblet cells secret mucin. This secretory product forms a crucial physiological barrier between the intestinal mucosa and the luminal environment [104]. The function of the mucus is not clear, but may be related to physical (e.g., lubrication of epithelial surfaces, protection of mucosa against proteases), chemical (e.g., diffusion barrier to nutrients, drugs, ions,

toxins, and macromolecules), and immunological protection (e.g., interaction with immune system and binding of bacteria, viruses and parasites) [105].

The most common epithelial cell is the enterocyte or absorptive cell [103]. It is highly polarized with distinct apical and basolateral membranes, which are separated by tight junctions (Fig.1-4). The apical membrane displays strikingly uniform microvilli measuring approximately 1μm in height in which disaccharidases and peptidases reside [106]. These modifications contribute to a magnification of the total surface area of the small intestine, up to 200 m^2 for an adult, i.e., a 600-fold increase. This large surface area facilitates mass transfer from the lumen of the intestine to enterocytes and further to the blood and lymph circulation [107]. The apical membrane (Fig.1-4) also expresses receptor-mediated transport systems, such as those for cobalamin (vitamin B_{12}) [108], specific ions, monosaccharides, amino acids, peptides, and fatty acids [106]. In contrast to the apical membrane, the basal membrane has smooth contours with no sugar or peptide hydrolases. However, Na^+, K^+-ATPase, glycosyltransferases and adenylyl cyclase are located in the basal membrane [106].

1.6.3 Intestinal transport and absorption

The terms transport and absorption often are used interchangeably and describe the movement of material from the intestinal lumen into the blood system. Transport of a molecule across the cellular membrane is a complex pathway that includes passage through the aqueous unstirred layer that surrounds the intestinal brush border membrane (Fig.1-4). This layer forms the major barrier to the absorption of lipids or lipophilic compounds (discussed later). The transport processes involve several mechanisms: pinocytosis (uptake of fluid phase proteins and ions by membrane engulfment) at the base of the microvilli, passive diffusion, facilitated diffusion, and active transport.

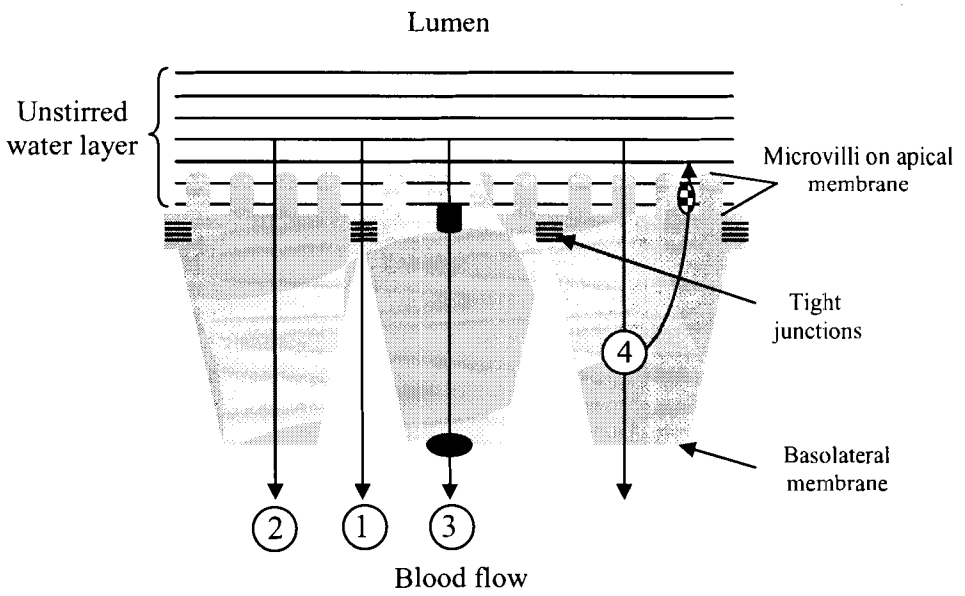

Figure 1-4. Transport routes in intestinal epithelia.

Solutes moving across the enterocytes from the intestinal lumen into the blood must traverse an unstirred layer of fluid. Passive transport of molecules across the epithelium of the small intestine can either occur through 1) the tight junctions bridging the intracellular space between the cells (the paracellular route) (primarily for ions), or 2) across the cell membranes (by the transcellular route) by passive diffusion, 3) carrier mediated diffusion, or 4) back into the lumen by an apical efflux mechanism mediated by membrane transporters.

The driving force for solutes during passive diffusion is the electrochemical gradient, in which the force driving passive diffusion of water is the osmotic gradient across the intestinal mucosa. Compounds can be absorbed across the intestinal epithelium in two ways, either through the cells (Fig.1-4, routes (2&3)), i.e., the transcellular route, or between the cells, i.e., the paracellular route (Fig.1-4, route (1)). Transport across healthy epithelium by the paracellular route is limited to small hydrophobic molecules due to the presence of the tight junctions [109]. Transcellular transport of a molecule can take place by a passive mechanism (pathway 2, Fig.1-4), or by a specific carrier (pathway 3, Fig.1-4).

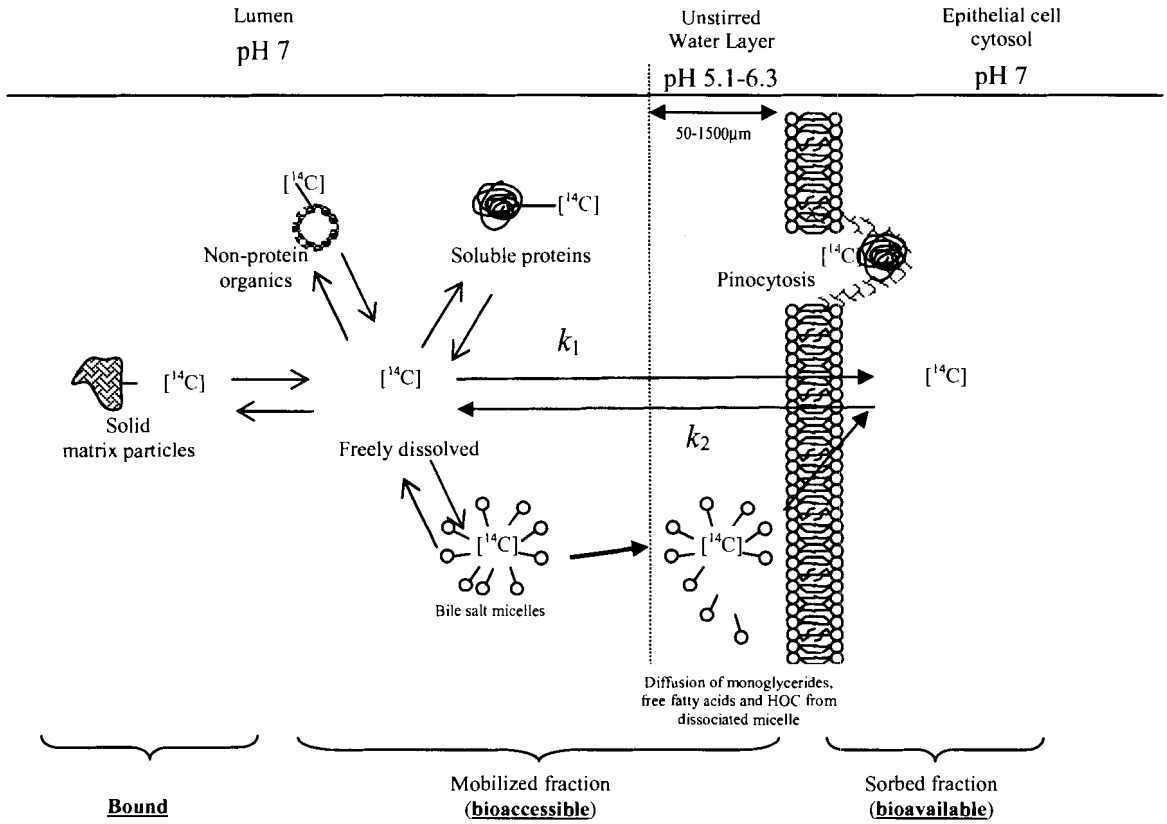

Figure 1-5. Schematic diagram of mobilization and partitioning of the HOC among various fractions of the gastrointestinal uptake of HOC.

During intestinal transit, the presence of intestinal components release HOCs bound to the solid matrix from the matrix particles. The mobilized and soluble fraction of chemicals in the gastrointestinal environment that include HOC associated with soluble proteins, fats, non-protein organics (i.e., humic acid), and freely dissolved HOC molecules make up the bioaccessible fraction. The bioavailable fraction is defined as the fraction that has diffused through the cell membrane. In the intestinal lumen, dietary fats (mostly triglycerides) are hydrolyzed by lipases to monoglycerides, fatty acids, and glycerol. The water solubility of these products is low, but they are well solubilize in the hydrophobic interior of bile salt micelles that are produced by the liver [110]. Bile salts enhance the absorption of dietary lipids and thus consequently HOCs by acting as lipid storage forms and by providing a vehicle to overcome the mucous unstirred water layer (UWL) adjacent to the intestinal wall [111]. The slightly more acidic (pH 5.1-6.3) environment of the UWL causes dissociation of the micelles resulting in the diffusion of fatty acids and HOC across the bilayer of the membrane. A decrease in pH promotes the diffusion of fatty acids across the membrane by reversing the ionization of free fatty acids in the aqueous phase. HOCs associated with soluble proteins can be dissociated or taken up by pinocytosis.

HOCs that enter a GIT have to overcome a series of barriers – chemical permeation through aqueous and lipid layers that determined by the resistance the HOCs experience in each phase. Earlier studies showed that the uptake rate constant (k_1)

increased with K_{ow} for organic chemicals having a log K_{ow} < 3, that k_1 was independent of K_{ow} for chemicals with log K_{ow} between 3 and 6 e.g. transfer in the lipid phase is rate-determining rate [112, 113]. It was also found that the elimination rate constant (k_2) was independent of K_{ow} for chemicals with log K_{ow} < 3 and decreased with increasing K_{ow} [112]. With increasing K_{ow} (log K_{ow} > 6), HOC transport in the aqueous phase of the adjacent unstirred water layer (UWL) becomes the more important and dominating step, meaning that k_1 increases over k_2 and controls the uptake kinetics by becoming the rate-limiting step. The uptake rate constant (k_1) is a measure of how fast concentrations in the organism will increase. The elimination rate constant (k_2) is a measure of how fast the concentration in the organism decreases and how fast steady-state is reached between concentrations in the organism and the ambient environment [114].

In summary, for passive flux of a molecule across a lipid bilayer to take place, the molecule must have the correct physicochemical properties, e.g. small size, no charge, log K_{ow}, and lipophilicity, to cross both membranes (apical and basal) [103]. However, compounds absorbed by this route may also become substrates for intracellular metabolism and apical transport (pathway 4, Fig.1-4) [115]. In addition, compounds can be also absorbed via carriers [103]. Some HOCs that associate with soluble proteins can be taken up by pinocytosis; however, receptor-mediated endocytosis of compounds is minimal and is not likely to be the mechanism of uptake for most xenobiotics [116].

Studies of the intestinal absorption and toxicity of xenobiotics have traditionally been performed in vivo in experimental animals. In recent years, in vitro models employing cells in culture have been proposed, both for the screening of the absorption of drugs and, more generally, for the study of toxicity and metabolism of xenobiotics. Several different approaches have been attempted with the aim of preserving, in vitro, the complex functional and morphological organization of the intestinal epithelium. These approaches include: primary cell cultures, cell lines from normal tissue, normal cell lines transfected with regulatory genes, and established cell lines of tumour origin [117].

Primary intestinal cell culture from the small intestine can maintain a variable degree of differentiation for three to six days, but the isolation of the epithelial cells leads

to rapid loss of their differentiated characteristics [117]. Moreover, they are not always easy to obtain in a reproducible and quantitative manner.

From primary cultures, it has been possible to isolate homogenous cell lines capable of proliferating and surviving for several in vitro passages before undergoing senescent changes or spontaneous transformation [118]. These cell lines are usually derived from rat small intestine and exhibit poorly-differentiated intestinal epithelium (i.e., IEC lines) [119]. The advantages and disadvantages of using these cell lines is discussed in detail in Chapter 2 of this thesis.

Cell lines obtained from human tumours express variable degrees of differentiation in culture that depend on the characteristics of the tumour origin [103]. Among numerous cell lines derived from human gastrointestinal adenocarcinomas, only three: Caco-2, HT-29 and T-84 express, in culture, the morphological and functional characteristics of some of the differentiated cytotypes of the intestinal mucosa [117]. The Caco-2 cell model is the best characterized among intestinal cell culture models with regards to the transport properties of pharmaceuticals [120], metals [121] and recently xenobiotics [122, 123]. Specific features of Caco-2 cells are discussed in more detail below.

1.6.4 Caco-2 cells

After 3 weeks in culture, the Caco-2 epithelial cell line derived from a human colonic adenocarcinoma [120] undergoes a spontaneous differentiation to a monolayer of highly polarized cells, joined by functional tight junctions, with well-developed and organized microvilli on the apical membrane [124] (Fig.1-5). Not only do Caco-2 cell monolayers morphologically resemble human small intestinal absorptive cells, they also express many brush border enzymes, such as microvillar hydrolases, including disaccharidases [125], peptidases [126], and alkaline phosphatase [127].

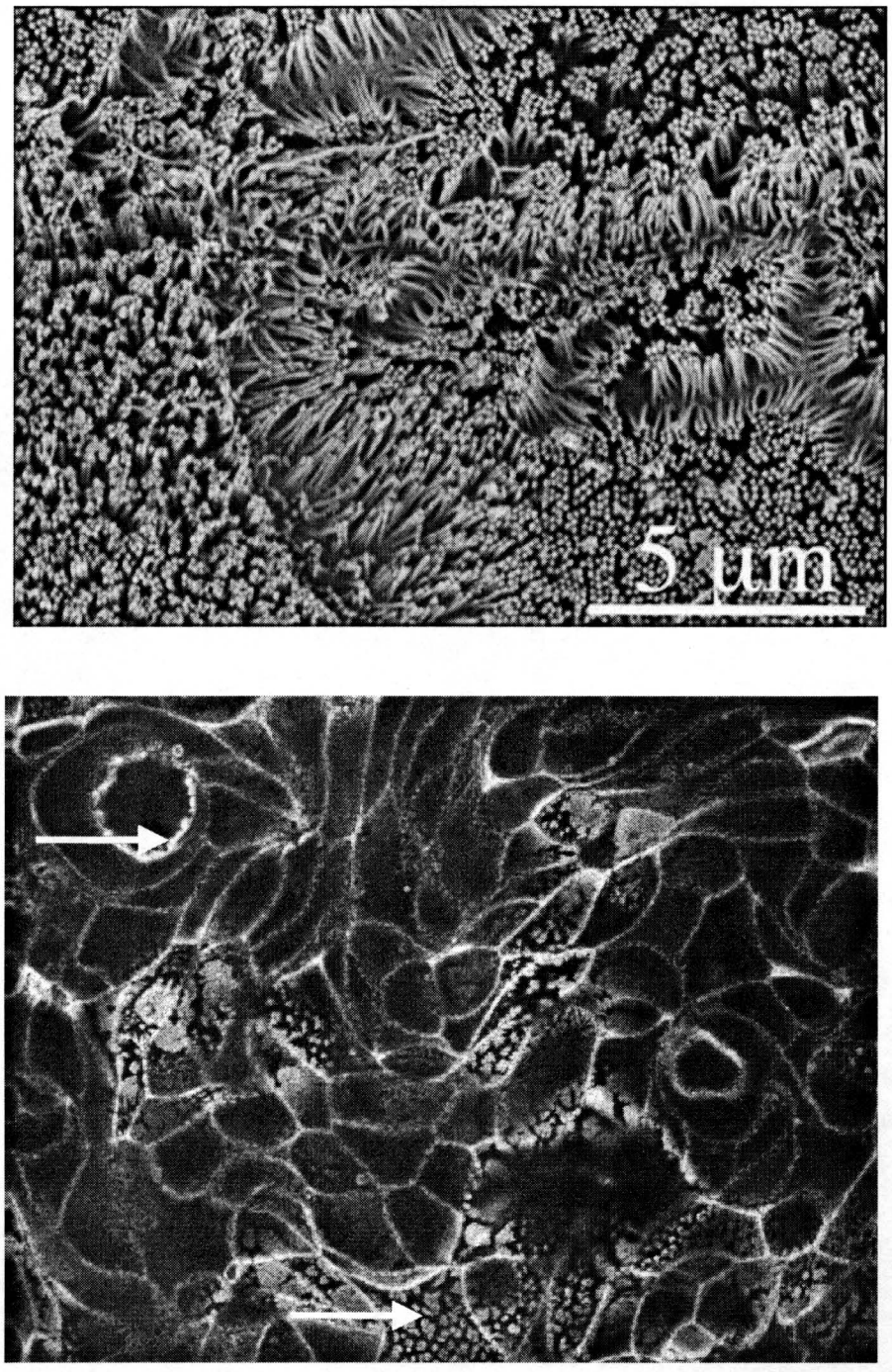

Figure 1-6. Scanning electron microscope image of polarized Caco-2 cells showing apical microvilli (A); localization of F-actin fibers of polarized Caco-2 with rhodamine phalloidin visualized using a confocal scanning microscope (B).

SEM imaging and confocal microscopy was performed by L. Vasiluk. Actin staining with rhodamine phalloidin has been used as an indirect method to assess the integrity of tight junctions, since actin distribution often correlates with changes in tight-junction properties [128]. Cells display punctate staining of actin microvilli bundles and a continuous belt-like pattern (arrows) at all sites displaying cell-to-cell contact (tight junctions). Arrows show actin bundles of microvilli in cross-section.

Changes to ZO-1 (*Zonula occludens-1*, a tight junctional protein, [128]) distribution during the formation of the monolayer are shown in Fig.1-6.

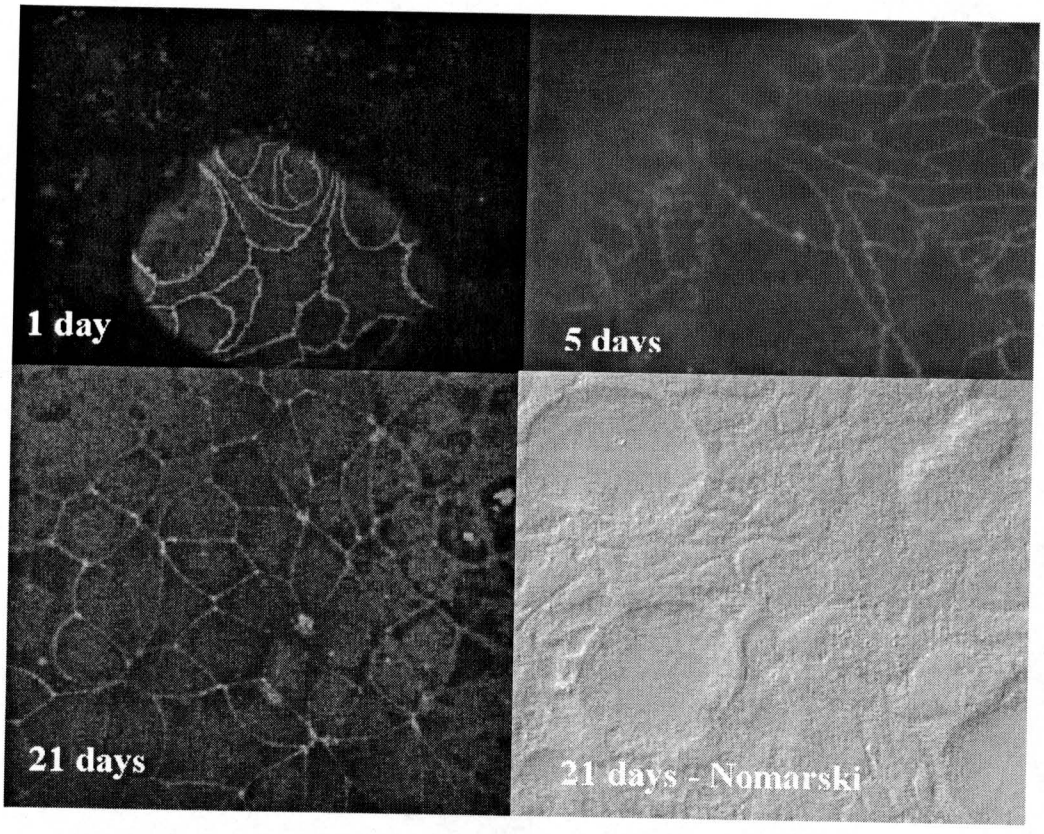

Figure 1-7. Immunofluorescence staining of the tight junctional protein, ZO-1.

Confocal microscopy was performed by L. Vasiluk. After 1 day in culture, ZO-1 appears in islands of cells and cell-cell contacts. These islands progressively enlarge and finally appear organized at day 8 in the characteristic honeycomb pattern that follows the cell borders. Between 8 and 21 days, this pattern does not change. Dome formation (21 days- Nomarski) is a lifting of the cell monolayer, to create a bubble of fluid between the cell layer and the culture dish. Domes do not occur on porous inserts, since fluid accumulation on the basal side is prevented.

When cultured on polyethylene terphthalate (PET) inserts (0.9 cm^2, 0.4μm pore size) for 3 to 4 weeks, Caco-2 monolayers become polarized and thus provide a good in vitro model for conducting intestinal transport studies [120] (Fig.1-7).

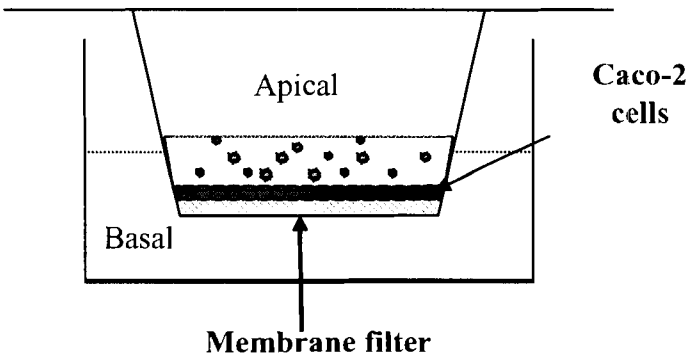

Figure 1-8. Schematic side-view of commercial cell culture wells used for transport studies in which Caco-2 cells are grown on PET inserts.

The Caco-2 transport system has an apical side, which represent the intestinal lumen and a basolateral side which represents the blood and lymph drain. Growth medium or buffer can be added to either or both the apical and basolateral chambers.

When transport and uptake experiments are performed, an unstirred water layer (UWL) or aqueous boundary layer is present on the surface of the cultured Caco-2 cell monolayers. Karlsson and Artursson [129] measured the permeability coefficient for testosterone and reported that the thickness of the UWL was similar to that estimated for human intestine (128-500μm).

Many studies have been conducted using Caco-2 cells to demonstrate the presence of active transport systems for nutrients, such as amino acids, biotin and bile acids. Dix [130] reported that due to their colonic nature, Caco-2 cells may poorly express transporters for vitamins, such as cobalamin. In contrast, studies of bile acid transport in the Caco-2 model supported the suitability of this model for intestinal drug absorption since the bile acid transport system is known to be present only in the small intestine [131].

The induction of P450 enzymes (CYPs) in Caco-2 cells has been confirmed [132], as well as the activity of some Phase II enzymes such as glutathione-S-transferase [133] and glucuronidase [134]. Various PAHs have been used to induce P450 isozymes. For example, 7-ethoxyresorufin-O-deethylase (EROD) activity (a surrogate of CYP1A1) was inducible by addition of the CYP inducer, β-naphthoflavone [135]. Cholesterol

metabolism has been studied in the Caco-2 cells. Caco-2 cells have been shown to synthesize and secrete lipoproteins [136].

Although absorption of drugs and other chemicals can be expressed in terms of their concentrations within various compartments in such an in vitro system, the extent of mobilization and absorption is influenced by not only the chemical concentration, but also by the sorptive properties of each compartment.

1.7 Predicting bioavailability using the fugacity approach

The fugacity approach is a useful tool that can contribute to a better understanding of the fate of toxic substances. If concentration data for a chemical can be monitored in several phases and the respective fugacity capacities are known, then concentrations can be converted to fugacities which can be compared [137].

The bioavailability of a chemical bound to a solid matrix (e.g., food, soil, sediment) is often related to the chemical potential of the contaminant in the matrix environment [138]. A convenient way of expressing the chemical potential is by use of the term "fugacity". Fugacity can be described as the tendency of a chemical to "escape" from a defined compartment in the environment into another and is measured in units of pressure (Pascal (Pa)) [8].

Thus, the fugacity (f, Pa) is a function of both concentration C (mol/m^3), and the intrinsic absorbing capacity of the matrix, referred to as fugacity capacity Z, ($mol/m^3 \times Pa$):

$$f = C/Z \qquad (1)$$

In materials with a high fugacity capacity for a chemical (high $Z_{material}$), more chemical (i.e., a higher concentration) needs to be added to achieve a one-unit increase in the fugacity compared to a material with a low Z. At a given fugacity, if Z is low, then even a small concentration of chemical will exhibit the tendency to leave that phase. HOCs tend to accumulate in phases where Z is high, and high concentrations can be reached without creating high fugacities [8]. For example, in biota, hydrophobic compounds tend to partition into lipid phases because the Z of lipids for HOC is much

greater that the *Z* of the other compartments, such as aqueous compartments or proteins. Therefore, if we can determine the Z of a substance for each compartment in the model we can predict/calculate how the substance will partition among the various phases. Fugacity calculations have been used to predict the static and dynamic behaviour of toxic compounds within an organism and the environment [137]. The thermodynamic concept of chemical potential describes passive diffusion of chemicals within and between phases that possess very different physical properties [8]. Working with fugacity rather than concentrations is particularly valuable when studying multi-compartment systems (such as solid matrix/gastrointestinal fluids/ intestinal epithelium), because the direction of the passive chemical diffusion is determined by the fugacity gradient rather than the concentration gradient. Chemical equilibrium is defined as equal fugacity in all compartments [8]. When compartments are not at equilibrium, thermodynamic equations can still be used to determine the likely direction of flow of a chemical as it moves towards equilibrium in a system. A high fugacity means that more chemical is likely to move across membranes and therefore, the chemical may exhibit greater bioavailability.

The oral bioavailability of matrix-bound chemicals is complex, as it is a function of matrix properties; (amount and type of hydrophobic sorbent, i.e. organic matter for soil or sediment); chemical properties (speciation, size, hydrophobicity); environmental factors (temperature, pH); and time (matrix-contaminant contact time, uptake kinetics).

Equation 1 indicates that as the fraction (or proportion) of soil organic matter increases, its ability to hold hydrophobic organic chemicals (chemicals with high log K_{ow}) also increases (i.e., *Z* increases) thereby reducing the fugacity (or bioavailability) of the chemical. However, as discussed in the previous sections, organic matter varies considerably in its ability to sorb contaminants. Therefore, we can expect the fugacity capacity of the soil to vary according to both the quantity and type of organic matter.

1.7.1 Gastrointestinal digestion, membrane permeation and fugacity

Food absorption and digestion can raise the fugacity of HOCs in the gastrointestinal tract over their fugacity in undigested food [139]. Food digestion alters the composition of the food, due to the absorption of lipids and other organic matter from

the food. Therefore, as food is digested, the fugacity capacity of the food decreases which leads to an increase in the fugacity of the chemical in the food being digested. The ultimate effect is to raise the fugacity of the HOCs in the gastrointestinal tract [140]. The increase in chemical fugacity in the gastrointestinal tract creates a fugacity gradient which is the driving force for chemical diffusion into the intestinal epithelium.

HOCs have to pass through a series of diffusion barriers during transport between the bound matrix and the lymph of the organism which leads to the organism's storage compartment [112]. Since HOCs are believed to undergo passive diffusion, as mentioned above, membrane permeation kinetics for these compounds can be related to their hydrophobicity [113]. Several studies have suggested that gastrointestinal fluid extraction fugacity gradient and the partitioning process of digested hydrophobic contaminants was dependent on the K_{ow} of the compounds [18, 141, 142]. The relationship between partitioning or absorption efficiency of various HOCs and their K_{ow} has been previously studied in several organisms, including humans [143, 144]. A relatively constant absorption efficiency was shown for low-K_{ow} chemicals (log K_{ow} <7), but decreases with increasing K_{ow}. It was suggested by Gobas and several researchers [111, 139, 145] that transport by micelles and/or diffusion across the membrane bilayer are the rate-limiting steps for low-K_{ow} substances, whereas diffusion through the unstirred water layer is the rate determining step for high-K_{ow} chemicals.

Another advantage of the fugacity approach is that it can be combined with physiological processes in the cell (i.e. uptake, transport, metabolism), to describe transport of a chemical without having to measure each physiological process individually [111].

The use of fugacity terms greatly simplifies the expressions describing bioavailability and thereafter biomagnification processes and may assist in the risk assessment for chemicals of human health concern.

1.8 Risk Assessment

A human health risk assessment evaluates the risks associated with human exposures to contaminants [146]. It consists of four primary elements: 1) data collection

and evaluation; 2) an exposure assessment; 3) a toxicity assessment; and 4) risk characterization [147]. Quantifying the magnitude of exposure (e.g., oral bioavailability of the contaminant) is a part of exposure assessment. Given the expenses and time constraints associated with in vivo testing, development and validation of an accurate and relatively inexpensive tests to predict relative bioavailability provides an opportunity to improve the accuracy of human health risk assessments. If the contaminant is matrix-associated, then estimating the oral bioavailability of the contaminant may require the use of an extraction test. In general, chemical extractions have been designed to simulate the biological system of interest and are usually referred to as physiologically-based extraction tests (PBETs) [34]. Simple extraction tests have been used for several years to assess the degree of metals dissolution in a simulated gastrointestinal tract [12, 148]. The fraction of metal that dissolves during the stomach and intestinal digestions represent the fraction that is bioaccessible (i.e., soluble and available for absorption). At this time, there is a PBET for lead that correlates strongly with in vivo results and therefore is accepted for generating relative bioavailability values for use in human health risk assessment in several regions of USA [34]. There is also a growing case for the ability of those tests to estimate the relative bioavailability of arsenic, cadmium, and mercury from soil [34].

PBETs for HOCs are less developed than those for metals. At present, there are no extraction tests for organic contaminants that have been validated in vivo.

Given the current interest in developing new rapid methods to provide an accurate estimate of the oral bioavailability of hydrophobic contaminants bound to a solid matrix (food or soil), it would ideal to have a simple, bioavailability-predictive extraction test combined with exposure to sorptive epithelium for HOCs of human health concern.

1.9 Outline of the thesis

Hydrophobic organic chemicals (HOCs) are known to sorb strongly to organic matter. At present, the amount of contaminant that is chemically extractable from soil is considered the exposure dose [6]. However, the fraction of the contaminants that is absorbed in the intestinal tract can be affected by other factors, in particular sorption to a

solid matrix (soil, food, sediments, etc). In recent years, hydrophobic partitioning (octanol-water partition coefficient K_{ow}) has been used as a predictor of bioavailability in studies of the environmental fate of HOCs. Because of their high K_{ow} values, hydrophobic chemicals partition to tissue to a greater extent than more polar compounds [8]. However, these high K_{ow} compounds also bind more strongly to the soil/sediment matrix [9], which can reduce their oral bioavailability. At present, these factors are not taken into account for risk assessment procedures.

At present, animal tests are used to determine the potential for systemic uptake of these compounds from the gastrointestinal tract. However, as these methods are time-consuming and expensive, animal testing of individual compounds is impractical for large-scale screening. As discussed above, various in vitro models and test procedures have been described in the literature to estimate oral bioavailability of pharmaceutical agents.

Although some investigations have employed synthetic digestion protocols, none of these models includes an intestinal membrane or surrogate membrane. Conversely, Caco-2 monolayers have been employed in a few reports to study HOC transport and uptake; however, none of these studies employed a physiological digestion protocol prior to membrane exposure.

The novelty of the approach used in this thesis was to combine the exposure to digestive fluids as well as exposure to sorptive epithelium or its surrogate; to perform a kinetic analysis of the combined data to generate a model of the distribution between compartments and the percent sorbed to the epithelium, and to express the data in terms of chemical activity (fugacity), so that the contaminant levels in the various compartments of the gastrointestinal tract can be compared.

The following objectives were established for this thesis:

1) To establish a model digestive tract using synthetic gastric and intestinal fluids and the polarized human epithelial cell line, Caco-2

2) To measure the transport of the hydrophilic herbicide (glyphosate) across two polarized intestinal epithelium cell lines; human Caco-2 and rat IEC-18; to

determine the direct toxicity of glyphosate to these cells assessed by changes in paracellular permeability, cytoskeletal disruptions and cell lysis, and to determine the extent of direct binding of [^{14}C]-glyphosate to cultured cells

3) To measure the mobilization of the HOC, [^{14}C]-chrysene from soil matrix, and to determine its distribution among different components i.e. digestive fluid, soil, food, sediments, epithelium, or its surrogate; to determine the effect of ageing of the contaminant onto matrix, and the effect of altering the digestive fluid composition on the mobilization of chrysene from soil

4) To compare two in vitro models of oral bioavailability using [^{14}C]-benzo[a]pyrene bound to indigestible matrix (soil) and to determine the effect of ageing and soil organic matter content on the partitioning of the contaminant into the various compartments

5) To determine the effect of metabolic CYP450 induction on mobilization and uptake of [^{14}C]-benzo[a]pyrene from a digestible matrix, and to obtain the metabolic rate constant for this contaminant in our model.

CHAPTER 2: ORAL BIOAVAILABILITY OF GLYPHOSATE: STUDIES USING TWO INTESTINAL CELL LINES

Published with the same title in Environmental Toxicology and Chemistry 24(1): 153-160.

Linda Pinto helped to perform confocal microscopy at the BioImaging Facility at the University of British Columbia.

2.1 Summary

Glyphosate is a commonly used non-selective herbicide that inhibits plant growth through interference with the production of essential aromatic amino acids. In vivo studies in mammals with radiolabeled glyphosate have shown that 34% of radioactivity was associated with intestinal tissue 2h after oral administration. The aim of our research was to investigate the transport, binding and toxicity of glyphosate to the cultured human intestinal epithelial cell line, Caco-2, and the rat small intestinal crypt-derived cell line, IEC-18. An in vitro analysis of the transport kinetics of [^{14}C]-glyphosate showed that 4 hours after exposure, ~8% of radiolabeled glyphosate moved through the Caco-2 monolayer in a concentration-dependent manner. Binding of glyphosate to cells was saturable and ~4×10^{11} binding sites/cell were estimated from bound [^{14}C]. Exposure of Caco-2 cells to ≥10 mg/ml glyphosate reduced transmembrane electrical resistance (TEER) by 82-96% and, increased permeability to [^{3}H]-mannitol, indicating that paracellular permeability increased in glyphosate-treated cells. At 10 mg/ml glyphosate, both IEC-18 and Caco-2 cells showed disruption in the actin cytoskeleton. In Caco-2 cells, significant lactate dehydrogenase (LDH) leakage was observed when cells were exposed to 15 mg/ml of glyphosate. These data indicate that at doses >10 mg/ml, glyphosate significantly disrupts the barrier properties of cultured intestinal cells.

2.2 Introduction

Glyphosate is a widely-used nonselective post-emergence herbicide. It inhibits plant growth through interference with the production of essential aromatic amino acids. Glyphosate is a competitive inhibitor of enolpyruvylshikimate phosphate synthase (EPSPS), an enzyme which is responsible for the production of an intermediate in phenylanine, tyrosine and tryptophan biosynthesis [149]. The resulting reduction in protein synthesis causes termination of growth and eventually, cellular disruption and death. The effectiveness of glyphosate as a phytotoxin is due in part to its low molecular weight and high solubility in water which aid its rapid absorption and translocation by plant tissues; there is very little metabolism of glyphosate by plant tissue [150].

Glyphosate is a weak organic acid that consists of glycine and a phosphonomethyl moiety. Due to its high polarity, glyphosate is practically insoluble in organic solvents and is therefore it applied in various aqueous formulations. These usually contain a salt of glyphosate as an active ingredient, with the addition of surfactants; the surfactant in the major formulation Roundup™ is polyoxyethylene amine. Following application, glyphosate rapidly binds to particulate matter suspended in surface water or to the soil substrate [151]. It is absorbed to many soils and is not readily leached [152], therefore ingestion of contaminated soil is a potential source of human exposure to glyphosate. Degradation of glyphosate in soil has been shown to vary between 3 to 122 days and was found to depend on soil type and climatic conditions. Biodegradation appears to be the predominant mechanism of removal [153].

Because the EPSPS pathway is absent in animals, glyphosate is not lethal to mammals (oral and dermal LD_{50} values in rats are greater than 5000 mg/kg body weight). However, little is known about the effects of glyphosate at the cellular level in mammalian tissue. Measurements of the daily human uptake of glyphosate via food and water are not available [149].

Technical-grade glyphosate has been evaluated in several subacute toxicity studies in mice and rats. In one study, after oral administration in rats, radioactive glyphosate was incompletely absorbed from the gastrointestinal tract and excreted in the

urine. The absorption in rats was reported to be 30-36% after a single oral administration [154]. The majority of the radioactivity was associated with the tissues of the small intestine 2 hours after administration; greater than 34% of the dose was bound to the small intestine. This value declined by 50% after a further 4.3 hours [154]. These results were supported by a report from the National Toxicology Program (NTP) [155], which showed that 30% of administered glyphosate was absorbed and 70% of the dose was eliminated in the feces after 24 hours. Tissue distribution data indicated that most of the radioactivity was found in the gastrointestinal tract for up to 24 hours.

To date, no direct examination of the interaction of glyphosate with human intestinal epithelium has been done. Therefore, the aim of this research was to examine the transport, binding and toxicity of glyphosate to cultured human intestinal cells, Caco-2. The Caco-2 cell model is the best characterized among intestinal cell culture models with regard to transport properties of drugs and metals [120]. Confluent monolayers of Caco-2 cells, a cell line from a human colon adenocarcinoma, have been used extensively to predict intestinal absorption [156]. Caco-2 cells spontaneously differentiate after reaching confluency, forming a highly polarized monolayer with a well-defined brush border on the apical surface and tight junctions, morphologically resembling small intestinal absorptive cells. However, it has been reported that the electrical properties, ionic conductivity and permeability characteristics of the differentiated Caco-2 cells resemble those of the colon crypt cells rather than small intestinal cells [117]. Furthermore, because considerable work has been done with glyphosate in rats [154, 155] we also monitored the effects of glyphosate in IEC-18, a rat small intestinal crypt-derived cell line [118].

The specific aims of this study were: (i) to measure the transport of glyphosate across two polarized intestinal epithelium cell lines; human Caco-2 and rat IEC-18, (ii) to determine the direct toxicity of glyphosate to these cells assessed by changes in paracellular permeability, cytoskeletal disruptions and cell lysis, and (iii) to determine the extent of direct binding of [^{14}C]-glyphosate to Caco-2 and IEC-18 cells.

2.3 Materials and methods

2.3.1 Cell culture

The human colorectal carcinoma cell line (Caco-2) and rat ileum epithelial cell line (IEC-18) were obtained from the American Type Culture Collection (ATCC catalog No. HTB-37 (Caco-2 cells); ATCC Catalog No. CRL-1589 (IEC-18 cells)). Cells were maintained in Dulbecco's Modified Eagle's Medium (DMEM) with high glucose (4.5 g/l) supplemented with 1% non-essential amino acids, penicillin (25 IU/ml) and streptomycin (100 Bg/ml), with 10% fetal bovine serum (FBS) for Caco-2 cells, and 5% FBS and 0.1 U/ml insulin (Sigma) for IEC-18 cells, at 37°C in an atmosphere of 5% CO_2 and 90% relative humidity. Caco-2 cells were used between passages 30-70. For transport experiments, cells (1-2x10^5 cells/insert) were seeded on Transwell polycarbonate cell culture inserts (Becton Dickinson) with 0.4μm pore size. Cells were incubated for three weeks and used between 21 and 26 days after seeding.

2.3.2 Transepithelial electrical resistance (TEER)

The transepithelial electrical resistance across the Caco-2 monolayers was measured using the Millicell-ERS epithelial voltohmmeter (Millipore Co.) at 1h time intervals. The TEER values of the Caco-2 monolayers were calculated using the following equation:

$$TEER_{cell\ monolayer} = (R_{sample}-R_{blank}) \times A\ (ohm \times cm^2) \qquad (1)$$

where R_{sample} is the resistance measured, R_{blank} is the average resistance of two control inserts without cells (approximately 100 ohm x cm^2), and A is the effective area of the cell culture insert (0.9 cm^2). Cell inserts with TEER values <200 ohm x cm^2 were excluded from transport experiments. Generally, mature Caco-2 monolayers that are suitable for transport experiments exhibit TEER values in a range of 200-1500 ohm x cm^2 [157].

2.3.3 Exposure of cells to glyphosate.

Transport experiments were carried out in Transwell inserts. The apical medium (DMEM) was replaced with 0.4 ml of Hanks Balanced Salt Solution (HBSS, Gibco) supplemented with 0 to 20 mg/ml of freshly dissolved non-radioactive glyphosate, approximately 95% pure (Sigma-Aldrich) and [^{14}C]-glyphosate (specific activity of 1.0 mCi/mmol, Sigma-Aldrich) to give 3×10^5 dpm per well. Every hour the inserts were transferred into new wells containing 1.5 ml of fresh HBSS. After 4 h of incubation in a 37°C incubator, the apical medium was removed and lactate dehydrogenase (LDH) release was measured (See section 2.3.4). Subsequently, the inserts with cells were used for the assessment of transepithelial permeability of [^{3}H]-mannitol (specific activity of 26.3 mCi/mmol, NEN Life Science products Inc.). The number of replicates was noted for each experiment separately.

2.3.4 Cytotoxicity assessment using the lactate dehydrogenase (LDH) assay

The LDH assay measures the extent of release of this cytosolic enzyme from damaged cells into the medium. LDH activity was measured in apical samples (50 µl) from each well using the Cytotox96 Non-Radioactive Cytotoxicity Assay kit manufactured by the Promega Corporation, following the manufacture's directions. Triton X-100 (9%) was used as a positive control.

2.3.5 Transepithelial transport of [^{3}H]-mannitol

Transport experiments were carried out in Transwell inserts with 0.4 ml of HBSS. [^{3}H]-mannitol was added to the apical compartment to prepare a final concentration of 10^6 dpm per well. To reduce the volume of the unstirred water layer and to provide mixing, the inserts plus wells were shaken at 70 rpm on a rotating platform at 37°C. The inserts were transferred to new wells containing fresh HBSS at 30 min intervals for 150 min after sampling. [^{3}H]-mannitol was analyzed in the apical and basal compartments by adding Biodegradable Counting Scintillant (Amersham) to 10 µl (apical) and 500 µl (basal) samples. Samples were counted on a Beckmann 6500 Liquid Scintillation Counter

with automatic quench correction. The apparent permeability, P_{app} (cm/s) was calculated according to the following equation:

$$P_{app}=k*V_R/A*60 \quad (2)$$

where k is the transport rate constant (min^{-1}); V_R is the volume (1.5 ml) of the receiver (basal) chamber; **A** is the surface area (0.9 cm^2) of the cell culture insert [157].

2.3.6 Visualization of F-actin filaments in cultured cells

Caco-2 and IEC-18 cells were seeded at 1 X 10^5 cells/well on 12-mm-diameter number 1 coverslips in 24-well plates (Falcon, Becton-Dickinson Canada Inc., Mississauga, Ontario, Canada). After three weeks of growth, the cells were exposed to 0, 10 or 20 mg/ml of glyphosate in HBSS for 4 hours at 37°C. At the end of the incubation period, coverslips with cells were fixed in 4% paraformaldehyde in PBS, pH 7.4 for 30 min, at room temperature. Cells were permeabilized in PBS/10% (v/v) bovine albumin serum (BSA) with 0.5% saponin (w/v) for 30 minutes, at room temperature. The F-actin fibers were labelled with rhodamine phalloidin (Molecular Probes, USA) (diluted 1:40 in PBS/10% (v/v) BSA) for 20 min at room temperature. Filters were then washed with PBS and mounted onto slides with ProLong antifade (Molecular Probes, USA). Samples were viewed with a Zeiss Axioplan 2 confocal laser scanning microscope (Germany) equipped with epifluorescence filters, using a 63x lens.

2.3.7 Statistics

Data are presented as means ± standard deviation. Data were analyzed using one-way ANOVA test, followed by Tukey's multiple-comparison procedure.

2.4 Results

2.4.1 Effect of glyphosate on transepithelial electrical resistance (TEER) of cell monolayers

Transepithelial electrical resistance is routinely measured to monitor electrophysiological properties of epithelial cells and to assess paracellular permeability of the monolayer [157]. Addition of 10 or 20 mg/ml of glyphosate in the apical compartment caused a significant concentration-dependent decrease in TEER values after 4 hours (Fig. 2-1), indicating that these concentrations increase the paracellular permeability of the monolayers. The reduction of the TEER caused by glyphosate was statistically significant at both concentrations. Within 2 hours of glyphosate exposure, most of the TEER reduction had already occurred. At a concentration of 20 mg/ml, the decrease in TEER values was pronounced even after one hour of exposure. After 4 hours of exposure to 20 mg/ml, TEER had declined by 96%. The glyphosate-induced decrease in TEER values was more pronounced in Caco-2 than in IEC-18 (data not shown). IEC-18 cells have lower baseline TEER values because of their elevated paracellular permeability [158, 159], so a smaller overall decline was observed. For example, the TEER of IEC-18 cells had a value of approximately 50 ohm $\times$ cm^2 before the glyphosate exposure and, this was reduced to 30 ohm $\times$ cm^2 by the highest glyphosate concentration (20 mg/ml).

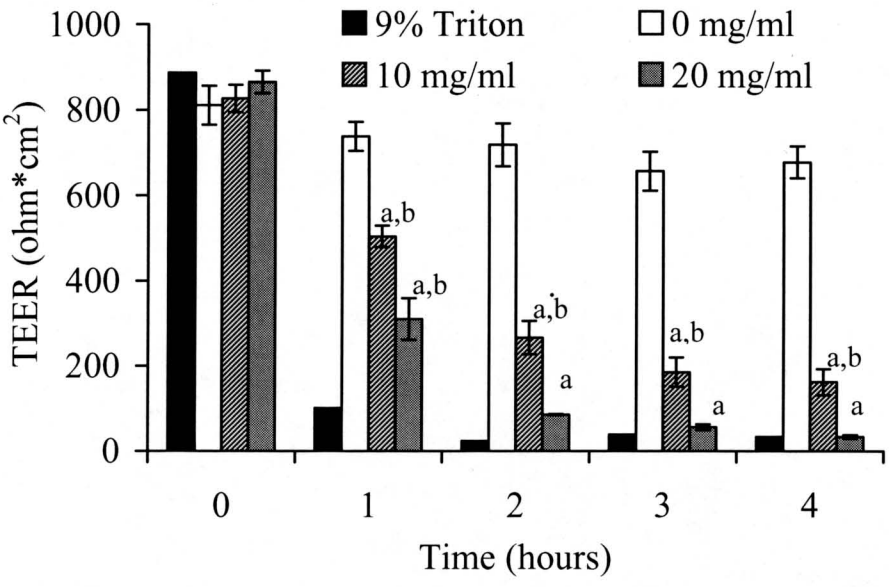

Figure 2-1. Effect of various concentration of glyphosate on the transepithelial electrical resistance (TEER) of Caco-2 monolayers grown on PET inserts.

Data are presented for two independent experiments with three replicates within each experiment and expressed as mean ± standard deviation. Triton X-100 (9%)was used as a positive control. [a] The value is significantly different from the value obtained with 0 mg/ml of glyphosate, $P < 0.0001$. [b] The value is significantly different from the value obtained with Triton X-100, $P < 0.0001$.

2.4.2 Effect of glyphosate on paracellular transport of [^{3}H]-mannitol by Caco-2 and IEC-18 epithelial cells

Another measure of paracellular permeability is [^{3}H]-mannitol transport across monolayers. The transport pathway of mannitol, a hydrophilic monosaccharide, is thought to be via the paracellular route, such that an increase in permeability to mannitol indicates an increase in paracellular permeability, or 'leakiness'. Even without glyphosate treatment, the IEC-18 cells were found to be 5-fold more permeable to [^{3}H]-mannitol than Caco-2 cells. The transport rates (apparent permeability, P_{app}) of IEC-18 monolayers were not affected by lower concentrations of glyphosate (5 mg/ml and 10 mg/ml) (data not shown). However, in the Caco-2 cell line, the P_{app} for [^{3}H]-mannitol was increased by glyphosate in a concentration-dependent manner (Fig.2-2). The apparent permeability of Caco-2 to [^{3}H]-mannitol was significantly increased above control (3.5 fold) at a glyphosate concentration of 20 mg/ml.

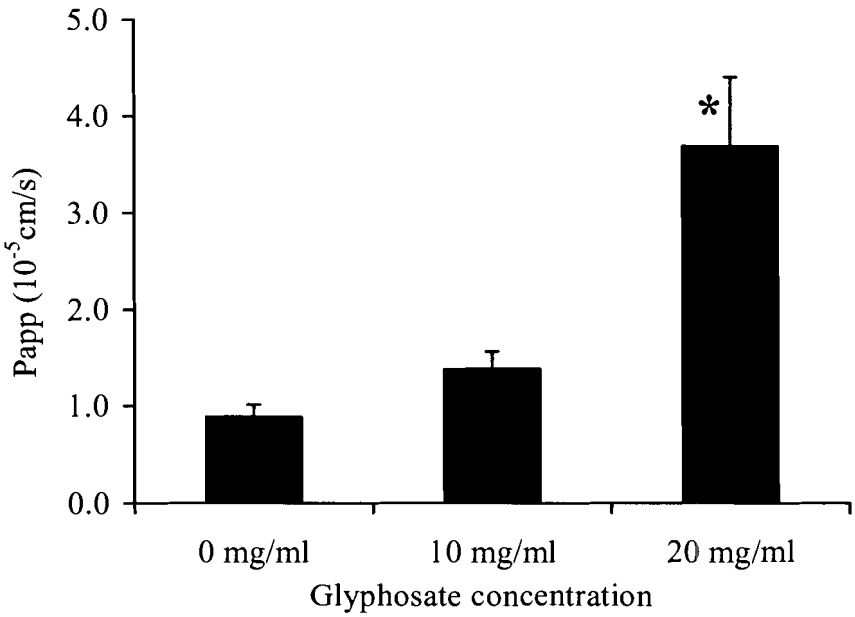

Figure 2-2. Effect of glyphosate on the apparent permeability of Caco-2 monolayers to [^{3}H]-mannitol.

Cells were exposed to glyphosate in HBSS at the concentrations noted for 4 hours at 37°C, then cells were washed with pre-warmed HBSS and [3H]-mannitol was added to the apical chamber to give a final concentration of 10^6 dpm per well. The basal media was sampled and [3H] mannitol measured using LSC. Results are representative of two independent experiments and expressed as the mean ± standard deviation. *An asterisk indicates that a value is significantly different from the value obtained with control (0 mg/ml), $P < 0.0001$.

2.4.3 Transport studies of [^{14}C]-glyphosate

Radiolabelled glyphosate (mixed with unlabelled compound to prepare the desired concentrations) was added to the apical ('lumenal') side of the Caco-2 monolayers and the (cumulative) amount of [^{14}C]-glyphosate in the basolateral ('blood stream') side was measured over time. Transport studies using Caco-2 cells showed that when exposed to 5 mg/ml of glyphosate more than 90% of [^{14}C]-glyphosate remained in the apical chamber, and less than 2% of the glyphosate was found in the basal chamber. The lack of transport was consistent with the previous TEER and [^{3}H]-mannitol transport results that showed that 5 mg/ml did not increase paracellular permeability (data not shown). In contrast, the transepithelial transport of glyphosate increased at 10 and 20

mg/ml glyphosate (Fig.2-3A). After exposure to the highest glyphosate concentration (20 mg/ml) for 5 hours, approximately 8% of the initial radioactivity moved across the monolayer into the basal chamber; a 4-fold higher transport than observed with 5 mg/ml (Fig.2-3A). Significant increases in [^{14}C]-glyphosate transport as a result of exposure to 10 or 20 mg/ml of non-radioactive glyphosate occurred 3 hours after exposure.

The baseline rate of glyphosate transport across IEC-18 cell monolayers was much higher than across Caco-2 cells, and it was also concentration-dependent (Fig.2-3B). This was not unexpected because of the higher baseline permeability of this cell line. At the lowest concentration, 5 mg/ml, transport of glyphosate across monolayers was 15 fold higher in IEC-18 than Caco-2 cells, which might indicate a toxic effect of glyphosate at lower concentrations. However, the difference in transport between IEC-18 and Caco-2 cells was less pronounced at higher concentrations of glyphosate (only 5-6 times greater with 10 and 20 mg/ml). After the first 2 hours of incubation with the highest glyphosate concentration we found an increased permeability to the radiolabeled glyphosate. Forty percent of the initial [^{14}C]-glyphosate dose was found in the basal chamber of IEC-18 cells after exposure to the highest concentration of glyphosate (20 mg/ml). In the presence of this concentration of glyphosate, damage to the IEC-18 cells was so extensive that the monolayers lifted from their filters in 4 hours (data not shown). A lag phase of approximately 3 hours found for transport of glyphosate across Caco-2 monolayers was not observed for IEC-18 cells.

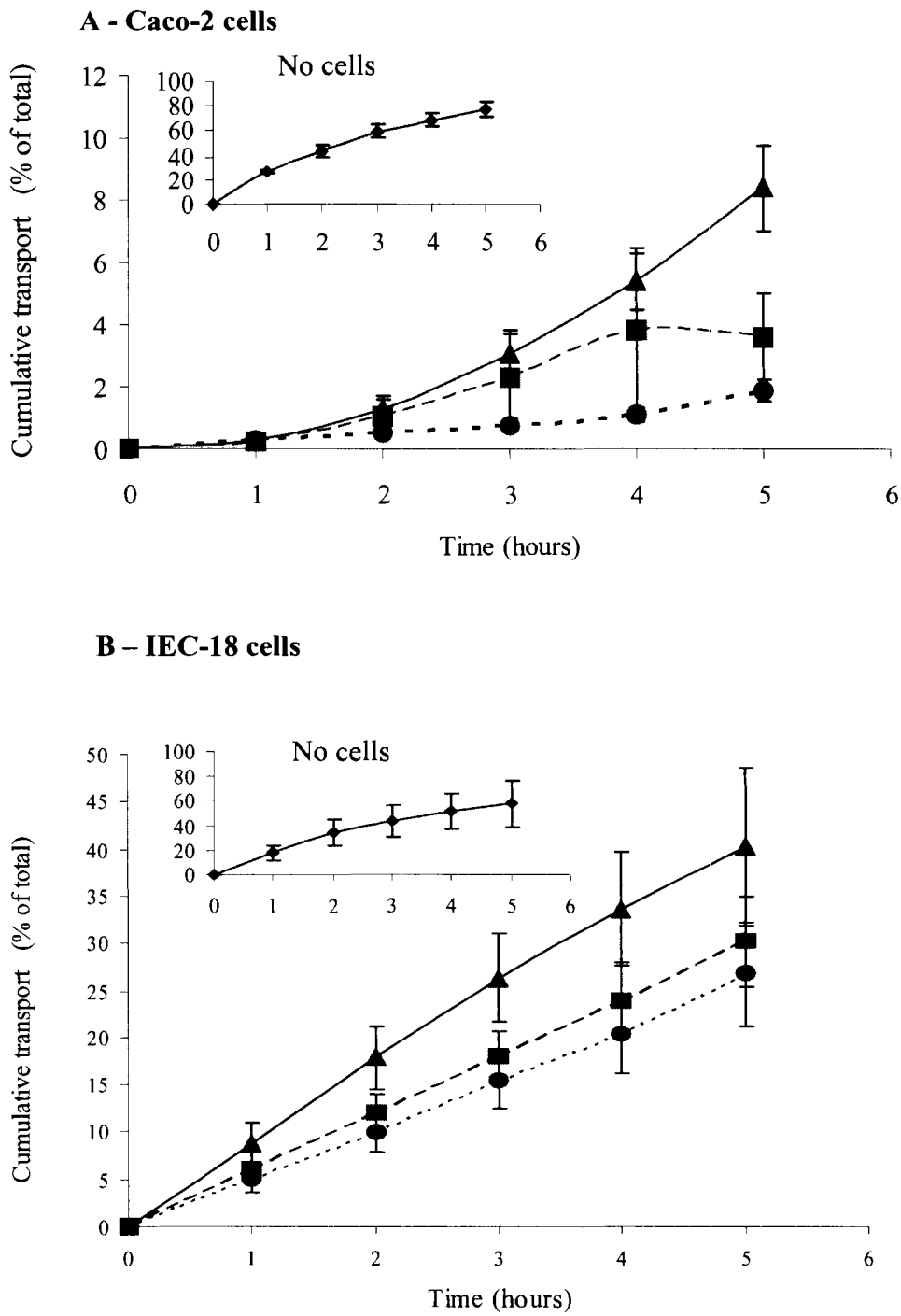

Figure 2-3. Cumulative transport of glyphosate across Caco-2 (A) and IEC-18 (B) monolayers.

[^{14}C]-glyphosate (3×10^5 dpm/well) was added to the apical compartment at t=0 at a concentration of 5 mg/ml (●), 10 mg/ml (■) and 20 mg/ml (▲) and the appearance of [^{14}C]-glyphosate at the basolateral compartment was measured by LSC. The data are mean ± standard deviation from three independent experiments.

At the end of the transport studies, the PET filters with epithelial monolayers were gently washed and cut out to measure the amount of sorbed radiolabelled glyphosate. Less the 1% of the [^{14}C]-glyphosate was sorbed to the Caco-2 epithelial cells at all concentrations (Table 1). A dose-dependent increase in binding was observed up to 5 mg/ml above which no further increases in binding occurred, suggesting that the number of binding sites was limited, i.e. binding was saturable. IEC-18 cells bound ~10-fold less [^{14}C]-glyphosate (~0.05%) than Caco-2 cells. As with Caco-2 cells, binding did not increase with increasing doses above 5 mg/ml though lower doses were not tested with this cell line.

Table 2-1. [^{14}C]-glyphosate binding to Caco-2 and IEC-18 cells after 4 hours of exposure.

The values represent the mean ± standard deviation of three independent experiments. [a] The percentage of initial radioactivity added to the cells. ND, not determined.

Glyphosate concentration (mg/ml)	*Caco-2 cells (%)*[a]	*IEC-18 cells (%)*[a]
1.75×10^{-3}	0.09±0.07	ND
1.75×10^{-2}	0.16±0.03	ND
0.7	0.16±0.10	ND
5	0.41±0.28	0.04±0.01
10	0.33±0.15	0.04±0.01
20	0.48±0.30	0.05±0.03

2.4.4 Effect of glyphosate on cell viability

The effect of glyphosate on epithelial cell integrity was determined by the LDH release. LDH content of the apical chamber was determined after 4 hours of pre-incubation of Caco-2 monolayers with different amounts of glyphosate. A statistically significant increase in LDH leakage was observed only with the two highest glyphosate

concentrations, 15 and 20 mg/ml (Fig.2-4). In contrast, the IEC-18 cells exposed to 5 and 10 mg/ml of glyphosate for 4 hours did not show a significant increase in the LDH leakage (data not shown).

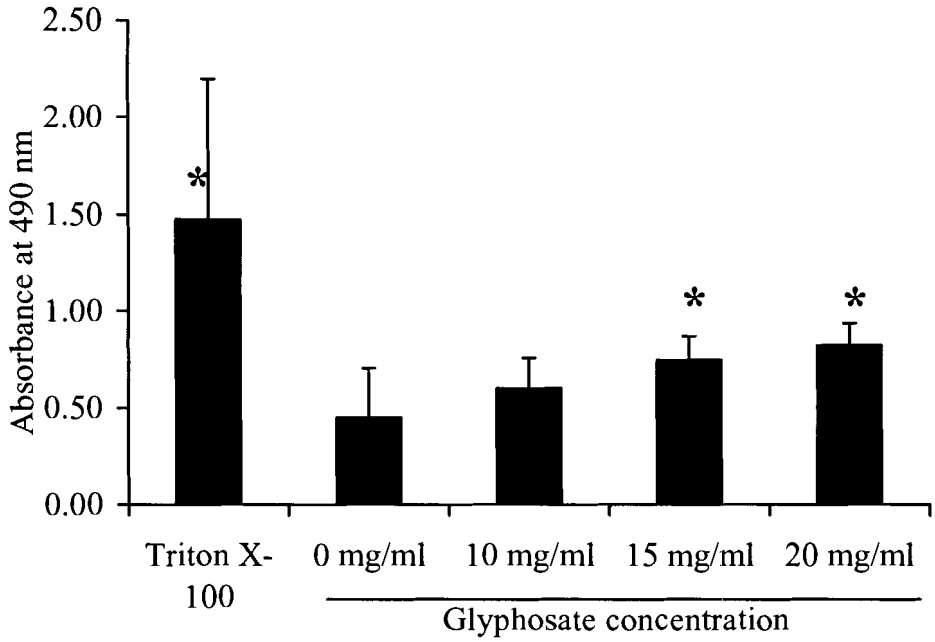

Figure 2-4. Cytotoxicity of glyphosate to Caco-2 cells, determined by LDH leakage.

The results are representative of four independent experiments and expressed as the mean ± standard deviation. 9% Triton X-100 was used as a positive control. *An asterisk indicates that the value is significantly different from the value obtained with control (0 mg/ml), $P < 0.01$.

2.4.5 Effect of glyphosate on F-actin arrangement in Caco-2 and IEC-18 epithelial cells

In fully differentiated gut epithelial cells, tight junctions establish cell polarity and regulate the movement of solutes across the epithelium. The tight junctions are connected to the actin cytoskeleton via tight junctional proteins, such as ZO-1, ZO-2 and ZO-3 [128]. Localization of F-actin fibers in untreated Caco-2 monolayers showed the expected punctate staining of actin microvilli bundles and a continuous belt-like pattern at all sites displaying cell-to-cell contact (Fig. 2-5A, arrows). After 4 hours of exposure to 10 mg/ml

of glyphosate, changes in the F-actin staining pattern occurred, as loss of some microvilli bundles became apparent (Fig.5B). Cell shapes were disrupted from the usual cobblestone pattern to disorganized whorls. This disruption was more severe after exposure to 20 mg/ml (Fig.2-5C, arrows). After 4 hours of exposure to 20 mg/ml of glyphosate, in addition to a loss of a definitive pattern, cell-cell junctions were diffuse and actin had polymerized in local areas.

When untreated IEC-18 monolayers were exposed to glyphosate and stained to visualize actin filaments, the cytoskeletal arrangement of actin filaments displayed the honey-comb arrangement typical for epithelial tight junctions and stress fibers, a less differentiated pattern compared to Caco-2 (Fig.2-5D). After exposure to 10 mg/ml of glyphosate, fibers were disorganized with more diffuse staining at cell-cell junctions (Fig.2-5E, arrows). Exposure to 20 mg/ml of glyphosate caused a complete loss of the distinctive staining of individual cells of the typical IEC-18 monolayers, as the F-actin fibers were severely clumped (Fig.2-5F).

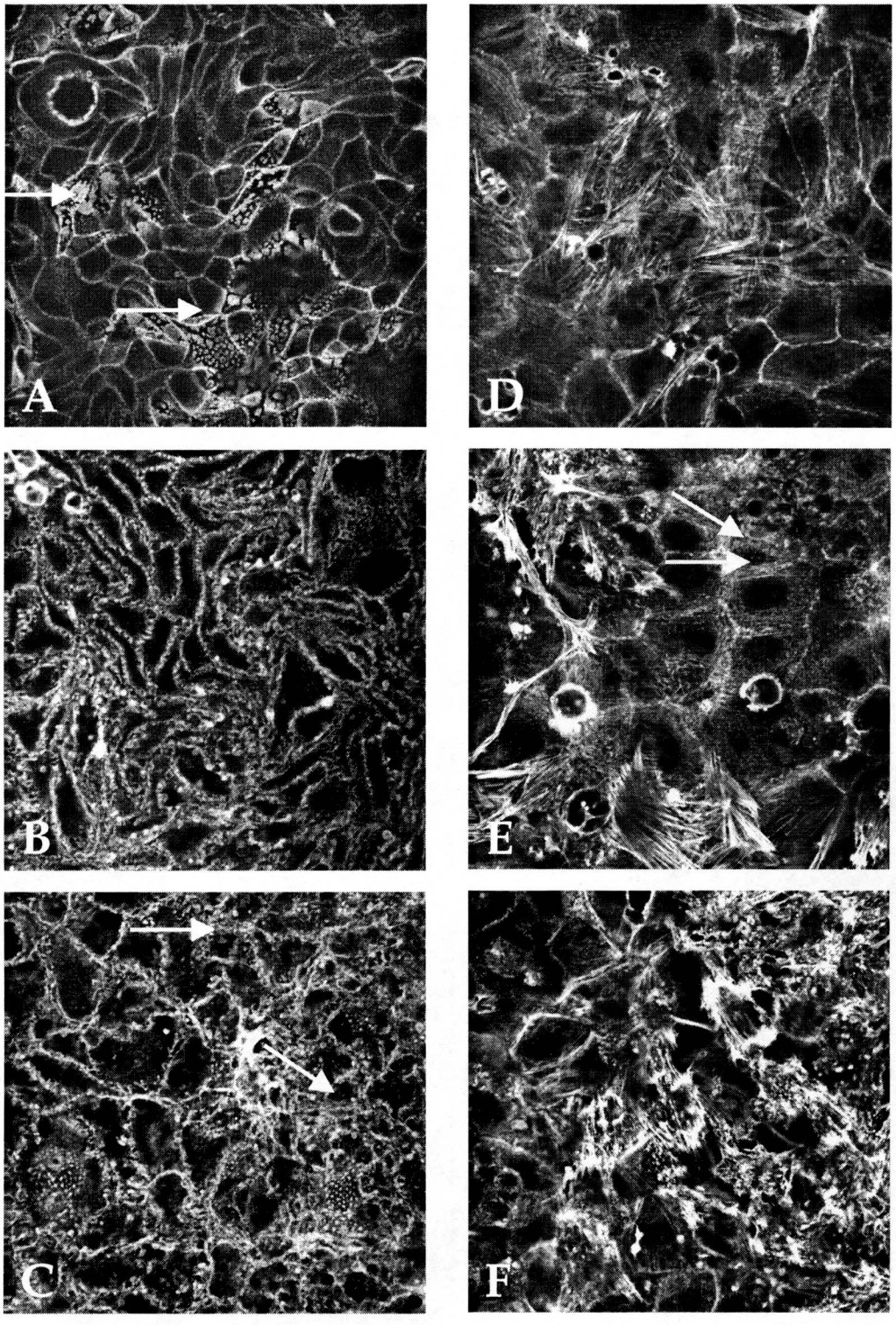

Figure 2-5. Localization of F-actin fibers of Caco-2 (A-C) and IEC-18 (D-F) cells.

The cells were grown on glass coverslips for three weeks and then exposed to various glyphosate concentrations: 0 mg/ml (A,D), 10 mg/ml (B,E) and 20 mg/ml (C,F) for 4 hours at 37°C. Following exposure, actin filaments were stained with rhodamine phalloidin and visualized using a confocal scanning microscope. The results are representative for two independent experiments. Original magnifications of the images were 630X (A) and 945X (B-F).

2.5 Discussion

Glyphosate is a widely used herbicide in agricultural and residential settings. It has been reported that glyphosate does not bioaccumulate in living cells due to its high water solubility and the absence of any active processes, which concentrate or conserve glyphosate [150]. However, many cases of acute toxicity with Roundup™, a commercial formulation of glyphosate have been reported [160, 161]. Acute human poisoning with Roundup™ produced gastrointestinal tract effects in 66% of the cases with levels of severity that depended on the volume of herbicide ingested [161]. Analyses showed that surfactants used in the formulation might be the main cause of toxicity, rather than glyphosate *per se* [162, 163]. However, no information is available on the absorption of technical-grade glyphosate into human intestinal epithelium. The fate of xenobiotics in the body is largely dependent on oral bioavailability, which, in turn, is mainly controlled by the passage of these chemicals across the intestinal epithelium. Several studies were conducted to investigate the fate of orally administered glyphosate in rats. A significant amount of radiolabeled glyphosate (~34%) was associated with small intestine tissue 2h after administration [154]. Thus, the possibility that glyphosate contributes to the gastrointestinal damage seen in cases of human poisoning by Roundup™ merits investigation.

In the present study, we characterized the effects of glyphosate exposure on the barrier function of intestinal epithelium. For this purpose, two polarized cell lines were employed; a human colonic cell line with enterocytic differentiation, (Caco-2), and a rat small intestinal crypt cell line (IEC-18). The apical membranes were exposed to glyphosate and the permeability of electrolytes (TEER), transport of [^{3}H]-mannitol, LDH release and F-actin arrangements were determined.

In this study, the effects of glyphosate on the epithelial barrier function were concentration- and time-dependent. The barrier function of the intestinal epithelium is due to highly regulated and organized tight junctions, which limit transport via the paracellular route. Thus, when tight junctions are perturbed by toxins, damage to the junctions alone may lead to the uncontrolled passage of xenobiotics into the blood

circulation. Determination of TEER was used as an indicator of this early, sub-lethal epithelial toxicity, as it signals even small changes in the structure of the tight junctions [117]. Measurements of the transepithelial flux of extracellular space markers such as mannitol have been utilized to determine the effect of toxic stimuli on the permeability of tight junctions [117]. Both increased transport of mannitol and decreased TEER values are generally considered to be indicators of increased paracellular permeability, although these parameters can also indicate loss of membrane integrity, rather than a specific effect on paracellular permeability. Treatment with glyphosate caused a rapid decrease in TEER and a concomitant increase in the permeability for mannitol in the Caco-2 cell line, indicating that paracellular permeability had increased. The finding that the increase in paracellular permeability was smaller for rat intestinal cells than for human colonic cells is supported by several studies [121, 159].

The human colon carcinoma cell line Caco-2 possesses several attributes that make it a suitable in vitro model system for the investigation of transport across the small intestinal epithelium. They are able to differentiate into mature enterocytes, as evidenced by the development of microvilli and the formation of tight junctions that separate the apical and basolateral domains, with the expression of lipids and proteins, including enzymes, specific for normal intestinal absorptive cells [164]. However, since the origin of Caco-2 is the colon, the differentiated Caco-2 cells may present a mixture of colonic and small intestinal characteristics [164, 165]. Furthermore, because of their tumor origin, Caco-2 cells may not represent a single cytotype, but may exhibit a mix of biochemical characteristics of normal small intestine, foetal colon, and normal colon [166]. The paracellular barrier presented by Caco-2 cells is much tighter than that of the small intestine and may result in underestimation of the bioavailability of transported compounds [164]. Furthermore, one needs to take into account that enterocytes such as Caco-2 cells are not responsible for the bulk of the intestinal mucous production in vivo, and the presence of mucous has been shown to inhibit the absorption of some chemicals [164]. The paracellular permeability in IEC-18 cells may be more comparable to that of the small intestine than the permeability in the Caco-2 cells [121, 159]. However, IEC-18 cells in culture do not form functional tight junctions, nor develop fully polarized columnar morphology, do not express significant levels of the small intestine enzymes

[117, 158] and have low carrier-mediated transport activities [164]. In this study, we found a 5-fold higher transepithelial passage of mannitol across IEC-18 compared to Caco-2 cells. Duizer et al., 1997 [167] found that the paracellular permeability of hydrophilic molecules across IEC-18 cells correlated with the intestinal permeability in vivo. However, the relative insensitivity of IEC-18 cells to small changes caused by toxic chemicals, measurable by TEER or [^{3}H]-mannitol transport, makes them less suitable for the transport studies in vitro.

In one study, the in vivo data from rats showed that greater than 34% of administrated glyphosate was transiently associated with the small intestine tissue at 2 hours after administration [154]. However, only 7.7% of radioactivity was found to be associated with small intestine tissue in the NTP study (3 h post-administration) [155]. In our study with Caco-2 monolayers, approximately 0.5% of applied glyphosate bound to cells with a surface area 0.9 cm^2, the equivalent of ~4 × 10^{11} sites per cell. Assuming that rat IEC-18 cells had the same cell density at confluency, the density of binding sites on IEC-18 cells were found to be ~10-fold lower. Snipes [168] estimated that the ground surface area of the flattened entire rat small intestine was on average ~113 cm^2, without taking into account the enlargement due to folds, crypts, mounds, plicae and villi. Assuming that binding sites are evenly distributed along the length of the small intestine, we calculate that approximately 6% of the dose applied to IEC-18 cells, would have bound to a rat small intestine. At present, the identity of the 'binding' sites is unknown. It was suggested by Brewster et al. [154] that the phosphoric moiety of the glyphosate reversibly binds to calcium ions in the bone matrix thereby slowing down elimination of glyphosate from this tissue. Sprankle et al. [151] showed that this type of binding occurred with glyphosate in soils. Calcium ion is critical for the maintenance of tight junctional integrity: removal of calcium ions is known to cause an increase in paracellular permeability associated with the loss of tight junctional strands [169]. It is possible that glyphosate prevents the entry of calcium and junction formation/maintenance in intestinal cells, leading to increase in paracellular permeability through the tight junctions.

To assess whether the increase in permeability was the result of membrane damage, rather than changes in paracellular permeability, we performed LDH assays. In previous studies, this assay has been shown to be very sensitive to the effects of

xenobiotics on intestinal epithelial cells [121, 156]. In the present study, leakage of the 140-kDa enzyme LDH through the apical membrane was only detected at glyphosate concentrations 1.5 times higher than those which decreased TEER values. For example, at 10 mg/ml glyphosate, significant declines in TEER were observed, but no significant increase in transport of mannitol or LDH leakage occured, suggesting that increased electrolyte permeability (indicated by TEER) is an early event in the response of Caco-2 cells to glyphosate. However, at 20 mg/ml of glyphosate or with Triton X-100, significant changes in TEER, mannitol permeability and LDH leakage were detected, indicating that both paracellular and transcellular transport were enhanced at this concentration.

There is considerable evidence that paracellular permeability is influenced by the status of actin filaments associated with the tight junctions [128]. Numerous second messenger molecules involved in signaling pathways, which are known to affect the assembly/disassembly of actin at the tight junctions also affects permeability [170, 171]. A few studies have shown that bacterial [172] or marine [173] toxins cause the loss of tight junctional integrity in Caco-2 monolayers leading to a decrease in TEER, increase in permeability to [^{3}H]-mannitol and depolymerization of the actin filaments. We hypothesized that the increased paracellular permeability caused by glyphosate would be accompanied by changes to the distribution of the actin cytoskeleton. Indeed, after exposure to 10 mg/ml glyphosate, Caco-2 cells displayed an abnormal actin staining pattern; microvilli bundles were lost and the definitive cobblestone pattern turned into disorganized whorls. At 20 mg/ml, we found even more severe damage in both Caco-2 and IEC-18 cells - a complete loss of the individual cell structure of the typical cell monolayers was apparent.

To eliminate the possibility that some of the observed changes were the result of increased osmolality [174] with the higher doses of glyphosate, we measured the osmotic pressure of the media used in our study. We found that 5 mg/ml of glyphosate exerted an osmolality of 350 mOsmol/kg; approximately the same osmolality as growth media (DMEM). An osmotic pressure of 460 mOsmol/kg was found for 15 mg/ml of glyphosate, a concentration at which significant damage occurred in Caco-2 monolayers. Parnaud et al. [175] have found that 10 mg/ml of polyethylene glycol (PEG) which exerts a comparable osmotic pressure (430 mOsmol/kg) did not affect the viability of Caco-2

cells after 5 days of exposure. These data suggest that the observed damage caused by 15 mg/ml of glyphosate was due to specific damage by glyphosate, rather than the hypertonicity of the treatment. At 20 mg/ml, the osmolality of the buffer increased by a further 20% at which point we cannot exclude the possibility that some proportion of membrane damage was caused by osmotic shock.

Our study showed that at low doses of glyphosate, the chemical was able to penetrate the epithelial barrier only to a small extent. However, at higher doses (10 mg/ml), reduction of TEER and increased permeability to mannitol had occurred, indicating that first signs of damage to epithelial cells are loss of paracellular barrier function at the tight junctions. This allowed glyphosate to cross the epithelial cells. The transitory association of glyphosate with intestinal tissue, which has been reported by several studies in rats, could be studied further in this system. Our study supports the validity of the Caco-2 in vitro system as a useful tool for modeling bioavailability of toxicants across human intestinal tissue and to predict the fate of the xenobiotics in the human body.

CHAPTER 3: MOBILIZATION OF CHRYSENE FROM SOIL IN A MODEL DIGESTIVE SYSTEM

In press with the same title in Environmental Toxicology and Chemistry (MS#05-345) From Environmental Toxicology and Chemistry, by Jaswinder K. Minhas*, Luba Vasiluk*, Linda J. Pinto, Frank A. P. C. Gobas and Margo M. Moore. **Joint first-authorship. Reprinted by permission of Alliance Communications Group, a division of Allen Press, Inc

Jas Minhas conducted soil experiments measuring partitioning of chrysene under full gastrointestinal digestion and measured the effects of ageing and altering the composition of GIF. Luba Vasiluk conducted the experiments comparing the fugacity capacity of EVA and Caco-2 cells, and conducted analyses of all the data. Frank Gobas provided valuable theoretical discussion and careful reading of the manuscript.

3.1 Summary

Accurate estimates of the oral bioavailability of hydrophobic contaminants bound to solid matrices are challenging to obtain because of sorption to organic matter. The purpose of this research was to measure the bioavailability of [^{14}C]-chrysene sorbed to soil using an in vitro model of gastrointestinal digestion and absorption to a surrogate intestinal membrane, ethylene vinyl acetate thin film (EVA). [^{14}C]-chrysene moved rapidly from soil into the aqueous compartment and reached steady state within 2 h. Equilibrium was reached in the EVA film within 32 h. Ageing the spiked soil for six or twelve months had no effect on chrysene mobilization. This was supported by the finding that the data best fit a one-compartment model. Despite significant decreases in [^{14}C]-chrysene mobilization when water or non-neutralized gastrointestinal fluids were used in place of the complete medium, the equilibrium concentration of [^{14}C]-chrysene in EVA remained the same in all conditions. Thus, the driving force for uptake was the fugacity gradient between the aqueous phase and the EVA. Cultured human enterocytes (Caco-2 cells) had a higher lipid-normalized fugacity capacity than EVA but the elimination rate

constants were the same suggesting that the rate was controlled by the resistance of the unstirred aqueous layer at the membrane:water interface.

3.2 Introduction

An important aspect of risk assessment is the determination of contaminant exposure. In human health risk assessment, ingestion of soil is considered an important route of exposure to many soil-borne contaminants in children due to their hand to mouth behaviour [176, 177]. Between 50 and 200 mg soil per day is ingested by children [178]. Besides unintentional ingestion of soil, some children with pica behaviour (profound soil ingestion) have been observed to ingest up to 25 to 60 g of soil during a single day [178].

At present, the concentration of contaminant that is chemically extractable from the soil is considered the exposure concentration [7]. Standard methods of contaminant analysis are not intended to quantify the bioavailable fraction yet the total amount of contaminant extracted during chemical extraction of bulk sediments or soils is often much greater than the amount of contaminant that can be absorbed from the soil by an organism [179]. Several studies [9, 32, 180] suggest that oral bioavailability of contaminants from soil can be significantly lower than that from matrices such as water or food. Therefore, these differences in bioavailability of contaminants ingested from different matrices can lead to significant errors in risk estimation.

In higher animals, >90% of nutrient absorption occurs in the small intestine. Absorption of soil particles in the gastrointestinal tract is thought to be negligible [181] and, in many cases, the particle-sorbed fraction of contaminant is considered to be unavailable for absorption. However, intestinal secretions and digestive enzymes could mobilize a proportion of the sorbed fraction during digestion and this mobilized fraction could ultimately be absorbed.

The gold standard used to determine bioavailability of persistent or bioaccumulative and 'inherently toxic' chemicals is a mammalian oral dose test, however, animal testing is expensive and may be considered unethical if applied to large numbers of chemicals. Therefore, rapid screening methods are required to select the chemicals with the greatest potential for absorption during oral exposure.

A number of in vitro procedures have been proposed to assess the bioavailability of organic compounds bound to soils. Methods include solid-phase extraction with C18

membranes [182, 183] or Tenax beads [184], organic solvent extraction using tetrahydrofuran [182] or alcohols [7], high temperature desorption [185], equilibrium partitioning [186], and matrix solid-phase microextraction fibers [187]. Artificial lipophilic materials (lipid containing semi-permeable membrane device or solvent filled dialysis membrane) to estimate bioaccumulation and bioavailability of hydrophobic organic contaminants (HOC) in natural waters have also been studied [29].

Wilcockson and Gobas [188] developed a thin film solid phase extraction technique with which they investigated the bioavailable fraction of semi-volatile and poorly volatile organic chemicals in air, biota, sediments, and soils. They used ethylene vinyl acetate (EVA) thin films, which exhibited quick absorption kinetics, resulting in chemical equilibria between the medium of interest and the solid phase after short application times.

In addition to the chemical assays, physiologically-based techniques have been investigated. Rotard et al. [189] proposed an in vitro digestion model using synthetically-prepared digestive juices. Unlike previous models, this model covered the entire route from mouth to small intestine. Minekus et al. [190] studied pharmaceuticals bound to food matrices using a model in which the fraction of test compound that diffused through hollow fibre membranes was defined as the "bioaccessible" fraction mobilized from soil during digestion.

The ultimate goal of this work is to develop a relatively rapid in vitro screening assay to determine the *relative* oral bioavailability of hydrophobic organic compounds (HOCs). The model should include exposure to simulated digestive fluids as well as to a sorptive epithelium or surrogate epithelial surface. This will yield a method by which the bioavailability of contaminant(s) from different matrices may be compared to a 'standard' (e.g., benzo[a]pyrene bound to a model soil). Values that exceed a pre-determined threshold may be further examined in vivo. The model HOC chosen for our study was chrysene, a four-ring polycyclic aromatic hydrocarbon (PAH) with log K_{ow} of 5.8. Chrysene occurs ubiquitously in environment in approximately the same concentration range as benzo[a]pyrene [36].

Two models of the gastrointestinal epithelium were employed in this study: EVA thin films [188, 191], and cultured Caco-2 epithelial cells. Caco-2 is a cell line derived from a human colorectal adenocarcinoma, which has become an established in vitro tool for studies related to intestinal cell function and differentiation. Caco-2 cells differentiate into an epithelial barrier with morphological and biochemical similarity to the mature intestinal columnar epithelial cells such as enterocytes [164]. Caco-2 cells have been widely used to study trans-epithelial transport and cytotoxicity of different nutrients and pharmaceuticals and more recently, of xenobiotics [122]. We compared the uptake of chrysene into EVA and Caco-2 cells.

The purpose of the present work was to establish which factors significantly affected the desorption of chrysene in a model digestive system. The specific aims of this project were to measure the mobilization of chrysene from soil particles, and determine its partitioning among different compartments of a model digestive system; to determine the effects of ageing chrysene onto soil on its partitioning into various compartments; to determine whether altering the composition of the gastrointestinal digestive fluids affected the mobilization of chrysene from soil; to compare the cultured human enterocyte cell line, Caco-2, with ethylene vinyl acetate (EVA) as a model sorptive surface.

Theory

Simple hydrophobic organic chemicals, including chrysene and other PAHs are absorbed from the gastrointestinal tract (GIT) as a result of simple passive diffusion where a difference in chemical potential or fugacity (in units of Pa) in the lumen of the intestinal tract (f_L) and the organism (f_{BVA}) is the driving force for net chemical transport N (in mol/day) from the medium with the higher chemical potential or fugacity to the medium with the lower chemical potential or fugacity:

$$N = D \times (f_L - f_{BVA}) \quad (1)$$

where D is the transport parameter (mol/Pa×d) for chemical diffusion between the lumen of the intestinal tract and the organism. Fugacity can be viewed as the escaping

tendency of a chemical from a medium and relates to chemical concentration C (mol/m^3) via the fugacity capacity Z (mol/m^3×Pa):

$$C = f \times Z \quad (2)$$

The net flux of diffusive transfer only corresponds to a difference in concentrations C, rather than fugacities, if the media involved in diffusion are the same. In the intestinal tract, chemical diffusion occurs between chemically distinct media. In addition, media (such as ingested food and soils) undergo changes in chemical composition during digestion, which can have large effects on the fugacity of the chemical and their rate of absorption [139, 145, 192, 193]. It is therefore important that the magnitude of absorption of hydrophobic organic contaminants from the GIT is viewed in terms of fugacities, rather than concentrations.

To measure the change in fugacity that hydrophobic organic substances undergo through digestion, we developed a thin-film extraction method following methods described in Wilcockson and Gobas [188]. This method relies on a chemical substance achieving a chemical equilibrium between the chemical concentration in a digestive medium (e.g. soil), and that in the film within a relatively short period of time. At equilibrium, the chemical fugacities in the gastrointestinal fluid (f_{GIF}) and the film (f_{EVA}) are the same, i.e. $f_{GIF} = f_{EVA}$. The fugacity of the chemical can then be determined when the concentration measured in the film (C_{EVA}), as $f_{EVA} = C_{EVA}/Z_{EVA}$, if Z_{EVA} is known. Z_{EVA} can be determined by a film-gas equilibration method discussed in Wilcockson and Gobas [188, 191]. However, in cases where changes in fugacity are of interest, it is not necessary to carry out this measurement, as differences in concentrations of the chemical in the film are directly proportional to differences in fugacity because the fugacity capacity of the film is constant throughout an experiment.

In this study, the partitioning behaviour of chrysene was expressed in terms of its chemical activity (fugacity) rather than its concentration. The purpose of this research was to determine the changes in the bioaccessible and bioavailable concentrations of chrysene in a model digestive system that employed either cultured human epithelial cells (Caco-2) or ethylene vinyl acetate (EVA) film as a surrogate epithelium.

3.3 Materials and methods

3.3.1 Experimental design

For these studies, we developed an in vitro model to measure the fugacity of soil-bound chrysene during digestion and absorption into model epithelia. The chrysene concentration of the soil used in our experiments was based on the concentrations found at contaminated sites [87]. The composition of digestive fluids, temperature, and transit times were based on human physiology and a surrogate sorptive surface in the form of a thin film of ethylene vinyl acetate (EVA) [188, 191] was employed. Care was taken to avoid the use of any other polymers in the experimental design.

Briefly, 100 mg aliquots of [^{14}C]-chrysene-spiked soil were introduced into 20-ml borosilicate scintillation vials, previously coated with a thin film of EVA. Ten ml of preheated (37°) gastric fluid was added to each and the vials were tightly capped. Vials were rotated horizontally on a rotator (Hybaid, Middlesex, UK) at 6 rpm and 37°C, which allowed thorough mixing of the contents and contact with the entire EVA-coated surface. After 1 h, 85 mg solid $NaHCO_3$ was added and 1.5 h after the start of the experiment, 1 ml intestinal secretions were added to each vial. Thus the soil-to-fluid ratio was 1:100 for the first 1.5 h and 1:110 subsequently. A soil-to-fluid ratio in the range of 1:100 to 1:5000 (w/v) was assumed to cover all physiological conditions in vivo [194]. For each time point, three vials were removed from the experiment, and the soil, fluids and EVA portions were analysed for [^{14}C]-chrysene. A schematic of this experimental set-up is shown in Figure 3-1A.

We also compared the uptake of [^{14}C]-chrysene dissolved in phosphate buffered saline (PBS) by Caco-2 cells and by EVA thin films. In these experiments, either Caco-2 cells grown on coverslips, or EVA-coated glass coverslips were placed into 2 ml glass beakers with PBS and the contents were mixed using an orbital shaker at 70 rpm (Fig. 3-1B).

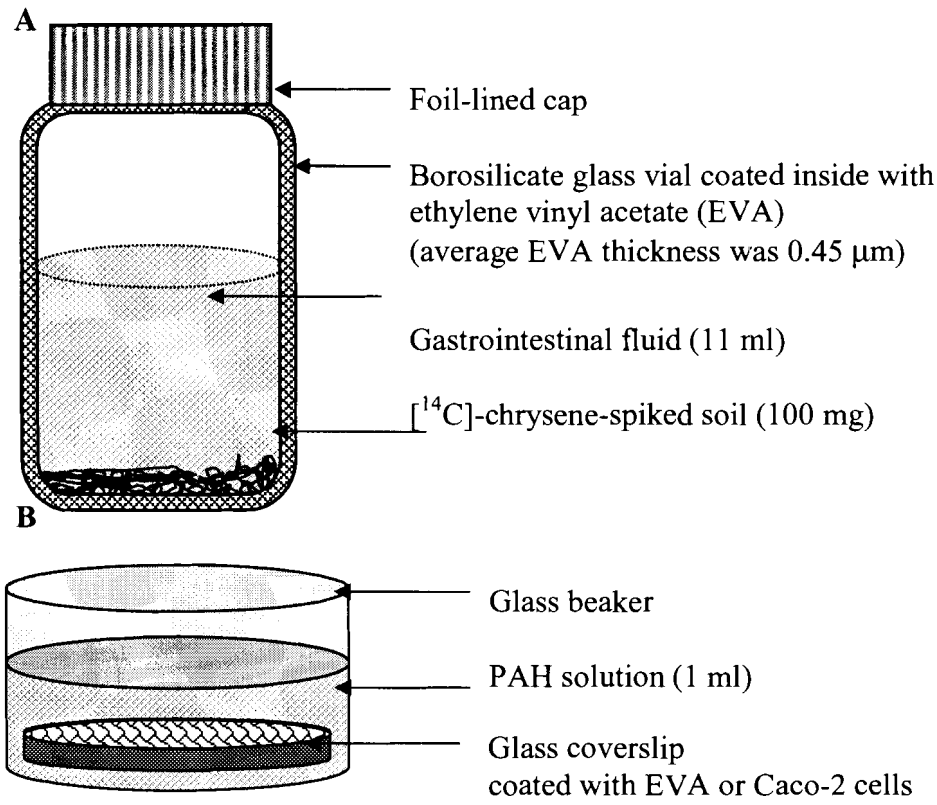

Figure 3-1. Gastro-intestinal digestion model.

A. Cell-free gastro-intestinal model: An ethylene vinyl acetate (EVA) coating was used to mimic the intestinal epithelium in our model. The concentration of [^{14}C] chrysene that partitioned into this coating was considered to be the bioavailable fraction.

B. Model for comparing [^{14}C]-chrysene uptake by EVA or Caco-2 cells. Glass coverslips were coated with EVA solution or Caco-2 cells. EVA coating was performed as outlined in the Materials and Methods. Cells were seeded at a density of 1-2×10^{5}cells/ml on glass coverslips and grown for 24 d. Coverslips with cells were fixed with 4% paraformaldehyde and washed with PBS prior to treatment with [^{14}C]-chrysene in PBS-Tween. For both EVA and Caco-2 cells triplicate samples were removed at specific times, rinsed with PBS and counted in a scintillation counter.

3.3.2 Model Soil

Subsoil was collected between five and twenty cm depth from Burnaby Mountain, BC. The oven-dried soil was fractionated in a mechanical shaker and the 125-250 μm soil fraction was used for this study. This fraction was chosen because it is more likely to adhere to the skin and be transferred by the hand-to-mouth activity of children [177]. The organic content of the soil was determined by loss on ignition to be 15.2% and the pH in water was 3.8.

3.3.3 [^{14}C]-chrysene

[5,6,11,12-^{14}C]-chrysene was obtained from Chemsyn Science Laboratories (Lenexa, Kansas, USA) (specific activity of 46.8 mCi/mmol) under the auspices of the NCI chemical carcinogen repository. The chemical was re-purified on silica gel to 98% purity before use. To prepare [^{14}C]-chrysene-spiked soil, 100 mg of dry soil was weighed into 20 ml borosilicate scintillation vials and 40 μl aliquots of toluene containing approximately 100,000 dpm of [^{14}C]-chrysene and 2 μg total chrysene were pipetted into each vial. The toluene was allowed to evaporate at ambient temperature. After spiking, the soils were kept in closed containers at room temperature for a minimum of 7 d prior to use. In some experiments, [^{14}C]-chrysene was aged onto soil for six months or one year.

3.3.4 Thin film preparation

In this study, EVA thin films were used as a surrogate for intestinal epithelium. Only freely-diffusible, unbound chemical enters the EVA film. Thus, chrysene that was mobilized from the soil into the digestive fluid and absorbed by the EVA film was considered to be the bioavailable fraction. The EVA thin film was prepared from pelleted Elvax 40W (gift of Dupont, Wilmington, DE, USA) which contained 40% VA and had a density of 0.965 g/ml.

To prepare the thin film, pre-cleaned 20 ml glass scintillation vials were rinsed with dichloromethane (DCM) and 250 μl of 0.6% (w/v) EVA in dichloromethane and 5

µl of 2% dichlorodimethylsilane (Aldrich Chemical, Milwaukee, WI, USA) in hexane was added to each vial. The silane prevented the EVA from detaching from the vial during the course of the experiment but had no measurable effect on the sorptive properties of the EVA (data not shown). The vials were then manually rolled until all of the solvent had evaporated leaving a thin film over the entire inner surface of the vial. The coated surface area of the vial was calculated to be 3412.5 mm^2 with an average thickness of 0.45 µm.

3.3.5 Model gastrointestinal fluids

The composition of synthetic gastric and intestinal fluids was based on in vitro digestion models designed by [32, 195] and modified to contain the following: synthetic gastric fluid (1 L) was prepared by dissolving 0.5 g sodium citrate (Analar, BDH, Toronto, Canada), 0.5 g malic acid, 420 µl lactic acid syrup (both from Sigma-Aldrich, St. Louis, MO, USA.) and 500 µl glacial acetic acid in deionized water. The solution was adjusted to pH 2.5 with 0.18M hydrochloric acid. Pepsin (Sigma-Aldrich, St. Louis, MO, USA) (12 mg/100 ml) was added just prior to use.

Transition from the stomach to the small intestine was mimicked by neutralizing the pH of the solution to pH 7 with 85 mg of sodium bicarbonate ($NaHCO_3$) per 10 ml gastric fluid. Once neutralized, one ml of freshly-prepared synthetic intestinal secretion was added which contained per ml: 4.0 mg bile salts (Sigma-Aldrich, St. Louis, MO, USA), 0.3 mg pancreatin (EM Science, Darmstadt, Germany), 10 mM calcium dichloride, and 0.04M Tris buffer, pH 7 (Caledon Laboratories Ltd. Ont. Canada).

Experiments were conducted to determine whether altering the gastrointestinal fluid composition affected chrysene partitioning. The procedures used were the same as described in previous sections except that one or more of the gastrointestinal constituents was withheld or replaced in each experiment.

3.3.6 Measurement of [^{14}C] in the soil, aqueous and EVA compartments

The protocol for measuring [^{14}C]-chrysene in the aqueous, EVA and cell compartments is summarized in Figure 3-2. Briefly, the contents of triplicate vials were

filtered through a 15 ml x 25 mm diameter glass vacuum filtration system (Millipore, Bedford, MA, USA) using 3.1 μm and 0.7 μm pore size glass microfiber filters (Ahlstrom, PA, USA) to obtain the aqueous filtrate. EVA-coated vials were rinsed with deionized water to remove any adherent soil particles. Light microscopy showed that no particles remained after washing. Biodegradable Counting Scintillant (BCS) (Amersham Canada, Oakville, ON) was added to the aqueous samples and these were counted in a Beckman LS 6500 multi-purpose liquid scintillation counter with automatic quench correction (Beckman Coulter, Fullerton, CA, USA). Subsequently, 10 ml of BCS cocktail was added to the rinsed EVA-coated vials, which were agitated to extract the [^{14}C] bound to EVA into the cocktail. The soil-bound portion of the chrysene was determined by subtraction as attempts to release the chrysene by solvent extraction or by high temperature oxidation and trapping of [^{14}C]-CO_2 were found to be unreliable.

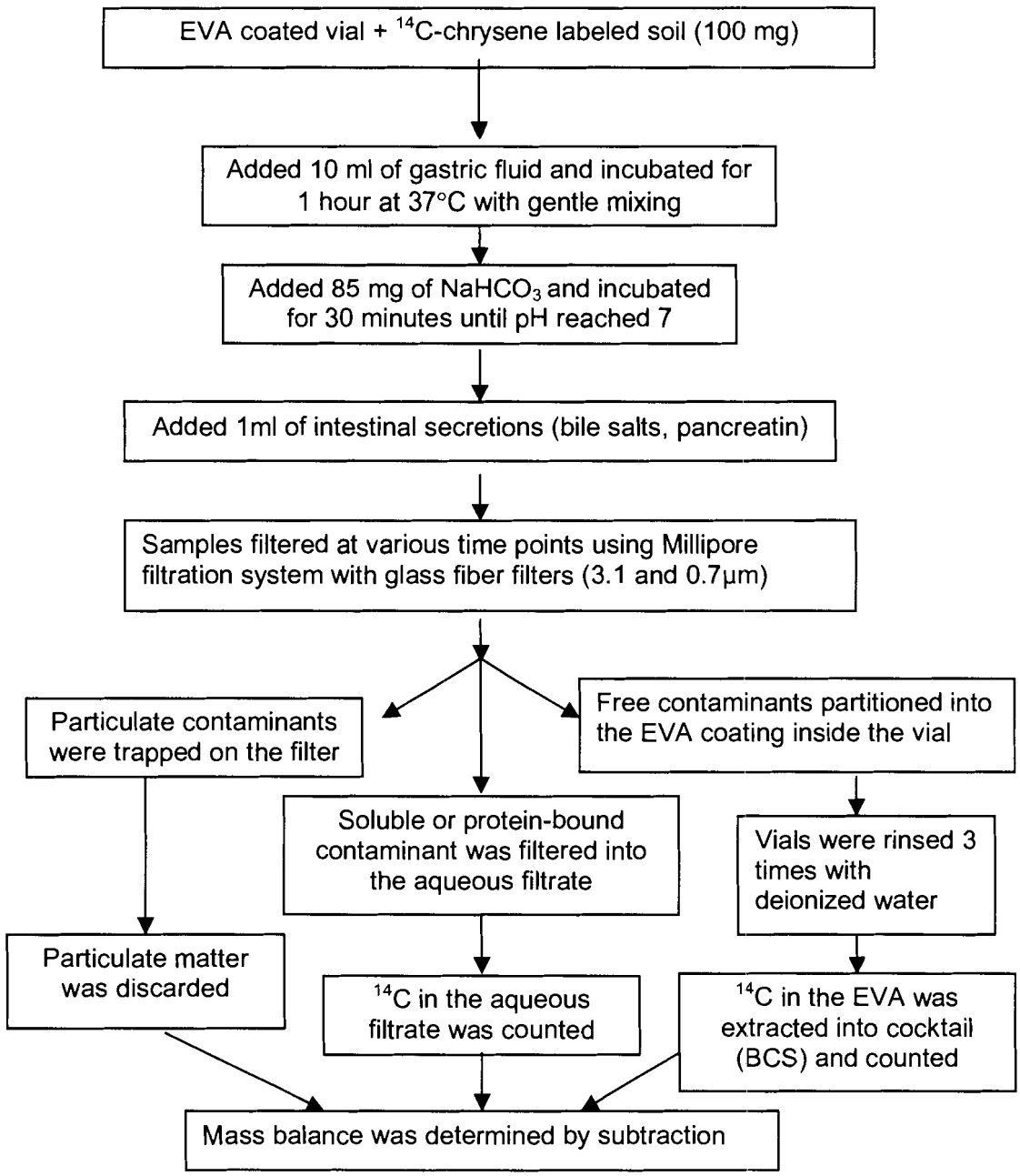

Figure 3-2. Schematic of the experimental procedure employed in this study.

3.3.7 Soil to Fluid Ratio

The soil-to-fluid ratio was 0.1g spiked soil: 10 ml gastric fluid (1:100) for the first 1.5 h and 0.1g soil : 11 ml intestinal fluid (1:110) subsequently. A soil-to-fluid ratio in the range of 1:100 to 1:5000 (g:ml) was assumed to cover all physiological conditions in vivo [194].

3.3.8 Comparing the relative sorptive abilities of EVA and Caco-2 cell monolayers

The EVA film was used as a model of the gastrointestinal epithelium to predict uptake in vivo. We also compared the fugacity capacity of the EVA film with a cultured human colon carcinoma cell line, Caco-2. Experiments with EVA and Caco-2 cells were conducted in triplicate using the experimental design shown in figure 1B and each experiment was repeated three times.

EVA: Glass coverslips (12 mm diameter, Fisher Scientific, Ottawa, ON) were rinsed with 40µl of DCM and then coated on one side with 40 µl of EVA solution (0.6% EVA and 0.04% silane). Custom-made borosilicate 2 ml beakers were placed in 12-well tissue culture plates (Becton Dickinson, Franklin Lakes, NJ, USA). A [^{14}C]-chrysene solution in 100% ethanol was added to PBS containing 0.05% Tween 20 to give ~100,000 dpm/ml and 1 ml of this solution was added to each of the beakers. Addition of Tween 20 reduced the time to achieve equilibrium (data not shown). The EVA-coated coverslips were added to the beakers and agitated on an orbital shaker at 70 rpm at 37°C. At specific time intervals, triplicate samples were removed. EVA coated coverslips were rinsed in PBS, extracted into BCS and [^{14}C] bound to EVA was determined by liquid scintillation counting.

Caco-2 Cells: The human colon carcinoma cell line Caco-2 was obtained from the American Type Culture Collection (Rockville, MD, USA). Cells were maintained in Dulbecco's Modified Eagle's Medium (Gibco BRL, Burlington, ON) with high glucose (4.5 g/l) supplemented with 10% bovine growth serum (HyClone, Logan, UT, USA), 1% non-essential amino acids, penicillin (25 IU/ml) and streptomycin (100 µg/ml) at 37°C in an atmosphere of 5% CO_2 and 90% relative humidity. Cells were used between passages

40-50. For absorption/partitioning experiments, cells (1-2 x 10^5 cells/well) were seeded on glass cover slips in a 24-well plate, and used between 21 and 26 d after seeding. Proteins in the cells were cross-linked by incubation with 4% (w/v) paraformaldehyde in PBS, pH 7.4 for 30 min, at room temperature. This prevented the monolayer from lifting during the experiment. Caco-2 cells were washed twice with PBS and covered with PBS until use.

Coverslips with Caco-2 cells were placed in the dishes containing the PBS-chrysene solution and incubated at 37°C at 70 rpm on an orbital shaker. At specific time intervals, triplicate coverslips were removed, rinsed gently using PBS, extracted in BCS and [^{14}C] bound to cells was counted in the scintillation counter.

3.3.9 Determination of the volume of lipid in Caco-2 cells

Caco-2 cells were seeded into 3-5 plastic tissue culture flasks with an area of 75 cm^2 each, grown to confluence (i.e., flask surface 100% covered by cell monolayer) and removed using 0.25% trypsin in 1mM EDTA. The combined cell pellet was washed once with PBS and then transferred to microcentrifuge tubes that had been oven-dried to a constant weight. The tubes were centrifuged to pellet the cells, which were then lyophilized and weighed. The lipid content of the dry cells was determined using a modification of the method of Bligh and Dyer [196]. Briefly, the pellet was resuspended in 200 µl PBS. Methanol and chloroform (2:1, v/v) were added, the tube was vortexed and allowed to extract for 2-3 h with periodic vortexing. The mixture was centrifuged and the supernatant was transferred to a 15-ml tube. The pellet was extracted twice more and the supernatants were pooled. PBS and chloroform were added to the combined extracts and the mixture was vortexed and centrifuged. The chloroform layer was transferred to an oven-dried glass vial and the aqueous phase was extracted twice more. The combined chloroform layers were dried under nitrogen at 40°C and the vial was reweighed. Phospholipids constitute about two thirds of the lipid in a non-adipose cell, and have a density of 1.0. The remaining one third is mostly triglycerides, which have a density (in humans) of 0.95 (Dr. R. Cornell, Simon Fraser University, Burnaby, BC, Canada, personal communication). Thus, we were able to calculate the percent lipid as mg

lipid/mg dry cells x 100, and to use the total weight of the extracted lipid to determine the volume of lipids in our experiments by assuming that 1 mg lipid = 1 μl of lipid.

3.3.10 Data handling and statistical analysis

All experiments were performed in triplicate and the results shown represent the mean ± one standard deviation of two to three independent experiments. The mobilized fraction of chrysene (i.e., the fraction desorbed into the aqueous phase - equivalent to the bioaccessible fraction) was calculated as follows:

$$\text{Mobilized Fraction (\%)} = \frac{\text{amount of } [^{14}\text{C}]\text{-chrysene in the gastrointestinal fluid}}{\text{amount of } [^{14}\text{C}]\text{-chrysene present in soil before digestion}} \times 100 \quad (3)$$

Fugacity calculations were performed as noted above. The raw data (sampling times and concentrations) were fitted using a one-compartment model assuming first-order kinetics.

$$C = A\,(1 - \exp^{-kt}) \quad (4)$$

where C is the concentration in the thin film (mol/m^3) at time t (in hours), k is the rate constant (h^{-1}) for uptake into EVA or Caco-2, and A is the concentration of chrysene in the EVA or Caco-2 cells at equilibrium. The one compartment model was fitted to the chrysene concentration in the EVA film using a nonlinear regression technique with software designed to minimize the sum of squared residuals (Systat 8.0, SPSS Inc., Chicago, IL, USA, 1998).

The data were analyzed by one-way analysis of variance (ANOVA) test, followed by Tukey's multiple comparison procedure using JMP version 5.0.1 (SAS Institute Inc., Cary, North Carolina, USA). For each comparison, significant differences were identified when $p \leq 0.05$.

3.4 Results and Discussion

3.4.1 Partitioning of chrysene into various compartments of the model digestive system

The objective of this research was to develop a method to measure the potential of soil-bound hydrophobic contaminants to desorb into the gastrointestinal fluids and/or into the intestinal epithelium. In vivo, the fraction of the ingested dose that reaches the systemic circulation is often considered to be the bioavailable fraction. In the present study, the contaminant that partitioned into the gastrointestinal fluid was the mobilized fraction, and because only the freely-available chemical can be absorbed, the concentration in the EVA was considered to be a measure of the bioavailable amount.

At the start of the experiment, a substantial amount of chrysene was assumed to have partitioned to the soil. After addition of soil to the gastric fluid, the [^{14}C]-chrysene moved from the soil matrix into the gastric fluid (Figure 3-3A), and within two hours, reached a steady state. The concentration of chrysene in the EVA film increased rapidly during the first eight hours and then reached a constant value after 32 h. A maximum of 4% of chrysene partitioned into gastrointestinal fluids whereas ~50% partitioned into the EVA film (C_{EVA}). Because losses to glass were negligible, and no [^{14}C]-chrysene was detected in the headspace gas (data not shown), the balance (~50%) of the [^{14}C]-chrysene remained in the soil.

The data from Figure 3-3A were recalculated to show the relative amount of [^{14}C]-chrysene in each compartment, normalized per cubic meter of soil, aqueous phase or EVA (Figure 3-3B).

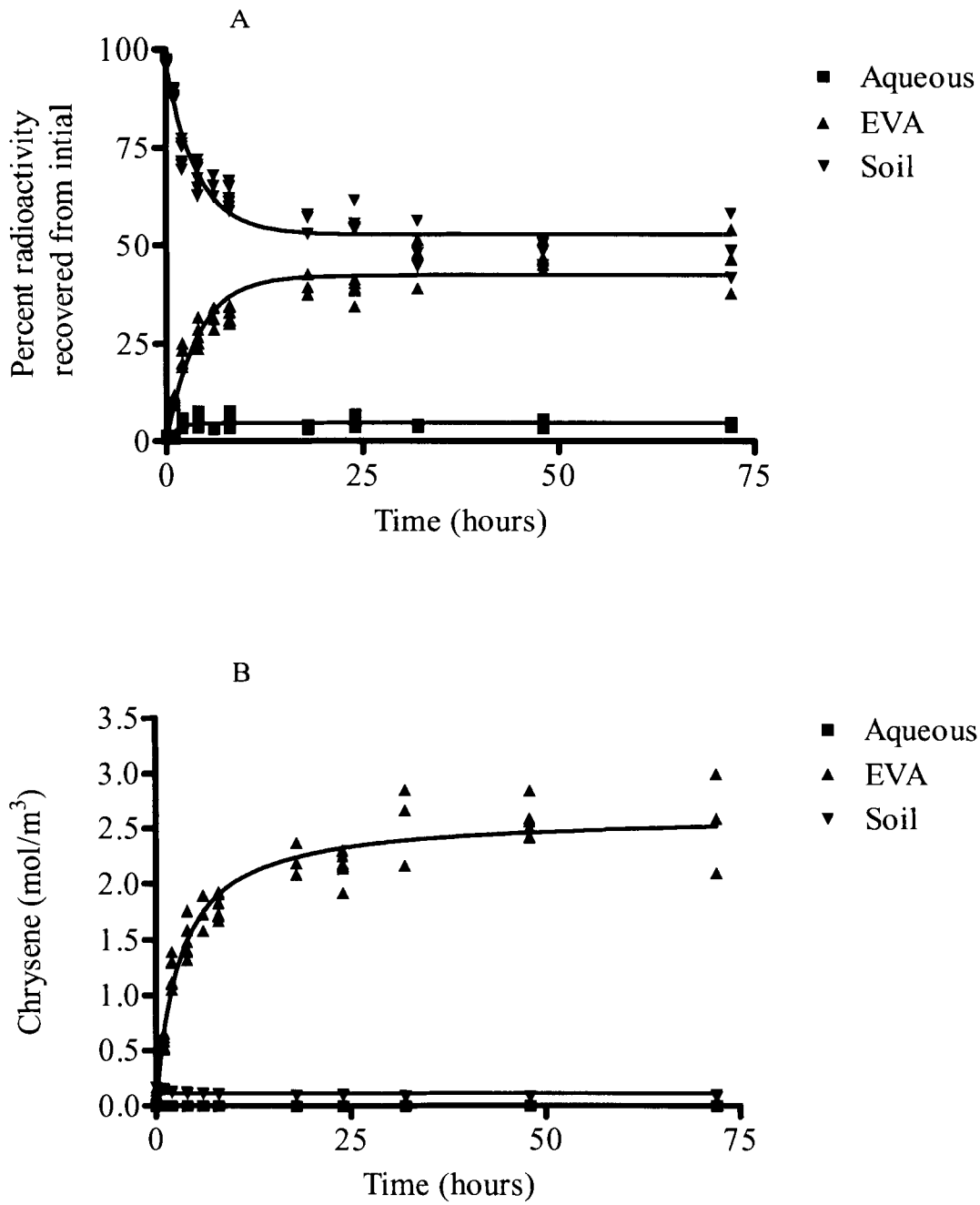

Figure 3-3. Partitioning of [^{14}C]-chrysene from soil into the aqueous and EVA compartments.

A. Partitioning of [^{14}C]-chrysene from soil into the aqueous (AQ) and EVA compartments of the in vitro digestive model when incubated for 48 h at 37°C. The data shown for of three independent experiments with triplicates within each.

B. The partitioning data from the experiment shown in Figure 3A was recalculated in units of mol chrysene per m^3 of each compartment versus time.

Chrysene moved rapidly from the digestive fluid into the EVA film as fugacity was high in the aqueous phase. As the experiment progressed, the aqueous compartment rapidly became saturated (Figures 3-3A and 3-3B).

At equilibrium, there was no net movement of chemical between the EVA and the gastric fluid, therefore, by definition, the fugacity of chrysene in EVA and gastric fluids were equal. Because the equilibrium concentration in EVA is approximately 7-fold higher than that in soil (organic matter), and approximately 10^5-fold higher than the aqueous phase (AQ) (gastrointestinal fluids), the relative fugacity capacities of chrysene in EVA, soil organic matter and gastrointestinal fluid are $Z_{EVA}:Z_{Soil}:Z_{AQ} = 7:1:10^{-5}$ (Table 3-1).

In the use of solid phase microextractions, it is recommended that extraction be non-depletive [187]. Because the goal of our research is to develop an accurate in vitro model of digestion, we were constrained in the amount of soil we could add to the vials to maintain a physiological soil: fluids ratio. In our model digestive system, a significant proportion (50%) of the soil-bound chrysene was mobilized and eventually taken up into EVA. This implies that the chrysene concentration in the EVA film does not reflect the absolute value of fugacity of the soil-bound chrysene in our physiologically-based model. To measure the absolute fugacity in the soil matrix using EVA films, it will be necessary to increase the soil to EVA mass ratio in the digestive systems. Nevertheless, the absolute fugacities are of secondary importance. Because our system achieved equilibrium, we are confident that the relative chrysene uptake values are valid.

Table 3-1. Comparison of concentration (C) of chrysene in the ethylene vinyl acetate (EVA), aqueous and soil compartments of the model digestive system, and the elimination (desorption) rate constant of chrysene from EVA.

Chrysene was spiked onto soil for a minimum of 7 days (non-aged) or aged for 6 or 12 months. The concentration at the plateau is expressed per volume of soil organic matter[a]. Values for k_2 represent the mean ± SE of triplicate samples.

Ageing	*Compartment*	*Concentration at plateau (C_p) (mol/m^3)*	*Elimination rate constant (h^{-1}) (k_2) (R^2 value)*
Non-Aged			
(3 days)	EVA	2.65	0.25 ± 0.02 (0.92)
	Aqueous	2.95×10^{-5}	-
	Soil[b]	0.35	-
6 – Months			
	EVA	2.31	0.31 ± 0.09 (0.98)
	Aqueous	1.05×10^{-5}	-
	Soil	0.38	-
12 – Months			
	EVA	2.46	0.39 ± 0.2 (0.71)
	Aqueous	2.49×10^{-5}	-
	Soil	0.35	-

[a]The volume of soil organic matter was $1.20\times10^{-8} \pm 3.18\times^{-10}$ m^3/100 mg dry soil.

[b]The concentration of chrysene in the soil at equilibrium was determined by subtraction.

3.4.2 Effect of ageing chrysene onto soil on its partitioning to EVA during an in vitro digestion process

Soil-PAH contact time (often referred to as 'ageing') is an important factor affecting the extent of absorption of PAHs by soil organic matter. As organic compounds persist in soil, they become progressively less bioavailable, and therefore less toxic [9]. To determine whether ageing affected the mobilization of chrysene in our in vitro model, experiments were conducted with chrysene-contaminated soils that were aged for either six or twelve months.

When chrysene was aged onto soil for six months, the aqueous phase concentration of chrysene was lower than that of non-aged soil; however, a similar reduction was not observed with the soil aged for 12 months (Table 3-1). For both aged samples, there was no decrease in the amount of chrysene that was taken up into the EVA coating compared to control (non-aged) soils indicating that ageing had no effect on the apparent fugacity of chrysene in this soil.

The fugacity capacity of EVA (Z_{EVA}) was 6 to 7-fold higher than soil regardless of whether the soil was aged; Z_{soil} did not change with ageing; Z_{EVA} was approximately 10^5 fold higher than the Z_{AQ} in all three groups; non-aged soils, soils aged six or twelve months.

3.4.3 Kinetics of chrysene uptake

A one-compartment model was fitted to the [^{14}C]-chrysene concentrations in the EVA data shown in Figure 3-3B using nonlinear regression analysis (SPSS). A one-compartment model was deemed appropriate because the concentration of chrysene in the aqueous phase remained constant throughout the experiment. The EVA to aqueous phase rate constants (k_2) did not vary significantly among the treatments (Table 3-1). In a study by Reeves et al. [197], desorption experiments with Tenax beads and coal tar contaminated soils resulted in rate constants ranging from 0.5 to 0.89 h^{-1} for 13 different PAHs; chrysene had a desorption rate constant of 0.5 ± 0.2 h^{-1} from non-aged soil and 0.7 ± 0.3 h^{-1} from aged (270 d) soil.

It is believed that during ageing, molecules slowly move into sites within the soil matrix that are not readily accessible [30] although the chemical nature of the sites may be more important than the pore size. For example, tests with beads having a pore diameter of 2.5–15 nm showed that phenanthrene was quickly desorbed and rapidly metabolized by microorganisms if the pores did not have hydrophobic surfaces, but desorption was slow and biodegradability was enormously reduced if the pore surface was hydrophobic [91].

In our study with six and twelve month aged soils, no reduction was observed in the fugacity or apparent desorption rate of [^{14}C]-chrysene uptake by EVA film in aged soils (Table 3-1). A likely explanation is that no sequestration of chrysene occurred because of the absence of non-aqueous phase liquids in the pristine soil. This is supported by the finding that the data best fit a one-compartment model (R^2=0.92). Significant differences in the maximum extent of desorption have been observed for aged soil. Increased soil-PAH contact time reduced the magnitude of the rapidly-desorbing phase and the extent of biodegradation [5, 11, 185] with the sorption of HOCs to sites in the condensed region of soil organic matter controlling the slowly desorbing phase [5, 185, 198].

3.4.4 Effect of altering the composition of gastrointestinal fluids on the mobilization of [^{14}C]-chrysene into the aqueous phase

Experiments were conducted to determine the effect of different gastrointestinal constituents on partitioning of chrysene into the aqueous and EVA compartments after 48 h of incubation at 37°C. When soil was incubated in complete gastrointestinal medium (Fig. 3-4A, 'Complete'), $3.7\times10^{-5} \pm 0.7\times10^{-5}$ mol/m^3 of the chrysene was found in the aqueous compartment, and 2.8 ± 0.1 mol/m^3 in the EVA. Substitution of gastrointestinal fluids with water significantly reduced the concentration in the aqueous phase by approximately 3-fold. This is likely due to the fact that the gastrointestinal fluid contained organic molecules with a high affinity for chrysene. Despite the significant reduction in the chrysene concentration in water, the concentration in the EVA film (and hence the fugacity of chrysene) did not change significantly. This implies that gastrointestinal fluid

has little effect on the fugacity that chrysene exerts in the model digestive system. This can be expected since soil is a poorly digested substance.

Pepsin is one of the most important of the digestive enzymes; it hydrolyses peptide bonds in proteins and polypeptides with a low degree of specificity. However, we observed no significant change in mobilization when pepsin was eliminated from the in vitro digestion protocol (Fig. 3-4A, 'Gastric, no pepsin') suggesting that the organic matter in our soil was recalcitrant to pepsin degradation. This agrees with the finding of Weston and Mayer [199, 200] who observed a lack of correlation between enzyme activities in the digestive fluid and the extent of PAH mobilization.

We also found that proteins differed in their ability to increase the concentration of chrysene and the fugacity capacity in gastrointestinal fluid. For example, substituting bovine serum albumin for pepsin ('Pepsin sub BSA') increased the concentration of chrysene and the fugacity capacity of the aqueous phase, even though BSA was present at half the molar concentration (Fig. 3-4A). Thus, the extent of mobilization was greatly affected by the type of protein present along with the contaminant. Nevertheless, this substitution had no effect on the concentration of [^{14}C]-chrysene in EVA (Fig. 3-4B).

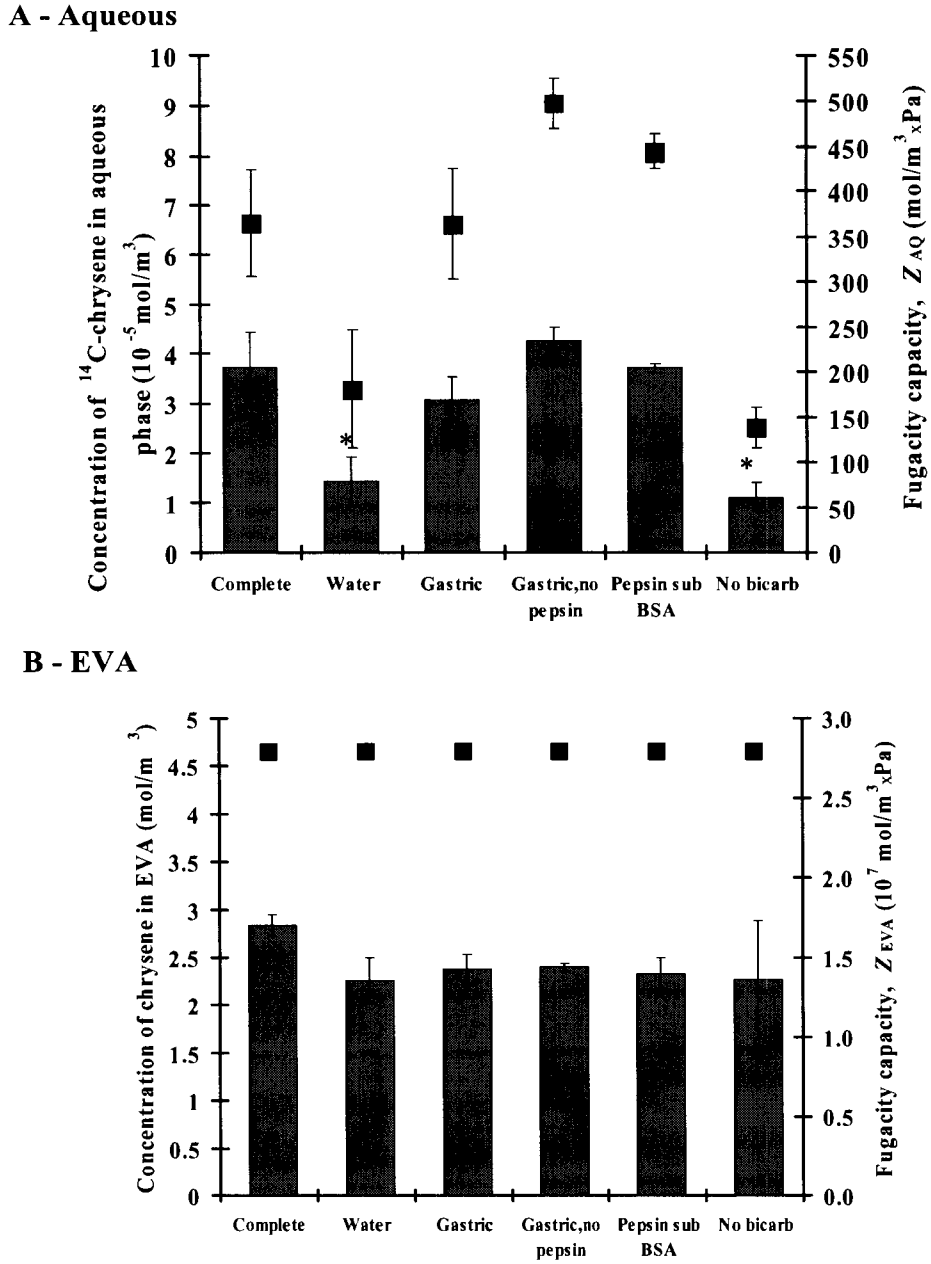

Figure 3-4. The effect of altering the composition of gastrointestinal fluids.

A. The effect of the composition of the gastrointestinal fluids on the aqueous concentration of [^{14}C]-chrysene (bars) and the fugacity capacity (Z_{aq}) (squares) in the aqueous phase. Different gastrointestinal compositions are defined as follows: 'Complete' (included all constituents); 'Water' (gastrointestinal fluids replaced by water); 'Gastric' (no intestinal secretion added); 'Gastric, no pepsin' (no pepsin nor intestinal secretions added); 'Pepsin, sub BSA' (complete gastrointestinal composition, but pepsin substituted BSA); 'No bicarb' (gastric fluid not neutralized by $NaHCO_3$ before intestinal secretion added). An asterisk indicates that the values are significantly different from the 'Complete'. **B**. The effect of the composition of the gastrointestinal fluids on the concentration of chrysene (bars) in EVA. The fugacity capacity (squares) of EVA (Z_{EVA}) for chrysene remains constant (2.8×10^7 mol/m^3×Pa).

Oomen et al. [97] suggested that bile salt micelles play a central role in mobilizing HOCs from a matrix. In their studies, 20-25% of total amount of HOCs (PCBs and Lindane) were sorbed to bile salt micelles [97]. In contrast, no change was observed in the mobilization of soil-bound chrysene when bile salts (or any of the other intestinal constituents, e.g. bile salts, pancreatin, $CaCl_2$) were absent from the digestive fluids ('Gastric'). The difference in our results may be attributed to the fact that the bile salt concentration employed in our digestive model was ~3-fold lower than that in Oomen's study. In addition, bile salts may have little effect on the soil matrix.

In our model, the increase in pH was the most important factor that mobilized PAH from soil (Fig. 3-4A). Substitution of Tris buffer for bicarbonate gave the same results as bicarbonate suggesting that it was the pH shift rather than another property of sodium bicarbonate that increased [^{14}C] chrysene concentration in the aqueous phase (data not shown).

Yang et al. [201] has also shown that desorption of soil-bound PAH compounds was pH dependent, with minimal release occurring at pH 2-3 and maximal release at pH 7-8 which is in agreement with the results from our study. Humic materials are considered precursors to mature geosorbents and have been shown to have a higher sorptive capacity for PAHs than bulk sediment or soil materials [202]. Geosorbents containing primarily humic type organic matter will allow faster and more complete desorption than those containing primarily kerogen-like organic matter, which is chemically reduced, physically condensed and relatively non-extractable [203]. The soil used in our study had an f_{oc} of 0.15, and, although it was not analyzed to determine the different types of organic matter, because it was near the surface, we predict that this soil has more humic and fulvic acids than humin, and does not have kerogen-like organic matter. The increase in PAH desorption with increasing pH in our study may be explained by pH-related changes in the humic structure as acidic groups become deprotonated and charged, thereby facilitating diffusion of PAH molecules through the organic matrix to the water interface. Fulvic and humic acids are protonated at lower pH and therefore would likely bind to chrysene by non-covalent interactions [204]. Engebretson et al. [204] also suggested that humic and fulvic materials dissolved in aqueous solution have a tendency to form micelle-like structures, with hydrophilic shells

facing the aqueous phase and hydrophobic cores in the centre of the aggregates. This self-organized structure acts to enhance the solubility of HOCs in such solutions by allowing them to penetrate the hydrophilic shells. At neutral pH, humic acids would be negatively charged which would decrease their affinity for chrysene as well as increase the water solubility of the humic acids. In support of this hypothesis, we observed that less colour developed in the digestive fluid when the pH was low (2.5) compared to the darker colour at higher pH (7) (data not shown). These data emphasize the importance of exposing the matrix to a complete in vitro digestion to estimate the fugacity changes that occur during digestion.

3.4.5 Effect of altering the composition of the gastrointestinal fluids on the uptake of [^{14}C]-chrysene into EVA

The extent of uptake of [^{14}C]-chrysene into the EVA film was measured in the same experiment shown in Fig. 3-4A. Despite significant decreases in the extent of mobilization when water or non-neutralized gastrointestinal fluids were used in place of complete medium (Fig. 3-4A), the amount of chrysene that partitioned into the EVA remained unchanged (Fig. 3-4B). Thus, measurements of mobilization alone would not have provided an accurate picture of the amount of [^{14}C]-chrysene sorbed to the surrogate membrane, i.e. the bioavailable fraction. In Fig. 4B, it is evident that the driving force for uptake is the fugacity gradient between the aqueous phase and the EVA. Because the Z_{EVA} is 4 orders of magnitude greater than Z_{AQ}, small differences in the Z_{AQ} caused by changes in gastrointestinal fluid composition had no significant effect on the uptake.

3.4.6 Comparing the fugacity capacity of EVA with the Caco-2 human cell line

Wilcockson and Gobas [188] suggested that there might be a useful relationship between the lipid-normalized concentration in biological tissue and the EVA film concentration. In our study, we determined the lipid content of Caco-2 cells and used the volume of lipid in these cells for fugacity calculations. However, the solubility of an HOC differs among various classes of lipids, and this may cause differences between lipid-normalized and thin film concentrations [188]. The entire lipid fraction of Caco-2

cells containing phospholipids, triglycerides and sterols was extracted and this fraction was used to determine lipid content.

We measured the partitioning of [^{14}C]-chrysene into Caco-2 cells and EVA (Figure 3-5) and the mean concentration at the plateau (C_p) for each compartment is presented in Table 3-2. Although equilibrium was reached by about 20 h, the extent of uptake by cells was significantly greater than EVA when the values were normalized to the volume of lipid present (Fig. 3-5 and Table 3-2): EVA accumulated approximately 10 times the amount of chrysene per m^3 when compared to whole Caco-2 cells; however, when the data were normalized to the lipid volume of the cells, the biological lipid bound 6-fold more chrysene per m^3 compared to EVA (Table 3-2). It was not possible to experimentally determine the fugacity capacity of the Caco-2 cells from this data; however, the results indicate that the apparent fugacity capacity of Caco-2 lipid was significantly higher than EVA.

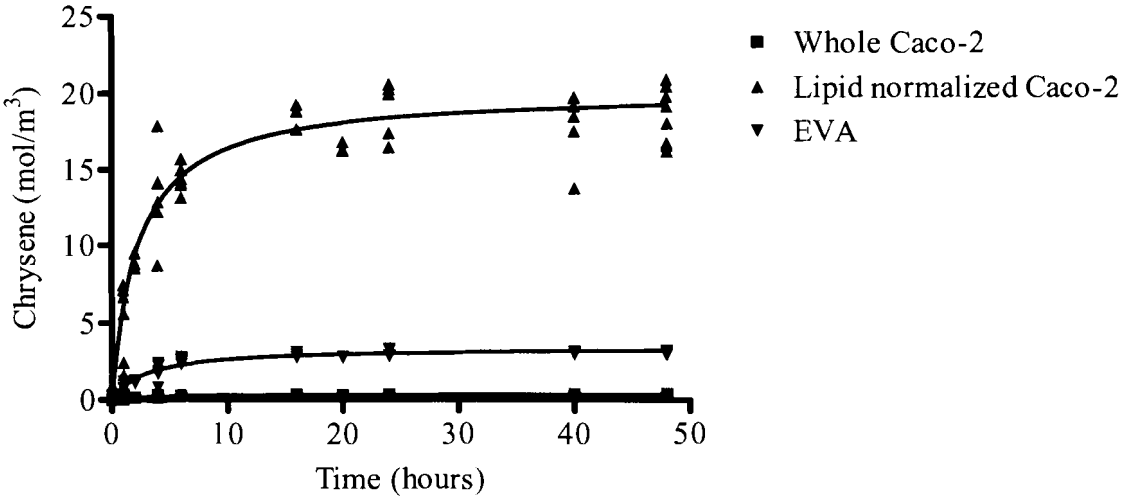

Figure 3-5. Uptake of [^{14}C]-chrysene from chrysene solution in PBS-Tween 20 to either EVA or Caco-2 monolayers.

For the Caco-2 cells, uptake was determined based on whole cells or normalized to the volume of lipid present in the Caco-2 cells.

Table 3-2. Comparison of the concentrations at plateau (C_p) and the elimination (desorption) rate constant, k_2, for [^{14}C]-chrysene uptake by ethylene vinyl acetate (EVA) or Caco-2 cells after incubation in phosphate buffered solution (PBS)-Tween for 6-44 hours at 37°C.

Values were calculated from the data shown in Figure 4. In the PBS/Tween experiments, cells or EVA were coated on coverslips. Rate constants for elimination of [^{14}C] chrysene from EVA or Caco-2 monolayers were derived from a one-compartment model. All values were calculated from triplicate experiments performed on three independent days and represent the mean ± Standard Deviation (C_p) or the mean ± Standard Error (k_2).

Compartment	*Concentration at the plateau (C_p) (mol/m^3)*	*Elimination rate constant (k_2) (h^{-1})*	R^2
EVA	3.10 ± 0.05	0.26 ± 0.02	0.93
Whole Caco-2 cells[a]	0.33 ± 0.01	0.31 ± 0.02	0.93
Caco-2 lipid[b]	18.45 ± 0.32	0.31 ± 0.02	0.93

[a]The volume of whole Caco-2 cells (2×10^{-9} m^3) was determined using the following parameters: coverslip surface area (1.13×10^{-4} m^2) × height of the Caco-2 cells (~17.7×10^{-6}m)

[b]The volume of lipid in Caco-2 cells was determined from 7 independent experiments as outlined in Materials and Methods. The mean value ± Standard Deviation was $3.7\times10^{-11} \pm 0.4\times10^{-11}$$m^3$.

Interestingly, when [^{14}C]-chrysene was incubated in a PBS-Tween solution, the rates of chrysene desorption from EVA or Caco-2 cells were not significantly different (Table 2). Furthermore, these rate constants were similar to the EVA desorption rate constant from soil experiments in which the aqueous phase was gastrointestinal fluid. Thus, the proportion of chrysene taken up per unit time was the same in the EVA and Caco-2 experiments. This suggests that the desorption rate was controlled by the resistance of the non-stirred aqueous layer at the membrane:water interface.

Summary statement

The physiologically-based extraction technique combined with the artificial intestinal membrane used in this study provides a potentially valuable approach for refining the input data used for formal risk assessment at sites subject to natural or anthropogenic soil contamination.

CHAPTER 4: MEASURING IN VITRO BIOAVAILABILITY OF BENZO[A]PYRENE FROM PRISTINE SOIL AND CONTAMINATED SEDIMENT

Manuscript in preparation with the same title as Luba Vasiluk, Linda J. Pinto, Zahra A. Walji, Wing Shan Tsang, Frank A. P. C. Gobas, Curtis Eickhoff and Margo M. Moore

Linda Pinto and Zahra Walji conducted the EVA studies with low organic matter soil. Wing Shan Tsang maintained tissue culture line Caco-2 cells required for the project. Luba Vasiluk conducted the remainder of the work with the assistance of Linda Pinto. Frank Gobas and Curtis Eickhoff provided valuable discussion and careful reading of the manuscript.

4.1 Introduction

Approximately 23,000 chemicals are awaiting categorization by the Canadian government for which there is little data on oral bioavailability in humans beyond the hydrophobic partitioning coefficient (octanol-water partition coefficient, log K_{ow}) [3]. This measurement is an excellent starting point for predicting the bioavailability of hydrophobic organic chemicals (HOCs) because these chemicals partion into tissues to a much greater extent than more polar compounds. The general rule is that the higher the log K_{ow} of a chemical, the more it will partition into tissue [30]. However, these bioavailability assessments do not take into consideration metabolic processes. Nor do they account for the strong binding of high log K_{ow} compounds to soil/sediment matrices [9], which can reduce their oral bioavailability.

Environmental toxicologists define "bioavailability" as the ability of a chemical to cross a cell membrane and enter a cell [30]. Currently, the bioavailability of sorbed contaminants is determined as the amount extracted by organic solvents. However, the total amount of contaminant extracted often is much greater than the amount of contaminant that is actually bioaccumulated [11, 30, 32]. It has been shown repeatedly

that many hydrophobic soil contaminants are less than 100% bioavailable, and that bioavailability further decreases over time [5, 197].

Normally, as the time of contact between a contaminant and the soil increases, there is a decrease in chemical and biological availability, a process called "ageing" [90]. The mechanism of ageing has been much investigated [30], particularly with polycyclic aromatic hydrocarbons (PAH). As a result, it is known that interactions between soil and PAH are affected by the soil organic matter, both in amount [90] and nature [89]; by inorganic components with particular reference to pore size and structure [91] and by microbial populations and the amount of contamination [35].

Furthermore, contaminant bioavailability is dependent on physicochemical properties of the soil/sediment matrix and therefore the bioavailability of the same contaminant from different matrices is expected to vary widely. In particular, the fraction of organic matter has been shown to significantly affect bioavailability. Chung and Alexander [205] reported that the degree of phenanthrene and atrazine sequestration during 200 days of incubation of 16 test soils had a very high correlation with organic carbon content. These measurements were based on both mild solvent extractions and microbial mineralization. However, the authors noted that organic matter may not have been the only soil property that was important; they found that minute pores or voids (nanoporosity of the soil) may also play an important role in sequestration of these organic chemicals. Soil organic matter is a highly heterogenous solid, with an abundance of such nanopores [5].

The main mechanisms of reduced chemical bioavailability during ageing are considered to be sorption and diffusion. In general, the sorption of organic contaminants to soil exhibits bimodal kinetics [5]. The first phase, in which a portion of the contaminant is sorbed rapidly via hydrogen bonds and van der Waal's forces [93] takes place over minutes to a few hours. The remaining fraction is sorbed more slowly, over weeks or months [5]. During this stage, the contaminant may create covalent bonds with organic matter, which results in stable incorporation into the soil [93]. Based on differences in sorption strength several authors have proposed two models to explain the process of ageing in soils. The first model described two phases of soil organic matter: a

glassy (solid fraction) and a rubbery (soft fraction) domain analogous to those found in synthetic polymers (reviewed in [5, 203]). While the sorption to a glassy organic matter fraction is irreversible, strong and slow, the sorption to the soft fraction of organic matter is weak, fast and reversible [5]. The second model is the sorption-retarded pore diffusion model wherein it is proposed that the rate-limiting process is molecular diffusion in pore water that is retarded by rapid-reversible local sorption on pore walls, which may or may not contain organic matter [30]. According to this model, the rates are dependent on the radii of soil particles, on the tortuosity of pores (bending and twisting interconnectivity, presence of dead-end pores) and on the constrictivity (steric interference) in the pores [5].

Ingestion of contaminated soil is the major route of exposure to many hydrophobic organic contaminants. The potential for exposure to contaminants via this source is greater for children because they are likely to ingest more soil than adults as a result of inadvertent soil ingestion among children through the mouthing of objects or hands [96]. For purposes of estimating risk to children, the US EPA assumes that most children ingest relatively small quantities of soil (e.g., <100 mg/day), while the upper 95th percentile is estimated to ingest 200 mg/day on average [95, 206]. For that reason, oral bioavailability values for ingested soil contaminants are critical for an accurate assessment of human health risk. Absorption of soil particles in the gastrointestinal tract of higher animals is thought to be negligible [181] and, in many cases, the sorbed fraction of contaminant is considered to be unavailable for absorption. Thus, a molecule must be desorbed to become bioavailable. Desorption may depend upon the release of a surfactant, emulsifier, or other endogenous molecules or by physical contact with hydrophobic constituents on the surface of an organism or tissue. It has been proposed that intestinal secretions and digestive enzymes could mobilize a proportion of the sorbed fraction during digestion and this mobilized fraction could ultimately be absorbed by the tissue [122, 141, 203].

Animal testing has been a gold standard in determining the bioavailability of environmental pollutants, however; it is expensive and unethical for large-scale screening. Thus, in vitro methods are urgently needed to screen compounds for their potential bioavailability. An in vitro method would also be useful in estimating the relative bioavailability of contaminants from a variety of matrices. Several reports have

focused on the development of in vitro methods designed to mimic gastrointestinal digestion as a means of estimating relative bioavailability. These models, based on human physiology are generally cheaper, faster, and more reproducible than animal tests. These tests simulate stomach and small intestinal digestions [32, 148]. The models used by various investigators differ in composition of synthetic digestive fluids, the duration of the elution procedure, the concentration of the contaminants or contaminated material, as well as the methodology applied for the separation of the mobilized fractions. These in vitro models have been successfully used for some time in the evaluation of the bioavailability of polar compounds such as pharmaceuticals and metals. Ruby et al [12] evaluated the relative bioavailability of lead in a weanling rat model and demonstrated that the stomach phase of the in vitro test correlated with the bioavailability values from the in vivo model. However, similar success with hydrophobic compounds has not yet been achieved and at present, these are few reports that evaluate the in vitro bioavailability of HOCs. Most digestive models are static gastrointestinal models which simulate mouth, gastric, and small intestinal conditions.

Some researchers have measured intestinal transport through cultured human enterocytes (Caco-2). Using a Caco-2 cell monolayer, Oomen et al. [122] showed that up to 54% of polychlorinated biphenyls (PCBs) were mobilized from spiked artificial standard soil after in vitro gastro-intestinal digestion, but <10% of these organic contaminants were transported across the Caco-2 monolayers to the basolateral compartment. Most of the PCBs were accumulated by the Caco-2 cells. A more recent study showed that Caco-2 may form a biochemical barrier for benzo[a]pyrene through extensive metabolism and subsequent luminally-directed active transport of polar metabolites [207]. However, these investigators did not include a digestion protocol in their experiments. Furthermore, the Caco-2 cells were exposed to contaminated buffers or medium. Hydrophobic compounds such as PAHs or PCBs are very poorly soluble in the aqueous phase; they tend to precipitate in the aqueous solution. Thus, investigating the oral bioavailability of these compounds may require binding to a solid matrix, such as food, soil, or sediment. Dynamic gastrointestinal models mimic the conditions during transit of ingested compounds through the digestive tract including exposure to cultured intestinal enterocytes.

The aim of the present study was to measure the mobilization of benzo[a]pyrene (BaP) from soil into gastrointestinal fluid, and sorption to epithelial cells or their surrogate (relative bioavailability). BaP, a 5-ring PAH (log K_{ow} of 6.04), is a pro-carcinogen of great concern as it is widely dispersed in the environment [36]. BaP is a very persistent chemical, and is therefore suitable for use in matrix ageing experiments.

Two models of the gastrointestinal epithelium were employed in the study: the EVA model proposed by Wilcockson and Gobas [188] and the Caco-2 cell model. Wilcockson and Gobas developed a thin film solid phase extraction technique with which they investigated the bioavailable fraction of semi-volatile and poorly volatile organic chemicals in air, biota, sediments, and soils. They used ethylene vinyl acetate (EVA) thin films, which exhibited quick absorption kinetics, resulting in chemical equilibrium between the medium of interest and the solid phase after short application times. EVA is more durable, and less expensive than cultured cells. We also employed the Caco-2 cell model which is the best characterized with regard to transport properties of drugs and metals [120]. Confluent monolayers of Caco-2 cells, a cell line from a human colon adenocarcinoma, have been used extensively to predict intestinal absorption of pharmaceuticals [117], and more recently xenobiotics [122, 141, 208]. Caco-2 cells spontaneously differentiate after reaching confluency, forming a highly polarized monolayer with a well-defined brush border on the apical surface and tight junctions, morphologically resembling small intestinal absorptive cells.

The specific aims of this study were to measure the extent of mobilization and uptake of [^{14}C]-BaP bound to soil using two in vitro models of digestion. Both models employed incubation in physiological gastric and intestinal fluids followed by exposure to either cultured Caco-2 cells, or an EVA thin film, Using these models, the effect of ageing and soil organic matter content were evaluated.

4.2 Materials and methods

4.2.1 Experimental approach to measure mobilization of BaP from a solid matrix during digestion

The digestion process was based on physiological constituents and transit times for fasting conditions in children, beginning with stomach digestion [32, 148, 209]. The BaP concentrations bound to soil used in our experiments were based on the concentrations found in contaminated sites [210]. Incubation of substrate ([^{14}C]-labeled BaP bound to soil) with gastric fluid was followed by pH neutralization and addition of bile salts and pancreatin to mimic digestion of the contaminant. The neutralized digestive mixture was then applied to one of two model epithelia, either a thin film of ethylene vinyl acetate or fixed Caco-2 cells on glass coverslips in 2 ml beakers or to live Caco-2 cells on the apical side of Transwell inserts. The amount of [^{14}C] in the aqueous compartment and in the Caco-2 cells or EVA film was monitored over time. In order to account for non-specific binding of the chemical, we performed a complete mass balance of the chemical movement in each experiment by determining the amount of [^{14}C] in each compartment of the system, including the tissue culture supports. The supports were flattened and packed up into scintillation vials, soaked in 10ml of Biodegradable Counting Scintillant (BCS) for an overnight and counted in a Beckman LS 6500 multi-purpose liquid scintillation counter with automatic quench correction (Beckman Coulter, Fullerton, CA, USA). 10-20% of [^{14}C] was associated with tissue culture supports and other plastic ware.

4.2.2 Soil characteristics

The model soil was collected between 0 and 15 cm (topsoil) and between 15 and 20 cm (subsoil) in depth from Burnaby Mountain, BC. The soil was fractionated into various particles sizes in a mechanical shaker. The 125-250 μm soil fraction was chosen because it is more likely to adhere to the skin and transferred by hand-to-mouth activity of children [95] (Table 4-1).

Sediment was collected from Sydney Harbour, Nova Scotia in September of 2002 by Environment Canada, stored in a sterilized glass jar and refrigerated until use. Prior to

the experiments, soils, and sediment were air-dried and autoclaved 3 times with a 24 hour interval between autoclaving to eliminate microbial populations.

Table 4-1. Properties of soil and sediment samples used in this study

	Topsoil	*Subsoil*	*Sydney Harbour sediment*
Depth	0 to 15 cm	15 to 20 cm	0 to 10 cm
Organic matter (%, loss-on-ignition)	28.9±0.1	11.0±0.2	8.8±0.0
pH in water	3.4	3.8	3.0
Particle size	125-250μm	125-250μm	66.4% <63μm (by mass)

4.2.3 Measurement of soil/sediment organic matter (Loss-On-Ignition method)[211]

The Loss-On-Ignition (LOI) method was modified from a method described by Ben-Dor and Banin [212]. Briefly, air-dried soil and sediment samples were added to tared crucibles and heated at 105°C for 24 hours. After obtaining the weights of crucibles with oven-dried samples, the samples were ignited in a muffle furnace at 400°C for 16 hours, then cooled in a desiccator under vacuum and the weight of ignited samples was determined. The LOI content of the sample was calculated as

$$\text{LOI, \%} = ((Sample_{105}\text{-}Sample_{400})/Sample_{105}))\times 100$$

where "$Sample_{105}$" is weight of soil sample after heating at 105°C and "$Sample_{400}$" is weight of soil sample after ignition at 400°C. The LOI was corrected for dehydroxylation of inorganic constituents through a regression analysis model: soil organic matter = (b×LOI)+a, (g/100 soil); where a and b are as 0.972 and -0.37, respectively, as determined by Ben-Dor and Banin [211, 212].

4.2.4 Spiking soil with [^{14}C]-Benzo[a]pyrene

[7,10-^{14}C]- Benzo[a]pyrene (BaP) was obtained from GE Healthcare (formerly Amersham, Oakville, ON, Canada,) (specific activity of 60 mCi/mmol). To prepare spiked soil, 10 mg soil was put into 20 ml borosilicate scintillation vials to which 10 µl of toluene containing [^{14}C]-labeled-BaP was added. The toluene was allowed to evaporate overnight at room temperature. After spiking, soils were kept in closed containers at room temperature in the dark for a minimum of 7 days prior to use. In experiments with Sydney Harbour sediments, after spiking with [^{14}C]-BaP as described above, samples were kept in sealed vials for four months under the same conditions. To ensure consistency of spiking procedures, the amount of [^{14}C] in three soil samples were determined at the beginning of each experiment.

4.2.5 Model gastrointestinal fluids

The composition of synthetic gastric and intestinal fluids was based on in vitro digestion models designed by [32, 195, 209] and modified as previously described [208].

The soil-to-fluid ratio was 10 mg spiked soil/sediment: 1 ml gastric fluid (1:100) for the first 1.5 hours and 10 mg soil : 1.1 ml intestinal fluid (1:110) subsequently. A soil-to-fluid ratio in the range of 1:100 to 1:5000 (g:ml) is assumed to cover all physiological conditions in vivo [32, 194].

One ml of gastric fluid was added to each vial with spiked soil matrix and vials were incubated for 1 hour at 37°C to mimic gastric digestion. Transition from the stomach to the small intestine was done by neutralizing the pH of the solution to pH 7 with 7 mg $NaHCO_3$ per 1 ml. Once neutralized, 100 µl of freshly-prepared synthetic intestinal secretion was added which contained per ml: 4 mg bile salts (Sigma-Aldrich, St. Louis, MO, USA) 0.3 mg pancreatin (EM Science, Darmstadt, Germany), 1 mM calcium dichloride, 0.04M Tris buffer pH 7.0 and 100 mg bovine serum albumin. (Caledon Laboratories, Georgetown, ON, Canada).

4.2.6 Cell culture

The human colorectal carcinoma cell line (Caco-2) was obtained from the American Type Culture Collection (ATCC catalog No. HTB-37). Cells were maintained in Dulbecco's Modified Eagle's Medium (DMEM, Gibco BRL, Burlington, ON) with high glucose (4.5 g/l) supplemented with 1% non-essential amino acids, penicillin (25 IU/ml) and streptomycin (100 μg/ml), with 10% fetal bovine serum (FBS), at 37°C in an atmosphere of 5% CO_2 and 90% relative humidity. Caco-2 cells were used between passages 30-70. For transport experiments, cells ($1\text{-}2x10^5$cells/insert) were seeded on transwell polycarbonate cell culture inserts (Becton Dickinson, Franklin Lakes, NJ, USA) with high pore density (0.4μm pore size). Cells were incubated for three weeks and used between 21 and 26 days after seeding. Lipid content of Caco-2 cells was determined as described previously [208].

4.2.7 Transport experiments

Caco-2 cells were grown to confluence on cell culture inserts as described above and formation of a sealed monolayer was confirmed by the measurement of transepithelial electrical resistance (TEER) as described in Vasiluk et al [213]. Cells were washed with buffered solution (pH 7.4) to remove culture medium and neutralized intestinal fluid from gastro/intestinal digestion was added to the apical chamber. Cells were incubated at 37°C with gentle shaking and hourly change of the basal media to mimic blood flow. Aliquots of 20 μl from apical and 0.5ml from basal medium were sampled over the next 6 hours. Apical samples were cleared of soil particles by centrifugation at 2000 g for 1 min. Uptake into the Caco-2 cells on the inserts was also measured at the end of the experiment. All samples were added to Biodegradable Counting Scintillant (Amersham Biosciences Oakville, ON, Canada, a division of GE Healthcare) and counted using a Beckmann 6500 Liquid Scintillation Counter with automatic quench correction.

4.2.8 Determination of fugacity capacity of Caco-2 cells

The fugacity (f) of a chemical represents its tendency to "flee" the system, and $f = C/Z$, where C (mol/m^3) is the concentration of the chemical in the medium and Z (mol/m^3×Pa) is the fugacity capacity of the medium for that chemical. The fugacity capacity represents the increase in the chemical concentration in a medium that has to be achieved to raise the fugacity of the substance in that medium by 1 Pa [8]. It can be considered as the capacity of the medium to hold the substance. Fugacity is generally determined from the concentration of chemical in the air above a sealed system [188], because, in air, the molar capacity of all chemicals is identical. However, it was not possible to accurately measure the concentrations of BaP in air even using radiolabeled BaP. Recently, Otton (M.RM. Thesis, Simon Fraser University, Burnaby, BC, Canada) suggested that K_{EA} (EVA/air partitioning coefficient) is 3.8 times the K_{OA} (octanol/air partitioning coefficient). By substituting the value of K_{OA} to K_{OW} [208] the fugacity capacity of EVA for BaP (Z_{EVA}) can be calculated from the K_{OW} of BaP and Henry's law constant as follows

$$Z_{EVA} = K_{ow} \times 3.8/H \quad (1)$$

Since the fugacities in each compartment are equal at equilibrium, and $f = C/Z$, then

$$C_{Lipid}/ C_{EVA} = Z_{Lipid}/Z_{EVA} \quad (2)$$

Thus, once the fugacity capacity of EVA is calculated and the concentrations of BaP in Caco-2 cells and EVA were determined experimentally, the fugacity capacity of Caco-2 cells could be calculated.

4.2.9 Data and statistical analysis

The raw data (sampling time and concentrations) were fitted to a one-compartment model assuming first order kinetics. The one compartment was fit to desorption data using a nonlinear regression technique with software designed to minimize the sum of squared residuals (SPSS 13.0, SPSS Inc., 2004).

$$C=C_p(1-e^{-kt}) \quad (3)$$

where C is the concentration in Caco-2 or EVA (mol/m^3) at time t (h), C_p is concentration in the sorptive epithelia at equilibrium (mol/m^3), and k is the apparent uptake rate constant (h^{-1}).

Data are presented as means ± standard error. Data were analyzed using one-way analysis of variance (ANOVA) test, followed by the nonparametric Wilcoxon rank-sum test.

4.3 Results and Discussion

4.3.1 The effect of varying percent of organic matter on bioavailability of [^{14}C]-BaP bound to soil

To measure the mobilization and sorption of soil-bound [^{14}C]-BaP from soil, we incubated soil containing 1 μg of [^{14}C]-BaP in simulated gastric and intestinal fluids, and then applied the intestinal fluid to the apical side of cultured human enterocytes, Caco-2 cells. Two different soils were compared that differed primarily in their proportion of organic matter; high (29%) organic matter, and low (11%) organic matter (Table 4-1). We found that uptake into gastrointestinal fluid achieved equilibrium with both types of soil within 5 h (Fig.4-1A). The release of BaP, identified as the fraction present in the 2000g supernatant of the digests, was considered as free or bound to soluble organic matter in the aqueous fraction. The higher organic matter content in the top soil may have resulted in significantly lower concentrations of BaP mobilized into aqueous solution (Fig.4-1A). Similar results were obtained when soils were spiked with 0.5μg and 1.7μg (data not shown), i.e., the lower organic matter soil released approximately twice as much radioactivity into the gastrointestinal fluids compared with the soil with the high organic matter content.

After 5 h, the levels of [^{14}C] (representing BaP and any BaP metabolites) associated with Caco-2 cells was measured. The amount of BaP sorbed into Caco-2 cells was significantly greater with low organic matter soil for all three BaP concentrations measured (0.5μg, 1μg and 1.7 μg of BaP) (Fig.4-1B), which correlated with the relative concentrations in the aqueous phase. Hack and Selenka [32] suggested that since

solubilization of HOC in digestive juices is a prerequisite for their absorption, the mobilized (or bioaccessible) amount can be a good estimate of bioavailability. In the present study, we found that, although the concentrations of [^{14}C] in the cells (bioavailable fraction) paralleled the concentrations in the gastrointestinal fluid (bioaccessible fraction) the bioavailable fraction was 100-fold greater.

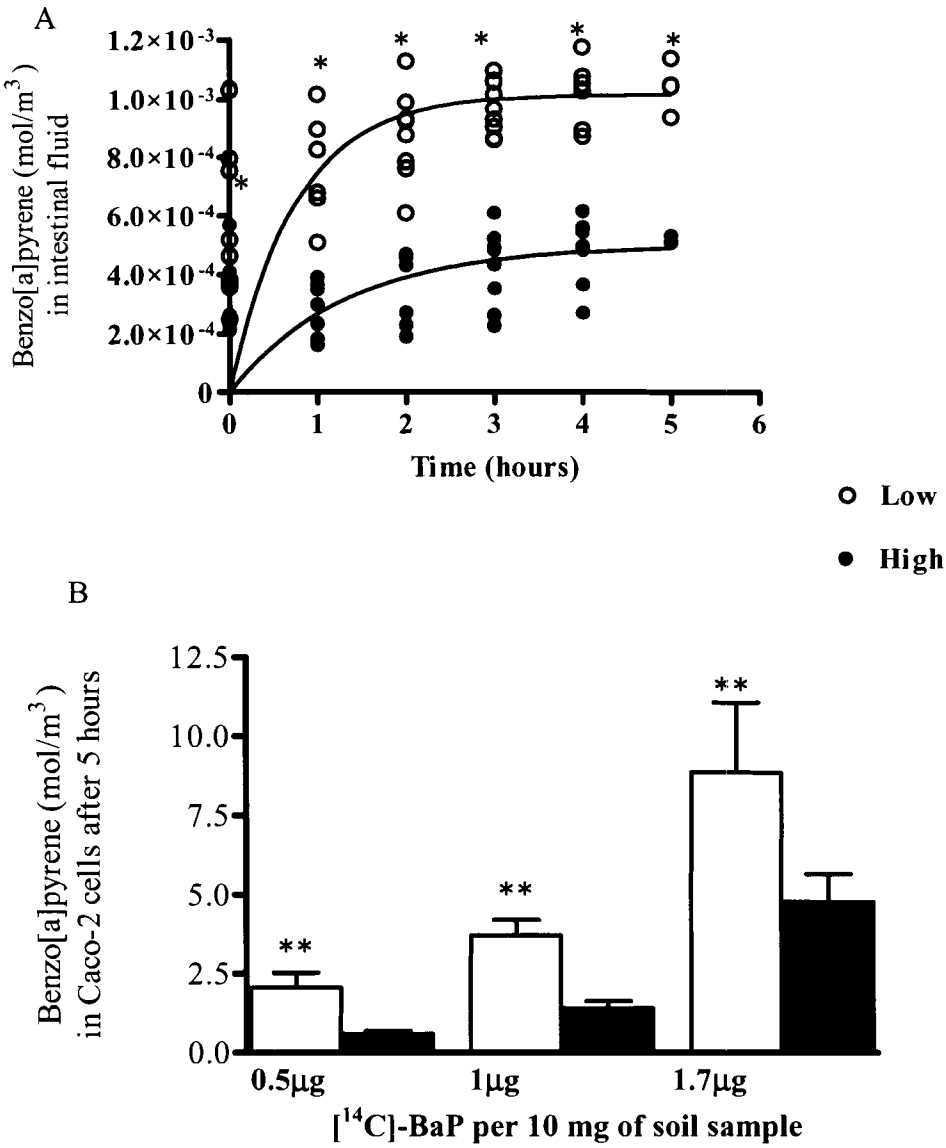

Figure 4-1. Partitioning of soil-bound [^{14}C]-BaP to gastrointestinal fluid and to Caco-2 cells: effect of soil organic matter content.

Two different soil samples were employed: high and low percent of organic matter values were 29% and 11%, respectively. A) Mobilization of [^{14}C]-BaP from soils into gastrointestinal fluids. Data shown are for 1mg of [^{14}C]-BaP per 10 mg of soil sample; B) [^{14}C]-BaP sorbed to Caco-2 cells 5 hours after exposure to epithelial cells. Asterisks indicate that the soils with low organic matter were significantly different from the high organic matter content soil: at $P<0.05$ (*), $P<0.01$ (**) and $P<0.001$ (***).

Due to its high K_{ow} value (log K_{ow} of 6.04), BaP in the soil would be expected to associate strongly with soil organic matter. Consequently, the higher the percent of organic matter, the higher the fugacity capacity of the soil. This is reflected in the lower fugacity of the BaP in gastrointestinal fluid during digestion of high organic content soil from which a lower amount of BaP was mobilized and sorbed to Caco-2 cells. Although the fugacity capacity of Caco-2 cells remained constant, the system was not at equilibrium. Hence, any changes in the extent of BaP mobilized into the aqueous phase were reflected in the BaP concentration in the Caco-2 monolayers.

4.3.2 Determining fugacity capacity of Caco-2 cells for BaP

Since Caco-2 cells cannot withstand incubation with gastrointestinal fluid for periods longer than 5-6 hours, we examined an abiotic substitute for the gastrointestinal epithelium. Ethylene vinyl acetate (EVA) thin film was chosen as a surrogate, because it has been suggested by Wilcockson and Gobas [188] that EVA exhibits quick absorption kinetics, resulting in rapid chemical equilibrium. In addition, they suggested that there might be a useful relationship between the lipid-normalized concentration in biological tissue and the EVA film concentration [188]. A previous study in our laboratory compared the relative ability of Caco-2 cells and EVA to sorb another PAH, chrysene [208]. In the present study, we experimentally determined the fugacity capacity of Caco-2 lipid, and compared the fugacity capacity of EVA thin film to the fugacity capacity of Caco-2 lipid over a range of BaP concentrations. The merit of experimentally determining the fugacity capacity of Caco-2 lipids is that the fugacity of cells can be determined from the measured concentrations, as $f = C/Z$. Because the fugacity capacities of the film or biological lipids are independent of the aqueous medium (here gastrointestinal fluid), differences in chemical concentrations in the film/lipid are a direct measure of differences in chemical fugacities between the media and aqueous phase.

[^{14}C]-BaP uptake into EVA and Caco-2 cells from soil spiked with five different concentrations of BaP is shown in Figure 4-2, expressed as the concentration at the plateau (C_p) for each level of BaP. Equilibrium was reached within 12 hours under all conditions (data not shown), therefore, the extent of uptake by cells or EVA film was measured after 14 and 16 hours. Caco-2 values were normalized to the volume of lipid

present. A linear relationship was found between BaP uptake into Caco-2 lipids and EVA thin film over the range of BaP concentrations measured (Fig.4-2).

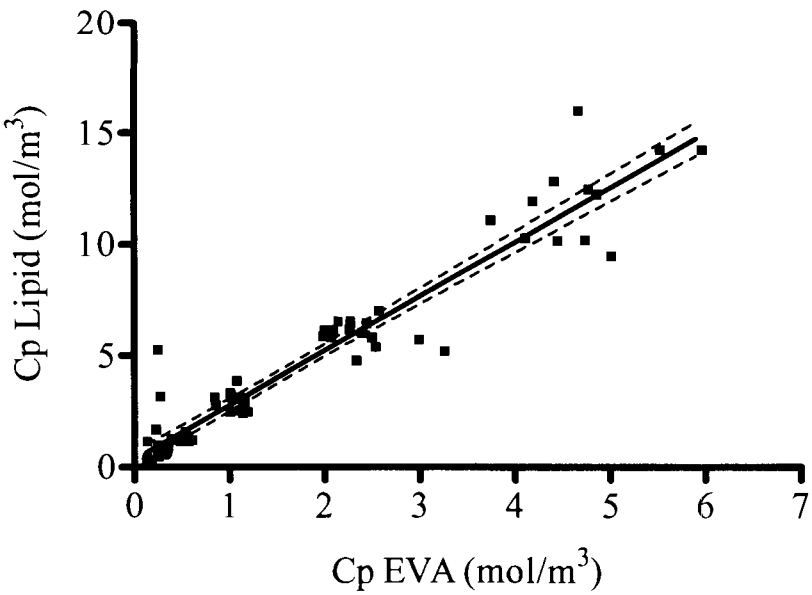

Figure 4-2. Uptake of [^{14}C]- BaP into either Caco-2 lipid versus EVA over a range of [^{14}C]-BaP concentrations.

Data are presented for three independent experiments with three replicates for each concentration of BaP. For the Caco-2 cells, uptake was normalized to the volume of lipid present in the Caco-2 cells. The dashed lines represent the 95% confidence interval (R^2=0.92).

The fugacity capacity of Caco-2 lipids was calculated using a linear bivariate fit equation (R^2=0.92) with 95% confidence (Fig.2) according to the following equation:

$$C_{Lipid} = 2.44 \times C_{EVA} \quad (4)$$

where C_{Lipid} is the concentration of BaP in Caco-2 monolayers at equilibrium (mol/m^3); C_{EVA} is the concentration of BaP in EVA films at equilibrium (mol/m^3). Substituting the concentration values with fugacity capacities from equation 2

$$Z_{Lipid} = 2.44 \times Z_{EVA} \quad (5)$$

Thus, the fugacity capacity of the Caco-2 monolayers was 2.44-fold higher than EVA. Using equation 1, the fugacity capacity of EVA film was calculated to be 2.78×10^{7} mol/m^3×Pa, therefore, the fugacity capacity of Caco-2 lipids was 6.77×10^{7} mol/m^3×Pa.

These results confirm our previous finding using another PAH, chrysene [208]. In that study, we calculated a higher $Z_{Caco\text{-}2}$ than Z_{EVA} and here we experimentally confirm the higher fugacity capacity of Caco-2 lipids. Nevertheless, EVA is a good surrogate for intestinal epithelium because of the linear relationship within the range of BaP concentrations tested.

4.3.3 Sorption of [^{14}C]-BaP bound to soil: comparison of Caco-2 cells with EVA

To obtain estimates of chemical equilibrium in Caco-2 lipids and to compare them to values at equilibrium in EVA films, we fixed coverslips coated with Caco-2 monolayers with paraformaldehyde as described previously in Minhas et al [208]. To measure the mobilization and sorption of soil-bound [^{14}C]-BaP from two types of soils at equilibrium, we incubated soils in simulated gastric and intestinal fluids, and then applied the intestinal fluid to coverslips with Caco-2 cells and EVA thin films.

[^{14}C]-BaP uptake into EVA and Caco-2 from the two soils is shown in Figure 4-3. EVA accumulated > 20 times more BaP per m^3 when compared to whole Caco-2 cells; however, when the data were normalized to the lipid volume of the cells, the biological lipid bound ~2.5-fold more BaP per m^3 than EVA, regardless of organic matter content (Fig.4-3). This was consistent with the results illustrated in Fig.4-2, which showed that the apparent fugacity capacity of Caco-2 lipid was 2.4 fold higher than EVA.

At equilibrium, we found that there was no significant difference in the amount of [^{14}C]-BaP sorbed between the low and high percent of organic matter soils for both the Caco-2 and EVA models. This was in contrast to the results obtained using Caco-2 cells; after 5 hours: cells accumulated significantly more [^{14}C] from low organic matter soil (Fig.4-1B). To determine whether the observed differences were due to differences in the rate of uptake, a first order uptake model was fit to the data shown in Fig. 4-3 (see section 4.3.5 for kinetics analysis).

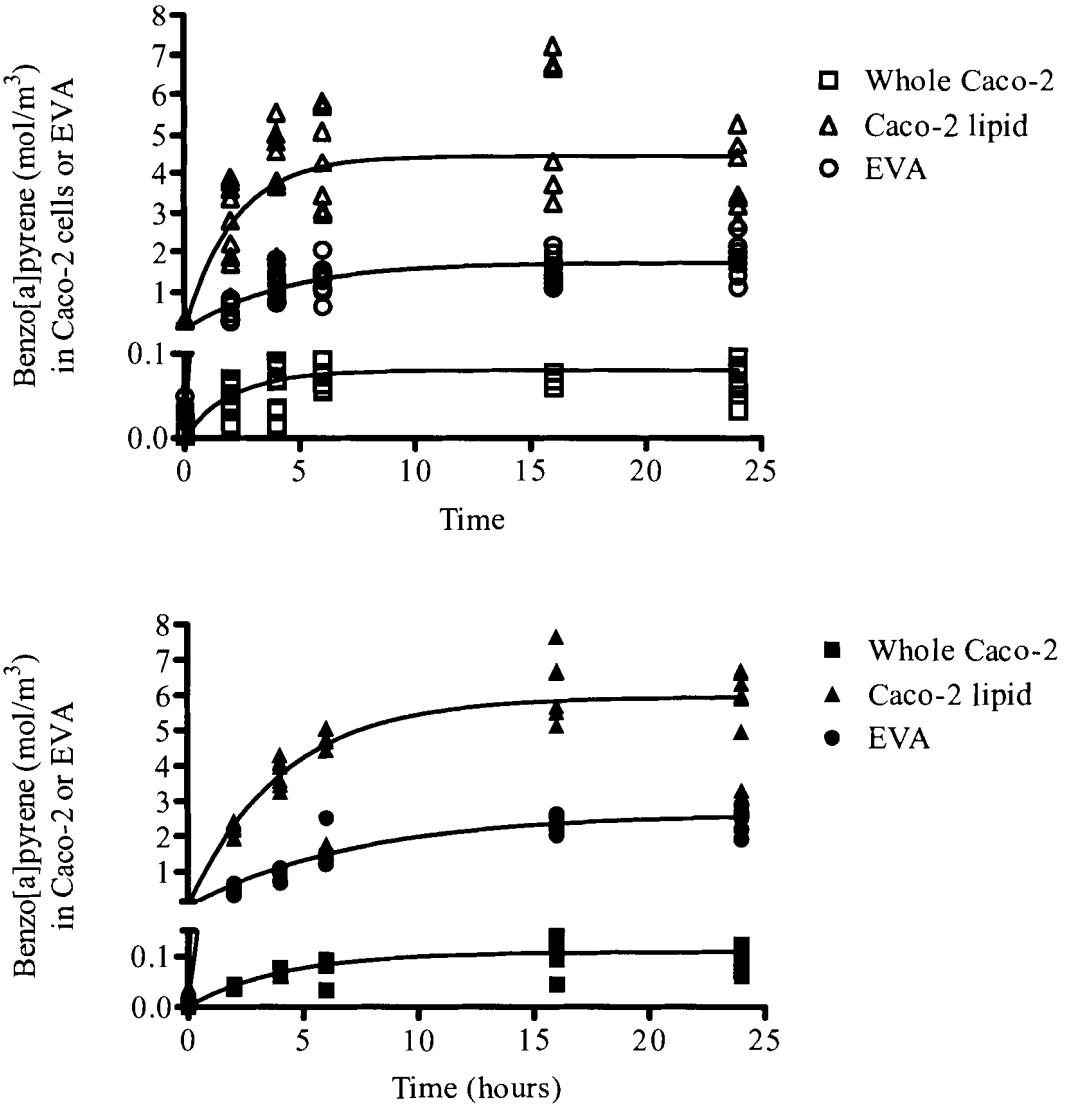

Figure 4-3. Uptake [^{14}C]-BaP from digested soils containing low (A, open symbols) or high (B, solid symbols) percent organic matter into EVA or fixed Caco-2 monolayers.

Data are presented for three independent experiments, each with three replicates. For the Caco-2 cells, uptake was determined based on whole cells or normalized to the volume of lipid present in the Caco-2 cells.

4.3.4 Partitioning of [^{14}C]-BaP bound to PAH-contaminated sediment: effect of ageing

It has been suggested by many researchers that organic compounds such as PAHs become less available in the soil over time, therefore probably exerting less toxic effect

[30, 197, 214]. It is believed that during ageing, molecules of the contaminants slowly move into sites within the soil matrix that are not readily accessed by microorganisms [30]. The major geosorbent is organic matter, though the nature of the organic matter can affect the extent of sorption. Sun et al [215] conducted desorption experiments with aged and non-aged naphthalene and pyrene onto artificial solids as absorbents with and without addition of organic matter. They reported that desorption from solids containing organic matter was difficult for both chemicals, and declined even more when the nanoporosity of the solids was increased.

Although Sydney Harbour sediment has approximately the same percentage of organic matter as the low organic matter soil used in experiments described above, the type of organic matter likely differed between the two samples: NAPL and carbon particles are likely to be present in sediment whereas humic and fulvic acids will be more common in the pristine soils. Furthermore, the surface area available for sorption in sediment is expected to be greater as 66% of the particles by mass were <63 μm in diameter (Table 4-1).

Sydney Harbour, Nova Scotia is a major industrial, transportation, and population centre. The Harbour has been the depository of industrial and anthropogenic contaminants, and as a result, the Sydney Tar Pond sediment contains elevated amounts of oils and tar [216]. Very high levels of toxic chemical contamination are present at this site owing to historical releases of hazardous substances from a number of municipal and industrial sources, principally PAHs (35.4 mg/kg), 5-10% of which is BaP, and includes other organic contaminants (such as PCBs as well as metals (Cd, Hg, Pb and Zn) [216]. Therefore, we conducted experiments with [^{14}C]-BaP-contaminated sediments from Sydney Harbor, that were aged for seven days or four months to determine the effect of ageing on the mobilization of BaP from a field-contaminated sediment. When BaP was aged onto sediment for four months, we observed a decrease in BaP uptake into either Caco-2 cells (fixed) or EVA, compared to non-aged sediments (Fig. 4-4 A and B).

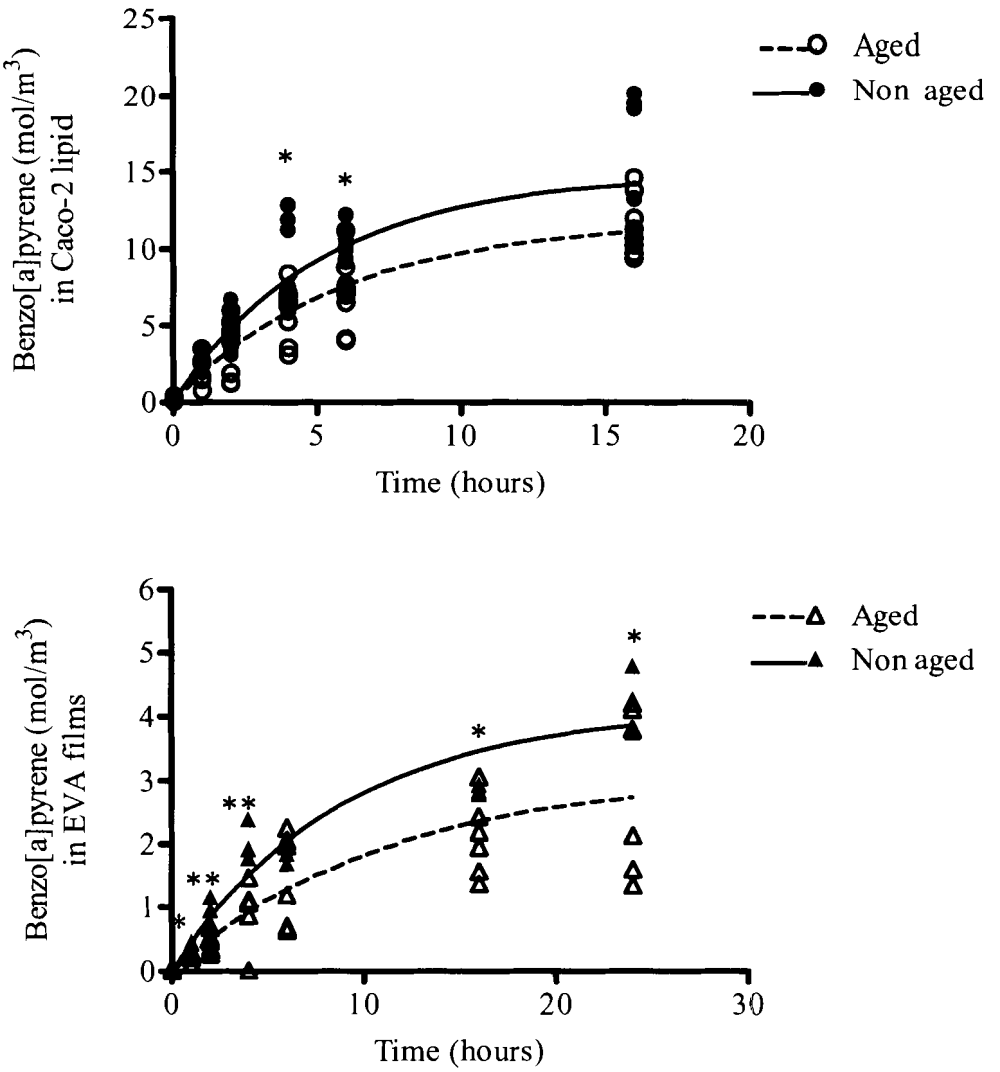

Figure 4-4. The effect of ageing on partitioning of [^{14}C]-BaP bound to Sidney Harbour sediment into Caco-2 cell lipids (A), or EVA film (B) during gastrointestinal digestion in vitro.

Values shown are from three independent experiments. Uptake 1 μg of [^{14}C]-BaP from digested sediments aged for 4 months (open symbols) or 7 d, non-aged (solid symbols) into EVA or fixed Caco-2 monolayers. Asterisks indicate that the contaminated sediment with aged BaP was significantly different from the non-aged sediment: at $P<0.05$ (*), $P<0.01$ (**).

However, the reduction observed with the aged samples was not significant at all time points during the experiment. The differences observed with EVA film were larger and more consistent than those observed with Caco-2 cells likely because of greater reproducibility of this technique (compare Figure 4-4 A and B). These data are in

agreement with our earlier observation that Caco-2 lipids have a greater fugacity capacity and/or rate of uptake compared to EVA; approximately 3-fold more [^{14}C]-BaP was taken up into Caco-2 lipids compared to EVA for both the aged and non-aged samples. Surprisingly, Caco-2 cells, which absorbed approximately 5-7 mol BaP/m^3 lipid from low percent organic matter soil after 20 hours of exposure, absorbed 10-20 mol/m^3 from Sydney Harbour sediment after 16 hours. Thus, despite the assumed presence of NAPL and soot in the Sydney Harbour sediment, there was a greater release of [^{14}C]-BaP compared to soil with a comparable percent organic matter. This is possibly due to the smaller particle size of the sediment providing greater surface area for desorption. It is also possible that BaP requires contact times longer than 4 months to become sequestered. However, we cannot exclude the possibility that the artificially spiked PAH will behave differently from the original contaminants. For example, it is unclear how ageing in nature should be simulated under laboratory conditions and spiking soil with contaminant dissolved in solvent may introduce artifacts into the experiment [30]. Although it is possible that a very small amount of toluene remained after incubating the soils for 7 days in the fume hood, we believe that toluene would not contribute significantly to the organic matter in the soils. After spiking, the soils were placed in the fume hood in uncapped containers overnight, and then with loose caps for 6 additional days. Toluene evaporates quickly at room temperature, particularly in the fume hood, where evaporation would increase even further due to the air flow. As reported by J. Peress, [217], the EPA method for determining evaporative losses from a solvent spill are related to many factors, including wind speed, temperature and vapour pressure. Specifically,

$$QR = 0.284 \times u^{0.78} \times MW^{2/3} \times A \times VP/82.05 \times T \qquad (6)$$

where A is surface area; MW is molecular weight; QR is evaporation rate; T is temperature, °K; VP is vapour pressure of liquid; and u is wind speed. For example, for toluene, a 1200 L spill at 25°C with a wind speed of 4 m/sec that has a depth of 1 cm, the rate of evaporation is ~8 kg/min. The toluene would be completely evaporated within 3-4 hours. Nevertheless, the properties of soil will retard the evaporation somewhat but given that there was a 7-day evaporation period, we assume 99% removal. Furthermore, Northcott and Jones [218] have calculated the amount of residual organic carbon

contributed by solvent for several common spiking solvents. Given the vapour pressure of toluene, if we assume 99% removal of toluene after 7 days at room temperature, the percent additional organic carbon content would be 1.6%. For these reasons, we do not believe that the contribution of solvent would have been significant in our study.

4.3.5 Uptake kinetics of BaP from soil during digestion

Because sorption is so important to the fate of hydrophobic contaminants in soil, it is essential to characterize both the thermodynamics and kinetics of sorption [184]. As stated above, sorption of PAHs to a solid matrix and its physicochemical interactions with soil particles often result in strong binding and slow release rates that significantly influence their bioavailability [5]. Desorption is often considered the rate-limiting step for soil systems [197].

To obtain estimates of equilibria in sorptive epithelia, first-order uptake models were fitted to the data obtained from fixed Caco-2 cells and EVA films using non-linear regression. Following a very basic uptake model, migration of test compounds from the matrix into sorptive epithelia can be described using Equation 3 (see Materials and Methods). A one-compartment model was considered to be appropriate because the amount of benzo[a]pyrene in the aqueous phase remained constant soon after the introduction of the intestinal components (Table 4-2).

Table 4-2. First order rate constant of [^{14}C]-BaP elimination from Caco-2 cells or EVA thin films from pristine soil samples and from Sydney Harbour sediment.

*All soils/sediment were spiked with [^{14}C]-BaP 7 days prior the assay except the aged sediment, which was stored for four months at room temperature in the dark prior to analysis.

*Soil type**	*Sorptive surface*	*k (h^{-1}) ± Std Error*	*R^2*
High organic matter	Caco-2	0.23±0.04	0.76
	EVA	0.09±0.02	0.89
Low organic matter	Caco-2	0.46±0.12	0.59
	EVA	0.24±0.04	0.76
Sediment (4 months aged)	Caco-2	0.17±0.02	0.85
	EVA	0.09±0.03	0.72
Sediment (non aged)	Caco-2	0.20±0.03	0.84
	EVA	0.11±0.02	0.91

The rate constant k was significantly higher for low organic matter soil when compared to high organic matter soil for both Caco-2 and EVA. This suggests that the presence of organic matter slowed the desorption rate of BaP from soil matrices. Sun and Li [219] reported that as the organic matter content of their soil samples was reduced from 18.7% to 0.6%, the percentage of pyrene accumulated by earthworms increased from 1.9% to 18.5% for non-aged soils, and from 0.9% to 3.7% for soils aged 120 days.

In addition, the rate of uptake into Caco-2 lipids was consistently double that of EVA for all matrices tested. Applying a fugacity approach, the transport parameter (D, mol/Pa×h) is determined by the rate constant k (h^{-1})of elimination [111], the volume V (m^3) and the fugacity capacity of the compartment (Z, mol/m^3×Pa).

$$D = VkZ \tag{7}$$

From equation 7,

$$k \propto 1/VZ \tag{8}$$

or for Caco-2 lipid

$$k_{Lipid} \propto 1/V_{Lipid} \times Z_{Lipid} \tag{9}$$

and for EVA thin film

$$k_{EVA} \propto 1/V_{EVA} \times Z_{EVA} \quad (10)$$

By substituting the value of Z_{lipid} from equation 5 in equation 9

$$k_{Lipid} \propto 1/V_{Lipid} \times 2.4_{EVA} \quad (11)$$

and measured volumes of EVA (2.5×10^{-10} m^3) and Caco-2 lipid fraction (3.7×10^{-11} m^3) we calculated that

$$k_{lipid} \cong 2.8\ k_{EVA} \quad (12)$$

Therefore we assumed that the consistent difference in the rate of elimination between EVA and Caco-2, where $k_{Caco\text{-}2\ lipid}$ appeared to be ~2 k_{EVA} for all solid samples, is probably also related to the higher volume of EVA compared to Caco-2 lipid.

Reeves et al [197] measured desorption rate constants for 13 different PAHs from coal tar contaminated soil using three aqueous extraction (phosphate-buffered water, distilled water and an acetic acid) and Tenax beads. The rate constants ranged from 0.03 to 0.9 h^{-1}. They found that the majority of the values in the desorption experiments were not significantly different between soils, nor between aged and non-aged samples of the 13 different PAHs tested, with only anthracene and indeno[1,2,3-cd]pyrene exhibiting a significant differences. Interestingly, in that study the researchers found that BaP had no differences in desorption rate constants between aged and non-aged soils (0.05 h^{-1} and 0.03 h^{-1}, respectively). When we compared the rates observed for aged and non-aged sediment we also found no differences in desorption rate constants between aged and non-aged sediments for both EVA and Caco-2 cells (Table 4-2). Sydney Harbour sediment had rates similar to high organic matter soil despite the fact that its percent of organic matter was comparable to low organic matter soil. This indicates that the organic matter in Sydney Harbour sediment may have a different binding capacity for BaP and acting differently than in pristine soil.

The results of Sydney Harbour sediment confirmed data obtained by Meloche (L. Meloche, M.RM. Thesis, Simon Fraser University, Burnaby, British Columbia, Canada) using thin-film solid phase extraction method [188] in coated glass vials to measure the uptake of PCB congeners from two spiked marine sediments (Port Moody Arm and

Robert's Bank) after two ageing periods. They observed a decrease in total EVA concentrations between the two samples, suggesting that some fraction of the chemical is no longer available for uptake. However, no significant differences in rates of PCB uptake between aged (102 days) and non-aged sediment were observed.

Summary and Conclusions

At non-equilibrium conditions, changes in the mobilized fraction of [^{14}C]-BaP were reflected in differences in the sorbed fraction. In contrast, at equilibrium (12 hours of exposure), sorbed concentrations of [^{14}C]-BaP in Caco-2 lipids or EVA films were not directly correlated with differences in the mobilized into gastrointestinal fluids fraction. Which condition is physiologically relevant? Performing experiments under chemical equilibrium conditions permitted us to measure the fugacity capacity of the Caco-2 cells for BaP and allowed us to make a comparison of the abiotic model (i.e., EVA) to biological lipid bilayer. The rough estimates for transit times in healthy humans following ingestion of a standard meal (i.e. solid, mixed foods) in the small intestines showed that 50% of the ingested food would be emptied in 2.5-3.4 hours [220, 221] with maximum prolonged transit up to 6 hours due to presence of solids (i.e. fiber), which makes the non-equilibrium conditions more applicable for the human health risk assessment. Therefore, we assumed that the results obtained under non-equilibrium conditions (up to 5 h) are more relevant from a physiological point of view. However, although the concentrations in the bioaccessible fraction paralleled the bioavailable fraction, the absolute amount of [^{14}C]-BaP accumulated by Caco-2 cells was two orders of magnitude greater than the mobilized fraction. In other words, in estimating only the mobilized fraction, one can underestimate the true bioavailable fraction.

CHAPTER 5:THE MOBILIZATION, TRANSPORT, AND UPTAKE OF BENZO[A]PYRENE FROM SKIM MILK POWDER IN AN IN VITRO MODEL OF DIGESTION

Manuscript in preparation with the same title as Luba Vasiluk, Linda J. Pinto, Wing Shan Tsang, Frank A. P. C. Gobas, Curtis Eickhoff and Margo M. Moore

Wing Shan Tsang maintained tissue culture line Caco-2 cells required for the project. Linda Pinto assisted in radioactive work with EVA and Caco-2 cells. Frank Gobas and Curtis Eickhoff provided valuable discussion and careful reading of the manuscript.

5.1 Introduction

Polycyclic aromatic hydrocarbons (PAHs) are a class of ubiquitous non-polar chemicals which are of great concern due to their toxic, mutagenic, teratogenic and carcinogenic characteristics [36]. PAHs are by-products of the incomplete combustion of organic matter and many studies have documented that PAHs are frequently found in cooked food, such as fish and meat, with concentrations ranging from 0.17 - 78 μg/kg [222]. Several PAHs have also been detected in milk and dairy products at levels of 1.5 to 7.5 μg/kg [60].

Benzo[a]pyrene (BaP) has been the PAH most commonly studied because it is the most carcinogenic of all PAHs [36]. Although tobacco smoke and polluted air are well-known sources of human exposure to BaP, it has been reported that for non-smokers, food is the main route of exposure to BaP, and accounts for 97% of the total daily BaP uptake [223]. Animal studies have shown that repeated BaP administration was associated with an increased incidence of tumors. Based on this data, an upper limit of the cancer potency (slope factor) for lifetime oral exposure to benzo(a)pyrene was determined to be 7.3 mg per kg body weight per day [224].

Hydrophobic organic contaminants (HOCs), such as PAHs, can enter the body as components of the diet where they may diffuse into the membranes of sorptive tissues,

i.e., the gastrointestinal epithelium. Dietary fat contains a hydrophobic domain that is maintained during lipolysis and the micellar dispersion of the lipolytic products [21, 107], and it has been postulated that many drugs, natural products, and xenobiotics may be bound to dietary fats [13]. The majority of the hydrophobic compounds that enter the gastrointestinal tract are dissolved in lipids, and because of the very low solubility of these compounds in the aqueous environment of the gut lumen, it has been proposed that dietary lipid assimilation might affect the uptake of extremely hydrophobic xenobiotics such as PAHs [23, 111, 141].

It has been shown that the intragastric administration of benzo[a]pyrene in mammals is followed by rapid physical adsorption to intestinal mucosa via passive diffusion into the intestinal epithelium [115]. Although the parent compound is relatively chemically unreactive, BaP metabolites are thought to be responsible for most of the mutagenic activity associated with BaP [36]. The human intestinal epithelium can metabolize a variety of HOCs, including BaP, via cytochrome P450 monooxygenase enzymes (CYPs).

CYP1A1 is an enzyme that is capable of metabolizing a wide spectrum of PAHs [225]. Individual compounds or mixtures of PAHs can regulate their own metabolism by inducing CYP1A1 via its transcription factor [4]. The capacity of CYP1A2 to metabolize PAH is less than CYP1A1; however,CYP1A2 has been reported to be induced by BaP in humans and rodents [225, 226]. CYP1B1 and CYP3A have also been shown to oxidize several PAHs in both humans [227] and rodents [228].

BaP is metabolized by CYPs to ~20 oxidized metabolites and a variety of conjugates. The glucuronides, sulphate esters and mercapturic acids (N-acetylcysteine derivatives resulting from gluthatione conjugates) are ionized at physiological pH, and therefore, are readily excreted. However, several of these metabolites can cause mutations, transform cells, and/or bind to cellular macromolecules. At present, 7,8-diol-9,10-epoxide is considered to be the ultimate carcinogenic metabolite of BaP [36].

Thus, the products of dietary fat digestion serve as delivery vehicle for lipophilic HOCs and increase their bioavailability at the absorptive surface of the intestinal epithelium. The inducible CYP isoenzymes in the intestinal tract could further influence

the development of tumors by metabolism to mutagenic metabolites. Culp et al [229] applied two different coal tar mixtures and BaP alone in food to mice over a lifetime. Dose-response assessment was carried out using BaP uptake as a surrogate for PAH uptake. With BaP alone (up to 100 ppm) they observed a higher incidence of fore-stomach tumors compared with controls, whereas with both of the PAH-rich coal tar mixtures (up to 3000 ppm) the tumor formation increased for various locations: lung, fore stomach, small intestine and various sarcomas. In a similar feeding study, Weyand et al [230] also found increased numbers of fore-stomach tumors.

It is believed that only the mobilized fraction of a contaminant is available for absorption in the digestive tract [32]. It has been assumed that hydrophobic compounds would exhibit low bioavailability due to their limited mobilization from the organic matrix or food under physiological conditions. To account for matrix effects, researchers have developed in vitro models that simulate human physiological conditions, often referred to as physiologically-based extraction tests (PBETs) [231]. One of these models, developed by Hack and Selenka [32] involves two steps, the first one represents the stomach digestion and the second, intestinal. The model was employed to evaluate the bioaccessibility of PAHs and PCBs bound to soil matrix with and without addition of lyophilized milk powder as a source of dietary lipids and proteins, which was added to the gastrointestinal fluid during artificial soil digestion. Van de Wiele et al [99] have established the Simulator of the Human Intestinal Microbial Ecosystem (SHIME) reactor to assess PAH release from PAH-contaminated soil. The SHIME model simulates transit along the stomach, small intestine, and colon including the addition of microbial degradation during gastrointestinal digestion. However, neither of these models included the exposure of gastrointestinal fluids to gastrointestinal membrane to estimate the sorbed fraction of the contaminants. A similar approach to Hack and Selenka has also been used for measuring availability of contaminants like organochlorine chemicals (PCBs) from soil as a matrix by Oomen et al [122] but included exposure to cultured human enterocytes to measure the relative bioavailability of PCBs from soil.

To date, there are no published studies of an in vitro model that employed PBETs with sequential exposure to gastrointestinal membrane, i.e., evaluating the effect of the digestible matrix on oral bioavailability.

Many laboratories have found that Caco-2 cells grown on permeable supports are useful for transport studies [232, 233] and can be adapted to create an in vitro model of the intestine [122, 213]. The Caco-2 cell line was originally derived from human colonic adenocarcinoma cells; however, they spontaneously differentiate leading to the formation of a monolayer of highly polarized cells, joined by functional tight junctions with well developed and organized microvilli on the apical side [232, 233]. Caco-2 monolayers closely resemble mature intestinal enterocytes, both morphologically and biochemically; expressing transport systems for sugars, amino acids, bile acids and dipeptides, and many brush border membrane enzymes [120]. The Caco-2 cell line also possesses several Phase I (CYP 1A1, CYP 1A2 [234, 235], CYP 1B1 [235], CYP 3A4 [123] and 3A5) and Phase II enzymes [236]. The Caco-2 cell lines have also been used as a model system to examine the process of lipid assimilation and lipoprotein production [111, 141]. Fatty acid uptake, triglyceride synthesis, and lipoprotein production by Caco-2 cells show many similarities to the mammalian small intestinal enterocytes although lipid assimilation functions much less effectively [237, 238]. Furthermore, trans-cellular transport of hydrophobic compounds such as PCBs and several PAHs has been confirmed in Caco-2 monolayers by several investigations [111, 115, 122, 123].

In the present study, we also used an in vitro model in which a surrogate membrane material was employed, ethylene vinyl acetate (EVA) [188]. Use of EVA permits the measurement of chemicals at equilibrium; measurements which facilitate fugacity calculations and which cannot be made with live cells due to their fragility after long incubation periods.

The objectives of the present study were to measure the rate and extent of uptake of [^{14}C]-BaP from skim milk powder into sorptive epithelium (Caco-2 cell line) or its surrogate, ethylene vinyl acetate (EVA). We have previously developed an in vitro model for the digestive system that combines synthetic gastro-intestinal digestion with uptake into model epithelium [208]. This model provides a means to accurately determine the rate and extent of [^{14}C]-BaP mobilization and uptake into cultured intestinal epithelial cells.

5.2 Materials and methods

5.2.1 Experimental approach

The in vitro model used in this study is described [208]. Briefly, the digestion process was based on physiological constituents and transit times for fasting conditions in children, beginning with stomach digestion [209]. Incubation of substrate ([^{14}C]-labeled BaP bound to skim milk powder) with gastric fluid was followed by pH neutralization and addition of bile salts and pancreatin to mimic digestion of the contaminant [124, 239]. The intestinal fluid and food (skim milk powder) was then applied to the Caco-2 monolayer. In order to account for non-specific binding of the chemical, we performed a complete mass balance of the chemical movement in each experiment by determining the amount of [^{14}C] in each compartment of the system, including the tissue culture supports. The supports were flattened and packed up into scintillation vials, soaked in 10ml of Biodegradable Counting Scintillant (BCS) for an overnight and counted in a Beckman LS 6500 multi-purpose liquid scintillation counter with automatic quench correction (Beckman Coulter, Fullerton, CA, USA). 10-20% of [^{14}C] was associated with tissue culture supports and other plastic ware.

5.2.2 Cell culture

The human colorectal carcinoma cell line (Caco-2) was obtained from the American Type Culture Collection (Manassas, VA, USA; ATCC catalog No. HTB-37). Cells were maintained in Dulbecco's Modified Eagle's Medium (DMEM, Gibco BRL, Burlington, ON) with high glucose (4.5 g/l) supplemented with 1% non-essential amino acids, penicillin (25 IU/ml) and streptomycin (100 μg/ml), with 10% bovine growth serum (HyClone, Logan, UT, USA), at 37°C in an atmosphere of 5% CO_2 and 90% relative humidity. Caco-2 cells were used between passages 30-70. For transport experiments, cells (1-2x10^5cells/insert) were seeded on 12-well Transwell polycarbonate cell culture inserts (Becton Dickinson, Franklin Lakes, NJ, USA) with high pore density (0.4μm pore size). Cells were incubated for three weeks and used between 21 and 26 days after seeding. The lipid content of the Caco-2 monolayer was determined as previously described [208].

5.2.3 Food matrix characteristics and spiking with [^{14}C]-BaP

To monitor the mobilization of [^{14}C]-BaP from food during digestion, we used skim milk powder as the food matrix. Skim milk powder (20 mg) was used for each sample. A liquid-to-solid ratio of 20 g/L was assumed to cover physiological conditions of dietary milk intake [240]. The BaP concentrations bound to skim milk powder used in our experiments were based on the concentrations found in food (smoked meats and fish [36]).

[7,10^{14}C]-Benzo[a]pyrene (BaP) was obtained from GE Healthcare (Amersham Biosciences Baie D'Urfé, QC, Canada) (specific activity of 60-61 mCi/mmol). To prepare milk powder spiked with [^{14}C]-BaP, non-sterile skim milk (20 mg) was put into 20 ml borosilicate scintillation vials and 10 µl of toluene containing 1 µg, 500,000 dpm [^{14}C]-labeled-BaP were added into each vial. The toluene was allowed to evaporate overnight at room temperature. After spiking, skim milk samples were kept in closed containers at room temperature for a minimum of 7 days prior to use. In experiments with aged skim milk samples, after spiking with [^{14}C]-BaP as described above, samples were kept in sealed vials for 6 months under the same conditions.

5.2.4 Model gastrointestinal fluids

The composition of synthetic gastric and intestinal fluids was based on in vitro digestion models designed by [32, 195, 209] and modified as previously described [208] to contain the following per litre: 0.5 g sodium citrate (Analar, BDH Inc. Toronto, Canada), 0.5 g malic acid, 420 µl lactic acid syrup (both from Sigma-Aldrich, St. Louis, MO, USA.) and 500 µl glacial acetic acid (Anachemia Canada Inc. Vancouver, Canada) in deionized water. The solution was adjusted to pH 2 with 0.18M hydrochloric acid. Pepsin (Sigma-Aldrich, St. Louis, MO, USA) (120 mg/l) was added just prior to the experiment.

Gastric fluid (1 ml) was added to each vial with spiked [^{14}C]-BaP skim milk powder, and vials were incubated with gentle shaking for 1 h at 37°C to mimic gastric digestion. Transition from the stomach to the small intestine was accomplished by neutralizing the pH of the solution to pH 7 with 7 mg of sodium bicarbonate ($NaHCO_3$)

per 1 ml. Once neutralized, 100 µl of freshly-prepared synthetic intestinal secretion was added which contained 0.4 mg bile salts (Sigma-Aldrich, St. Louis, MO, USA) 0.03 mg pancreatin (EM Science, Darmstadt, Germany), 1 mM calcium dichloride, 0.1 M Tris buffer pH 7 and 10 mg bovine serum albumin (Caledon Laboratories, ON, Canada).

5.2.5 Sorptive surfaces

In some experiments, a thin film of ethylene vinyl acetate (EVA) [188] was used as a model of the gastrointestinal epithelium to predict sorption in vitro and compared to fixed human cultured enterocytes, Caco-2 cell line.

EVA: Glass coverslips (12 mm diameter, Fisher Scientific, Ottawa, ON, Canada) were rinsed with 40µl of DCM and then coated on one side with 40 µl of EVA solution (0.6% EVA and 0.04% silane).

Fixed Caco-2 Cells: For absorption/partitioning experiments, cells (1-2 x 10^5 cells/well) were seeded on glass cover slips in a 24-well plate, and used 21 d after seeding. Proteins in the cells were cross-linked by incubation with 4% (w/v) paraformaldehyde in PBS, pH 7.4 for 30 min, at room temperature. This prevented the monolayer from lifting during the experiment. Caco-2 cells were washed twice with PBS and covered with PBS until use.

The fixed Caco-2 or EVA-coated coverslips were added to 2-ml glass beakers with intestinal digestion material and agitated on an orbital shaker at 70 rpm at 37°C. At specific time intervals, triplicate samples were removed. EVA or Caco-2 cell-coated coverslips were rinsed in PBS, extracted into BCS and [^{14}C] bound to Caco-2 cells or EVA was determined by liquid scintillation counting.

5.2.6 Transport of [^{14}C]-BaP from the apical into the basolateral compartment of polarized Caco-2 monolayers

[^{14}C]-BaP spiked milk powder was incubated in glass scintillation vials with the model gastric fluid followed by conversion to intestinal fluid. The digested material in gastrointestinal fluid was transferred onto the apical side of Caco-2 monolayers on inserts immersed in DMEM (Basal compartments). Cells were incubated at 37°C and the basal

medium was changed every hour to mimic blood flow and to allow measurement of basal [^{14}C]-BaP. Aliquots of 20 µl from apical and 0.5ml from the basal medium were sampled over the next 6 hours. Cells plus membranes were cut from the inserts at the end of the experiment and all samples were added to Biodegradable Counting Scintillant (Beckman) and analyzed by liquid scintillation counting in a Beckman LS 6500 multi-purpose liquid scintillation counter with automatic quench correction (Beckman Coulter, Fullerton, CA, USA).

5.2.7 Induction and inhibition of CYP isozymes in Caco-2 cells

To induce metabolism of [^{14}C]-BaP during the transport experiment, β-naphthoflavone (β-NF) an inducer of CYP1A1 and CYP1B1 (Sigma-Aldrich, St. Louis, MO, USA) was added to both compartments 24 h prior to the initiation of experiments (final concentration 50 µM). Transport experiments were performed as described above. To inhibit the CYP1A1 and CYP1A2-mediated metabolism of [^{14}C]-BaP, α-naphthoflavone (α-NF) (Sigma-Aldrich, St. Louis, MO, USA), was added to both apical and basolateral compartments at a final concentration of 200 µM [115] 0.5 h prior to the experiment. Transport experiments were performed as described above.

5.2.8 Separation and quantification of Phase I and Phase II metabolites of [^{14}C]-BaP by thin layer chromatography and LSC

The supernatants of the apical compartments were analyzed by thin layer chromatography (TLC) following solid-phase extraction. Samples were added to solid-phase Extrelut^{TM}-cartridges (Merck Eurolab Ltd., Darmstadt, Germany). Radioactive substances were extracted with diethylether/ethanol (9:1) and, after evaporation under vacuum; the eluate was dissolved in 100-µl methanol. The samples were applied to thin-layer chromatography (TLC) plates (Silica Gel 60F_{254} 20×20, Merck Eurolab Ltd.) to a horizontal origin half way up the plate. Separation of BaP and Phase I metabolites was achieved with a petrolether/ethyl acetate mixture (4:1) (Fig. 5.1A). BaP and its non-conjugated metabolites were detected by UV illumination and identified by comparing the R_f values with standards (Midwest Research Institute, Kansas City, MI, USA). Conjugates remained at the origin. BaP and Phase I metabolites were cut from the TLC

plate and extracted into liquid scintillation cocktail. After drying, the conjugates were separated by running the same TLC plate in the opposite direction using ethyl acetate/methanol (65:35) as the mobile phase (Fig. 5.1B). Conjugates were identified by comparison to R_f values of non-radioactive standards (Midwest Research Institute, Kansas City, MI, USA). Regions of the plate containing conjugates were extracted into liquid scintillation cocktail and [^{14}C] quantified by LSC as described above.

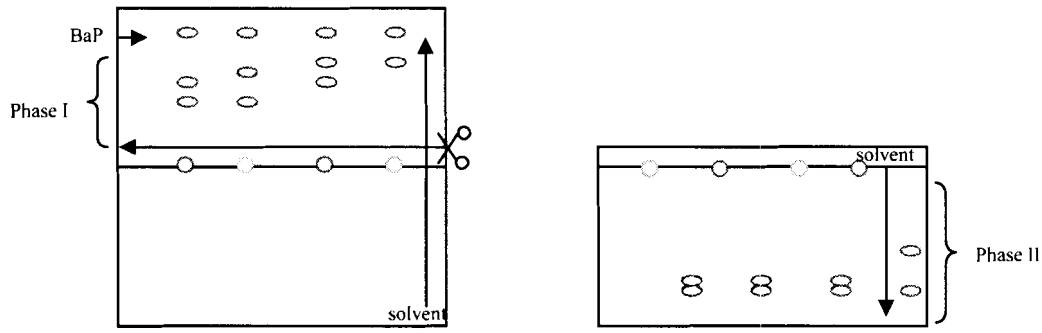

Figure 5-1. Radio thin layer chromatography analysis of [^{14}C]-BaP/metabolites from gastrointestinal fluids.

A. The samples were applied to thin-layer chromatography (TLC) plates to a horizontal origin half way up the plate. Separation of BaP and Phase I metabolites was achieved with a petrolether/ethyl acetate mixture (4:1). B. BaP and Phase I metabolites were cut from the TLC plate and extracted into liquid scintillation cocktail. After drying, the conjugates were separated by running the same TLC plate in the opposite direction using ethyl acetate/methanol (65:35) as the mobile phase.

5.2.9 The fugacity approach

Various studies have used the fugacity approach for the partitioning and transport of hydrophobic organics such as PAHs and PCBs in the environment [208]. Differences in fugacity, rather than in concentrations, determine the direction of chemical diffusion in the model [8]. Transport of chemical from one compartment (gastrointestinal fluid) to another (EVA thin film) will occur if the fugacity of the chemical in these compartments is not equal. The fugacity f (Pa) of a chemical can easily be related to its concentration C

(mol/m^3) by the fugacity capacity Z ($mol/m^3 \times Pa$) of the phase in which the chemical is dissolved [137]:

$$f=C/Z \quad (1)$$

Knowing that the intrinsic holding capacity (fugacity capacity) of EVA film or Caco-2 cells for BaP remains constant, regardless of the differences occurring during gastrointestinal digestion, any changes in EVA fugacity will be reflected in BaP concentration in EVA film [188].

5.2.10 Data and statistical analysis

The raw data (sampling time and concentrations) were fitted using a one-compartment model (equation 2) assuming first order kinetics and using a nonlinear regression technique with software designed to minimize the sum of squares residues (SPSS 13.0, Spss Inc., 2004).

$$C=C_p(1-e^{-kt}) \quad (2)$$

where C is the concentration of BaP in the sorptive epithelia or its surrogate in mol/m^3 at any given time, C_p is the maximum BaP concentration (at equilibrium), t is time (h) and k is the rate constant (h^{-1}) for desorption from matrix or uptake by epithelium.

Data are presented as means ± standard deviation. Data were analyzed using a one-way analysis of variance (ANOVA) test, followed by a nonparametric Wilcoxon rank-sum test.

5.3 Results and Discussion

5.3.1 Mobilization and uptake of [^{14}C]-BaP into EVA during full gastrointestinal digestion

This experiment was conducted to determine the effect of different phases of digestion on the partitioning of [^{14}C]-BaP bound to skim milk powder. Figure 5-1A shows the concentration of [^{14}C]-BaP in the aqueous phase, whereas Figure 5-1B shows the level in EVA film at the same time points. EVA was chosen as the surrogate

epithelium for these studies because this allowed us to examine the gastric as well as the intestinal portion of digestion, as EVA films are able to withstand the low pH environment of the artificial gastric digestion. Furthermore, the films are stable for at least 24 h that allowed us to bring the system to near equilibrium.

We found that some BaP was mobilized from the coagulated skim milk into the gastric fluid almost immediately, and the BaP concentration rose 1.5 fold the first hour of digestion (Fig. 5-1A). With the addition of $NaHCO_3$ after 1 h, complete solubilization of the milk occurred (data not shown). Within 30 min after neutralization the concentration of BaP in the aqueous phase had increased about 5.5 fold further, reaching a concentration of 3.45±0.13 $\mu mol/m^3$. 30 min after neutralization, the intestinal components (bile acids, pancreatin) were added. The aqueous concentration of [^{14}C]-BaP declined slowly after this point, likely as a result of uptake into EVA film.

The amount of BaP taken up by EVA thin films after only 90 s of gastric digestion was more than 1000-fold higher than the concentration in the aqueous phase (Fig. 5-1B). Furthermore, within one hour of incubation with gastric fluid, concentrations in the EVA had increased four fold and these doubled again after neutralization. After 24 h, the concentration of BaP in the EVA film was ~2000 times higher than the concentration found in the gastrointestinal fluid.

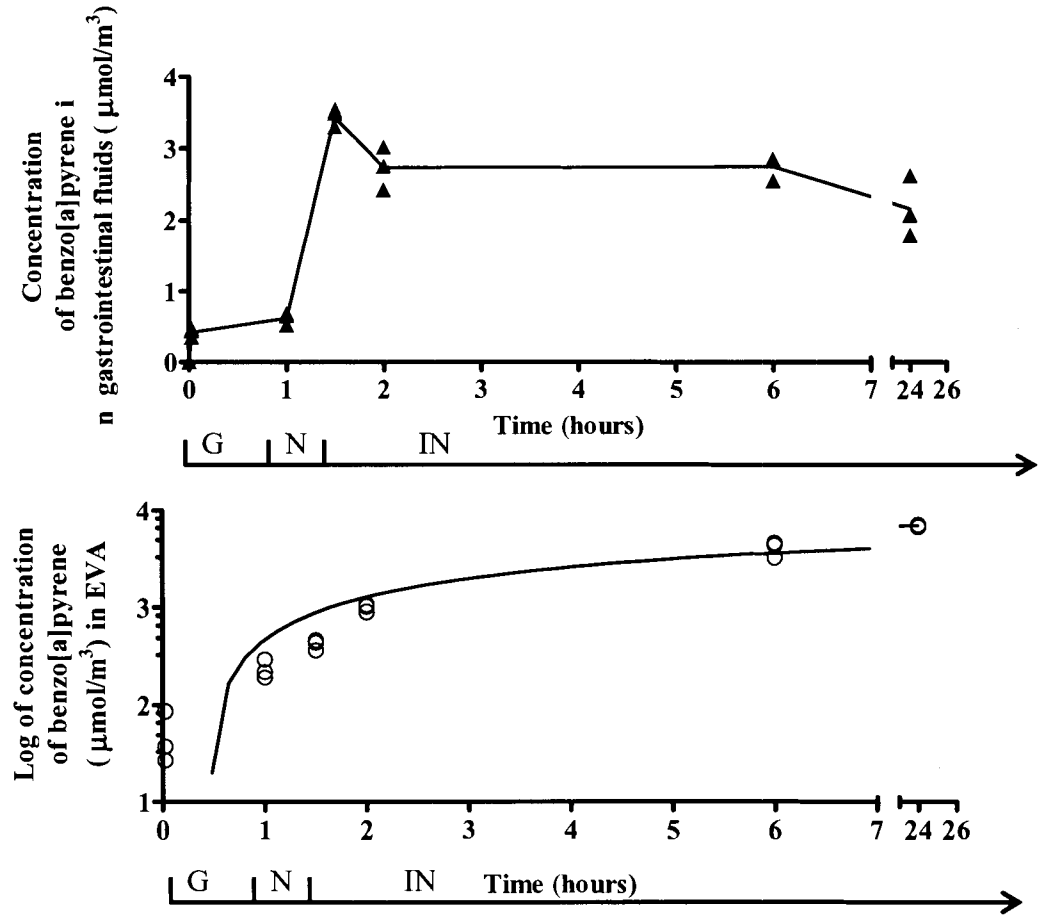

Figure 5-2. Mobilization and uptake of [^{14}C]-BaP into EVA during in vitro gastrointestinal digestion.

A)Mobilization of [^{14}C]-BaP into gastric ("G", from 0 h till 1 h at pH 2; "N", neutralized 1h till 1.5 h) and intestinal fluids ("IN", from 1.5 h till 24 h) during full gastrointestinal digestion (▲). The line represents the mean value for each time point. B) Partitioning of [^{14}C]-BaP from skim milk powder into the EVA-coated coverslips of the in vitro digestive model (○). Note the differences in the Y axis scales in A and B.

As the skim milk was digested, the BaP concentrations and fugacity in the intestinal fluid would be expected to increase because the digestion of the skim milk concentrates BaP in a reduced and compositionally-altered skim milk matrix. This causes a fugacity pump into EVA consistently with the results shown in Fig. 5-1B. This gradient drives the net passive absorption of BaP. Because EVA is metabolically inert, the chemical concentration and the fugacity in EVA will increase to match that in the

gastrointestinal fluid. Despite the lack of carrier-mediated uptake by EVA, a significant proportion of BaP (~46%) was taken up by the film.

In our model, the solubilization of the milk solids resulting from the change of pH from acidic to neutral appears to be the most important factor affecting the amount of BaP in the aqueous compartment. In contrast, the change in pH in the digestive fluids during the experiment had no significant effect on sorption by EVA suggesting that the uptake of BaP into EVA film was dependent on the fugacity capacity of the EVA film for hydrophobic BaP. This is in agreement with results of Minhas et al [208] who demonstrated that changes in the composition of gastrointestinal fluid had little or no effect on the amount of chrysene taken up by EVA film. Despite significant decreases in the extent of mobilization when water or non-neutralized gastrointestinal fluids were used in place of complete medium, the amount of chrysene that partitioned into the EVA (several magnitudes greater than into aqueous fluid) remained unchanged. In subsequent experiments, we therefore focused on the uptake during only the intestinal digestion.

The mechanisms by which hydrophobic molecules (nutrient lipids or/and lipophilic contaminants), travel through the absorptive surface of the enterocytes is not well understood. HOC as well as fatty acids and monoglycerides are believed to diffuse passively through biological membranes due to their lipophilicity and do not require active transport for absorption [21, 107, 110, 142]. However, the intestinal microvilli are bounded by some of the most viscous and high melting–point membranes in the body [21], there is no clear understanding of how efficiently passive diffusion occurs across this membrane. Although EVA offers a durable surrogate of intestinal membranes, the biochemical properties of EVA differ from intestinal epithelium in many ways. A fatty acid transport protein (FATP) has been isolated from mammalian intestinal epithelium that is thought to be involved in the protein-facilitated diffusion of fatty acid monomers [241]. Moreover, the intestinal absorption of fat-soluble vitamins appears to occur by carrier-mediated diffusion as well [21]. Caco-2 cells have been shown to not only transport and absorb xenobiotics, but also to carry out the metabolic transformation of BaP. Therefore, we next employed the Caco-2 cell line in our in vitro digestion model.

5.3.2 BaP transport across human intestinal epithelia

Radiolabeled BaP was added to the apical (luminal) side of the Caco-2 monolayers and the cumulative amount of [^{14}C]-BaP in the basolateral (systemic circulation) side was measured over time. Skim milk with bound [^{14}C]-BaP was incubated in gastric fluid as described in the Materials and Methods, the solution was neutralized and intestinal components were added. This solution was applied to Caco-2 monolayers grown on inserts (Fig. 5-2). Up to 5% (1.5-5%, 0.05-0.13 $\mu M/m^3$) of the skim milk-bound BaP moved into the basal compartment. Transport across the Caco-2 cells to the basal compartment was linear (Fig. 5-2) suggesting that a steady-state net flux was rapidly achieved in this compartment. Previous experiments in our laboratory showed that when the same amount of [^{14}C]-benzo[a]pyrene was added to high organic matter soil rather than skim milk, ~60% less [^{14}C]-BaP was transported to the basal compartment (see Chapter 4). These data suggest that the fugacity capacity of skim milk was less than the soil organic matter. These results may support the fat-flush diffusion hypothesis of Schlummer et al [143]. Their model is based on the principle that the lipid influx into intestinal epithelium acts to enhance gastrointestinal magnification by increasing diffusive uptake from intestinal contents. In other words, the fugacity capacity of Caco-2 cells increases during food digestion due to an increase in internal lipid content. Dietary lipid is hydrolyzed to monoglycerides and fatty acids in the lumen and resynthetized into triglycerides in Caco-2 cells. According to Dulfer et al [111], the fugacity capacity of triglycerides is much greater than that of the monoglycerides or fatty acids in the lumen (apical compartment), and therefore the diffusion gradient is enhanced towards the intestinal enterocytes. Simultaneously, the fugacity in the apical compartment is increased due to lipid transfer into the enterocytes and reduction in fugacity capacity of the food matrix (skim milk), which creates a positive unidirectional fugacity gradient towards the intestinal epithelium cells, resulting in the net passive diffusion of BaP into Caco-2 cells.

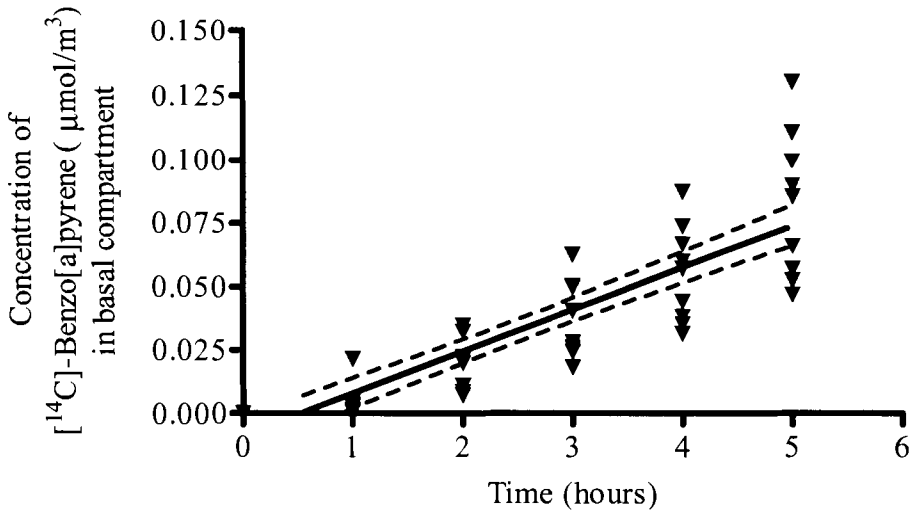

Figure 5-3. Cumulative transport of [^{14}C]-BaP across Caco-2 monolayers.

[^{14}C]-benzo[a]pyrene (~5×10^5 dpm/well or 1µg of BaP per well) was added to the apical compartment at t=0 (immediately after addition of intestinal secretions) and appearance of [^{14}C]-BaP at the basolateral compartment was measured by using LSC. The data represent three independent experiments. The slope of the best fit line yielded k=0.004 h^{-1} (R^2=0.75). * The dashed lines represent the 95% confidence interval.

5.3.3 Directionality of bound-BaP uptake and transport in Caco-2 cells

The enterocyte utilizes nonpolar substances, i.e. lipids, lipoproteins, PCBs and PAHs differently, depending upon direction from which they are presented to the cell. Greater uptake across the apical membrane has been demonstrated [141, 242]. The direction of exposure on the uptake and transport rates of [^{14}C]-BaP/metabolites for 150 min is shown in Fig. 5-3. The skim milk samples spiked with [^{14}C]- BaP were subjected to in vitro gastrointestinal digestion and incubated with Caco-2 monolayers either on the apical side (AB) or the basolateral side (BA). The amount of [^{14}C] transported to the opposite side and accumulated in the Caco-2 lipids were measured over time, and flux was determined. The amount of radioactivity that was transported across Caco-2 monolayers was linear over time at both surfaces (data not shown). The total fluxes (J_{tot} in pmol/cm^2/mm) were similar regardless of whether the partially digested skim milk-bound BaP was added to the apical or basolateral chamber (Fig. 5-3A). These results suggest that BaP mobilized from skim milk during gastrointestinal digestion diffuses passively across Caco-2 monolayers. Trotter and Storch [242] have measured the apical

and total membrane areas of Caco-2 cells, thereby determining the area of the basolateral portion of the membrane. They found an average apical area of 4,123 ± 391 μm^2 and a basolateral area (all membrane below the tight junctions) of 12,414 ± 1055 μm^2. If the flux values are normalized to membrane surface area, the apical to basal flux is 3-to 4-fold higher than the basal to apical flux (Fig. 5-3B). Interestingly, the differences in flux were reflected in the differences in uptake by the Caco-2 cells. The amount of [^{14}C] that accumulated in the cells was approximately 4-fold higher (P<0.0001) when the BaP was presented at the apical side compared to the basolateral side (Fig. 5-3C). Trotter and Storch [242] reported a similar difference in the flux of palmitate bound to BSA between the apical and basolateral surfaces of Caco-2 cells. In their study, the palmitate flux was 6-fold higher from the apical surface when flux was normalized per unit membrane surface area. These data support the theory of unidirectional transport of nonpolar substances, such as lipids, lipoproteins, PCBs [141] and PAH. The observed prevailing uptake of [^{14}C]-BaP into Caco-2 cells from the apical compartment compared to the basolateral may also be caused by the more rapid metabolism of apically-absorbed BaP. CYP enzymes may have been localized to the apical membrane of intestinal epithelial cells. Thus, Phase I oxidation of BaP results in faster removal from the aqueous phase preferentially at the apical membrane. The preferred uptake from the apical side is also in agreement with the "fat flush theory" in which it is postulated that lipid transport processes aid in the uptake of xenobiotics [143].

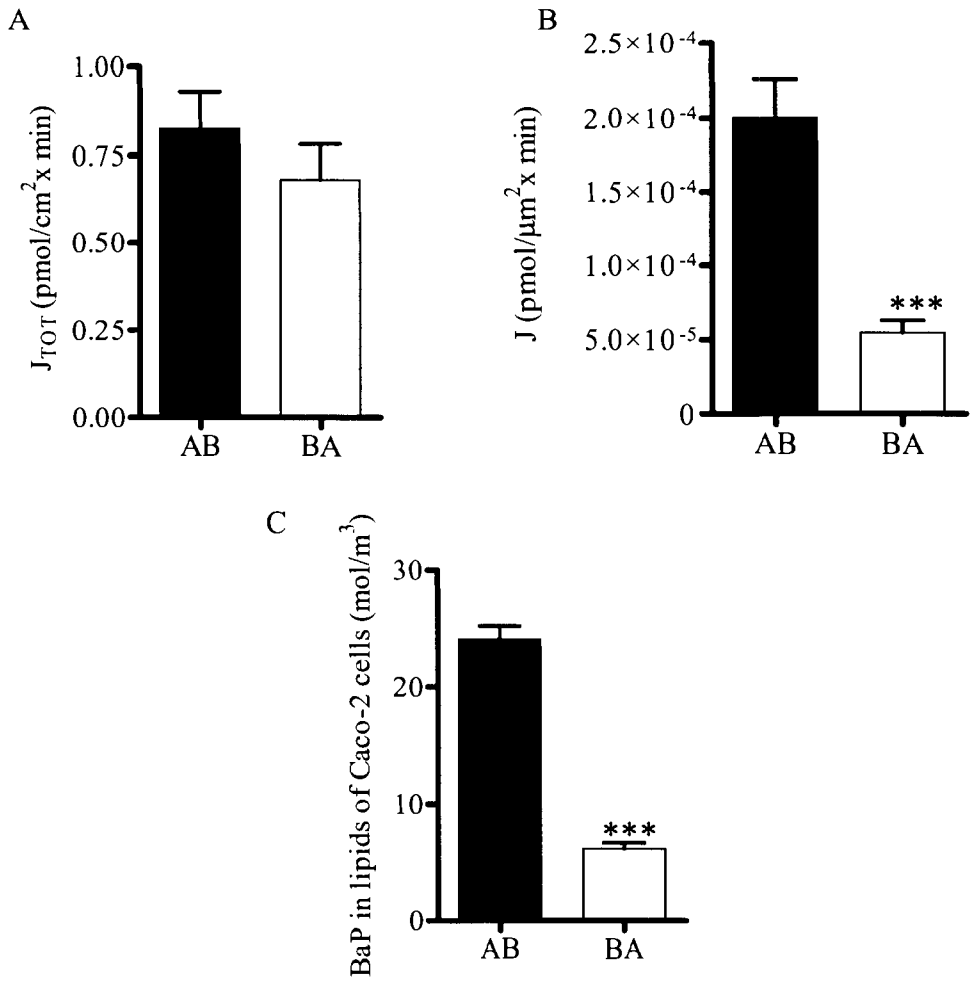

Figure 5-4. Effect of direction of exposure on uptake and transport of [^{14}C]-BaP bound to skim milk in the apical to basolateral (AB) and basolateral to apical (BA) directions after gastrointestinal digestion.

A) The cumulative amount of [^{14}C] appeared in the receiving (basolateral for AB and apical for BA) chamber over time. Linear regression analysis was used to calculate the flux rates J_{TOT} (pmol/ cm^2× min) from the linear portion of the slope. B) The flux rates normalized per surface area of the exposed membrane, J (pmol/µm^2×min). C) Concentrations of [^{14}C]-BaP in lipids of Caco-2 cells at 150 min of exposure presented apically or basolaterally. Asterisks indicate that concentrations of [^{14}C]-BaP in the lipids of Caco-2 cells exposed apically were significantly greater than when presented basolaterally, P<0.001. Note the difference in the Y-axis scales in A, B and C.

5.3.4 The effect of ageing on bioavailability of [^{14}C]-BaP bound to skim milk powder

Experiments were conducted with BaP-spiked skim milk powder samples that were aged for different periods to determine if ageing affected the mobilization of [^{14}C]-

BaP. [^{14}C]-BaP (1µg per 20mg of skim milk, w/w) was added to the skim milk powder and the skim milk powder was aged in the dark at room temperature for either seven days or six months. Solubilized milk in intestinal fluid was applied to the apical side of Caco-2 inserts as described above and the radioactivity in particulate and non-particulate phases of the apical fluid was measured over 5 h. During this time, the concentration of [^{14}C] in the aqueous fraction declined by almost 40% for both aged or non-aged skim milk (Fig.5-4A). However, the amount of [^{14}C]-BaP measured from aged skim milk compared to freshly spiked milk powder was significantly lower (Fig. 5-4A).

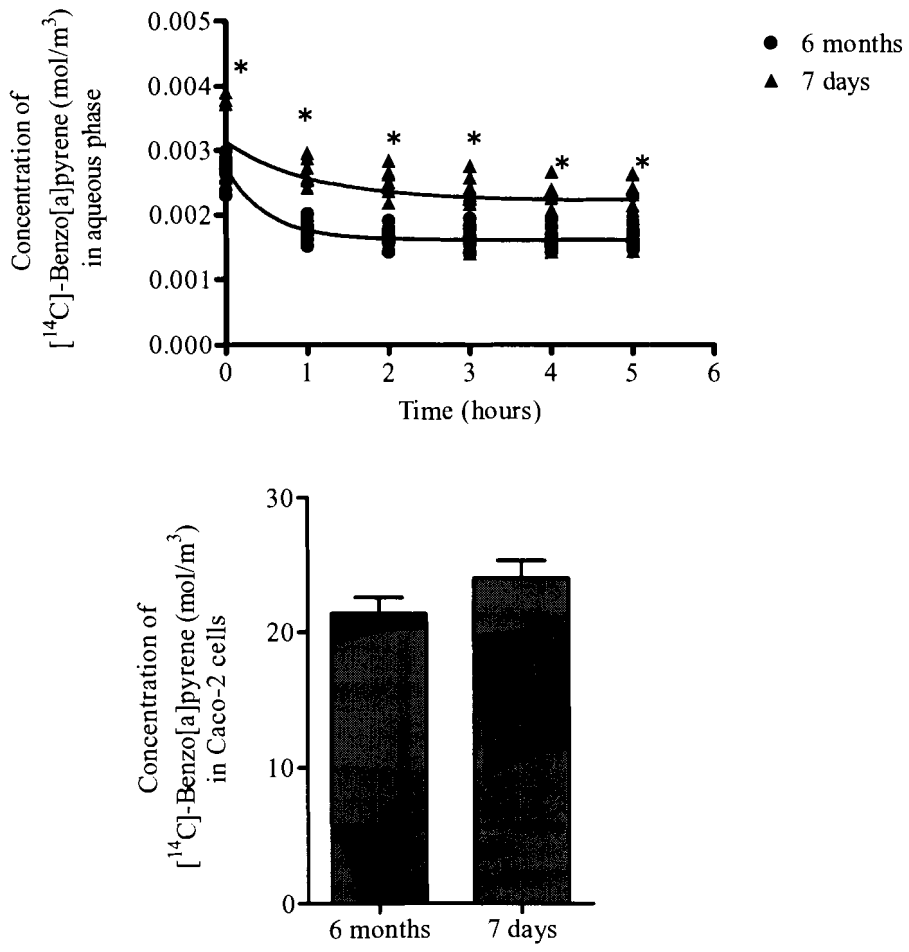

Figure 5-5. The effect of ageing on partitioning of [^{14}C]-BaP bound to skim milk powder into aqueous phase and Caco-2 cells.

A) Bioaccessible fraction - BaP mobilized into gastrointestinal fluids. An asterisk indicates that the values for skim milk aged seven days were significantly different from the values obtained with skim milk aged for six months; B) Bioavailable fraction (BaP sorption to membrane) Caco-2 cells after five hours of exposure. No significant difference was observed in [^{14}C] accumulated by Caco-2 cells between aged and non-aged samples. Note differences in the Y axis scales in A and B.

At the end of the transport studies (after five hours), the epithelial monolayers were gently washed and excised to measure the amount of sorbed radiolabeled material. We observed no significant difference in the level of [^{14}C]-BaP sorbed to Caco-2 cells (Fig. 5-4B) between aged and non-aged samples. Assuming that the fugacity capacity of the skim milk powder did not change during the four months of ageing (i.e., $Z_{AGED} = Z_{NON\text{-}AGED}$), and that the initial concentrations of BaP were the same ($C_{AGED} = C_{NON\text{-}AGED}$), it follows that the fugacities of the matrix prior to digestion remained unchanged regardless of the length of [^{14}C]-BaP exposure, i.e., $f_{AGED} = f_{NON\text{-}AGED}$ ($f = C/Z$). Despite significant decreases in the amount of [^{14}C] in the aqueous phase of aged samples (Fig. 4A), the amount of [^{14}C]-BaP that partitioned into the Caco-2 cell remained unchanged (Fig. 4B). Thus, measurements of mobilization alone would not have provided an accurate picture of the amount of [^{14}C]-BaP sorbed to the intestinal epithelium, i.e., the bioavailable fraction. These data supported by our previous studies with chrysene [208], where the fugacity capacity of EVA (Z_{EVA}) was found to be 4 orders of magnitude greater than fugacity capacity of aqueous compartment (Z_{AQ}), therefore changes in the mobilization into gastrointestinal fluid had no significant effect on the uptake.

5.3.5 Uptake of BaP/metabolites into Caco-2 cells over time

In the transport experiments, at each time point, the epithelial monolayers were gently washed and the amount of sorbed [^{14}C]-BaP was measured by LSC. Because BaP is sequestered almost entirely in fat [4], the Caco-2 concentrations were expressed on a volume lipid basis. The concentration of radioactivity found in Caco-2 lipids (Fig. 5-5) after six hours of incubation in intestinal fluids was approximately 2.5 fold higher than the concentration of BaP found in EVA film (Fig. 5-1B). This finding supports the results from our previous studies that comparing uptake of [^{14}C]-BaP or [^{14}C]-chrysene bound to soil into EVA and Caco-2 cells (see Chapter 4)[208]. From these studies, we determined that EVA film has a lower fugacity capacity for BaP compared to Caco-2 lipids, i.e., for BaP $Z_{Lipid} = 2.4Z_{EVA}$ (see Chapter 4). Because the relationship is linear over a large range of BaP concentrations, the concentrations in Caco-2 cells expressed on a lipid weight basis can be estimated from BaP concentrations in EVA film.

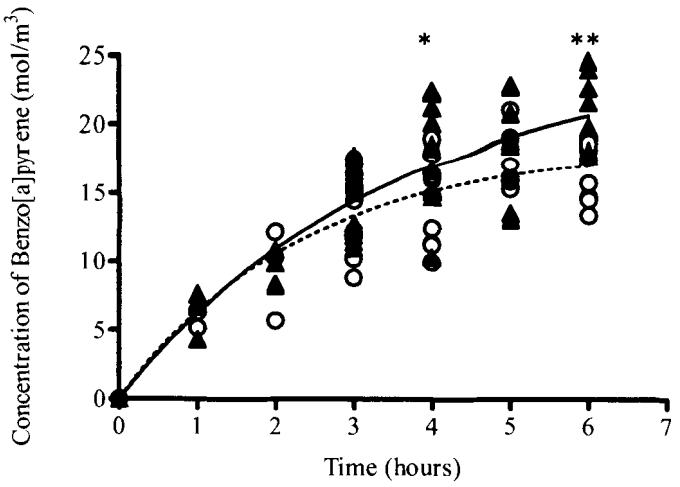

Figure 5-6. Levels of radioactive material in Caco-2 monolayers during six hours of exposure to skim milk powder contaminated with [^{14}C]-BaP in the presence of an inhibitor of CYP-mediated metabolism (α-naphthoflavone) (triangles), and without inhibitor (open circles).

Best fit lines were determined by non-linear regression (solid line (with inhibitor), dashed line (without inhibitor)). *An asterisk indicates that the values for inhibited Caco-2 cells were significantly different from the values obtained with metabolically active cells, at $P<0.05$ (*), $P<0.01$ (**). Note that concentrations on the Y axis are expressed in mol/m$^3_{LIPID}$ rather than μmol/m$^3_{LIPID}$.

It has been previously reported that Caco-2 cells exhibit increased transport of polarized metabolites towards the apical side, which can affect the rate of uptake of the BaP/metabolites into enterocytes. In the presence of metabolism by CYP isozymes up to 16% of the [^{14}C] was sorbed to the Caco-2 epithelial cells (Fig. 5-5). Addition of an inhibitor of CYP1A1, 1B1 and 3A4 (α-NF) increased the amount of radioactivity bound to cells, and significant differences in [^{14}C]-BaP were observed after 4h (Fig. 5-5). When CYP450s were inhibited, radioactive material was eliminated more slowly (k=0.282 h^{-1}) in Caco-2 monolayers compared to cells with active BaP metabolism (k=0.413 h^{-1}). The 2-fold difference in the rates was probably due to Phase I oxidation of [^{14}C]-BaP, which allowed faster elimination of the more polar metabolites from the untreated cells and support our earlier hypothesis about apical localization of CYP enzymes.

The rough estimates for transit times through the small intestine of healthy humans following ingestion of a standard meal showed that 50% of the ingested food would be emptied in 2.5-3.4 hours [220, 221] with a maximum prolonged transit of up to

six hours due to the presence of solids (i.e., fiber). We therefore used 6 h as the maximum incubation time in our studies. One goal of this study was to use a fugacity approach in order to describe the bioavailability of BaP from a digestible matrix. The classical fugacity approach assumes an equilibrium partitioning process; however, after 6 hours, our system has not reached equilibrium. In non-equilibrium conditions, rates can be used to describe transport processes (D), where D is the fugacity-based first order rate constant [243].

5.3.6 Measuring bioavailability of BaP bound to skim milk for metabolic conversion

The next step in our study was to measure the extent of metabolic conversion of BaP bound to skim milk powder during gastrointestinal digestion (Fig. 5-6). Previously, Buesen et al [115] reported that the major Phase II metabolites of BaP formed by Caco-2 cells were actively transported back to the apical (luminal) compartment of the tissue culture system and that the amount of Phase II metabolites peaked after a short period of exposure (four hours for transport and eight hours for metabolism studies). In their study, BaP was not bound to a solid matrix. In the present study, [^{14}C]-BaP bound to skim milk powder was subjected to full digestion with synthetic gastrointestinal juices and then this was applied to the apical side of Caco-2 monolayers. The amount of metabolite formation was measured exclusively in the apical aqueous phase over 6 h of incubation.

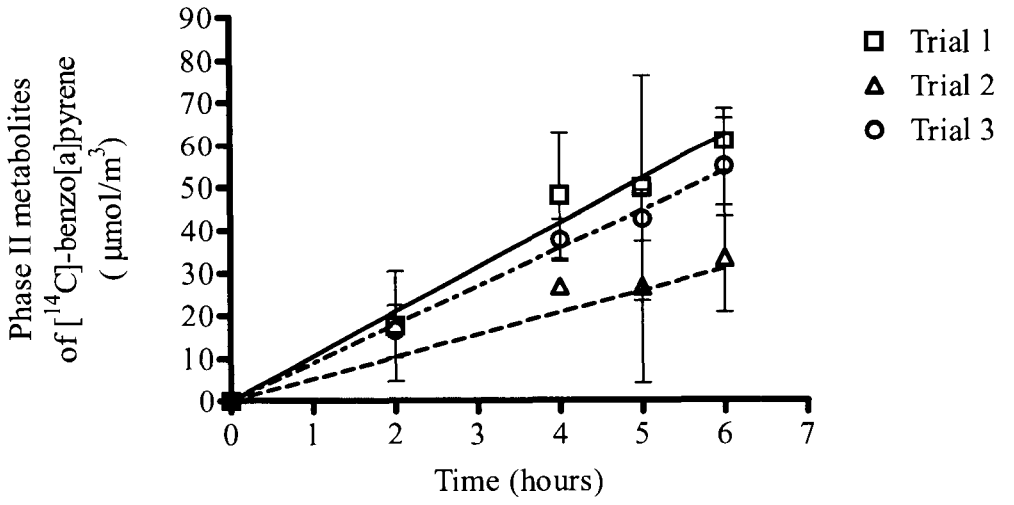

Figure 5-7. Extent of metabolic conversion of bound BaP.

Appearance of Phase II metabolites in the apical compartment during six hours of intestinal digestion.

[^{14}C]-labeled material ([^{14}C]-BaP and [^{14}C]-BaP metabolites), was extracted from the apical phase and BaP and polar metabolites were separated by bidirectional radio-TLC as described in the Materials and Methods. The radioactivity was extracted into BCS for quantification by liquid scintillation counting. Caco-2 cells converted BaP to both Phase I and Phase II metabolites only when a CYP inducer (β-NF) was added 24 h prior to the experiment (data not shown). Addition of α-NF abolished the appearance of Phase II metabolites (data not shown), indicating that the measured levels were specific for BaP metabolism, as previously reported [115, 227]. The level of Phase I metabolites did not increase during the experiment. Phase II metabolites accumulated in the apical compartment throughout the 6-hour period (Fig. 5-6) reaching a maximum of 75 µmol/m^3 (1.8% of the initial radioactivity). This is 40-fold lower than the value reported by Buesen et al [115], who showed that Caco-2 metabolized >70% of total free BaP to Phase II metabolites. The lower rates of metabolite formation are likely because the [^{14}C]-BaP was bound to skim milk powder in our experiments, and this reduced the bioavailability of BaP. Although binding to lipids probably dominated the interaction of BaP with skim

milk, proteins may also reduce bioavailability [244]. The extent of binding of HOC to protein depends on the affinity of an HOC for hydrophobic protein binding sites, HOC free concentration, and the protein concentration. For example, Seiber et al [244] showed that the relative potencies (EC_{50} values) of several halogenated hydrocarbons were strongly reduced by addition of 4% bovine albumin (w/v).

It has been previously reported that the highly polar metabolites of BaP (Phase II) are subject to an apically-directed transport [115]. In the present study, the radioactivity in the basal media was below the limits of detection. It has been demonstrated previously by Cavret et al [123], that the majority of the radioactivity recovered in the basal medium was metabolites. Almost all the BaP that reached the basal compartment in their studies seemed to have been in a metabolized form, an observation which is supported by the in vivo observation with fish and rats that about 90% of ingested BaP which can be withdrawn from the portal vein has been metabolized [24].

We observed a complete solubilization of skim milk as a solid matrix for BaP during gastrointestinal digestion, i.e., BaP was in the soluble fraction in the digestive fluid. Hack and Selenka [32] measured mobilization of PCBs and PAHs from contaminated soil using artificial gastrointestinal digestion and suggested that measurement of the mobilized fraction can be a good estimate of the bioavailable fraction. Because we employed a sequential exposure of the contaminated matrix to gastric digestion, followed by intestinal digestion and the introduction of the mobilized fraction to cultured human enterocytes, we were able to measure the fraction sorbed to the epithelium or its surrogate, which allows us to distinguish between the soluble, and the sorbed fraction that can reach the systemic circulation. If oral bioavailability is defined as the fraction of administered dose taken up into cells or reaching the systemic circulation of the organism then the fraction that is soluble in the gastrointestinal environment and available for absorption is defined as bioaccessible fraction [231]. Despite significant changes in the amount of [^{14}C] in the aqueous compartment that represents the bioaccessible fraction, the amount of [^{14}C]-BaP that partitioned into the Caco-2 cell or its surrogate remained unaffected. Thus, measurements of bioaccessible fraction alone would not have provided an accurate picture of the bioavailable fraction. In other words, the bioaccessible fraction did not always parallel the bioavailable fraction.

Furthermore, our system showed that even if food is solubilized in gastrointestinal fluids, its presence can reduce the bioavailability of the hydrophobic contaminants in the intestine.

CHAPTER 6: GENERAL DISCUSSION

Anthropogenic activities have created enormous amounts of chemicals that are eventually released into our environment, either deliberately for industrial or agricultural purposes or due to accidents. The Canadian government has established a Priority Substances List (PSL) that identifies substances to be assessed on a priority basis to determine whether they pose a significant risk to the health of Canadians or to the environment [3]. Currently there are ~23,000 listed substances that are awaiting evaluation for their bioaccumulation potential as one of the persistent, bioaccumulative, toxic (PBT) screening criteria. The potential of a chemical to bioaccumulate in organisms and food webs depends upon the properties of the chemical (e.g. hydrophobicity, lipophilicity, and resistance to degradation), environmental factors (e.g. salinity, temperature and concentration of other organic chemicals), biotic factors (e.g. the organism's mode of feeding, trophic position, lipid content and metabolism), and bioavailability (e.g. current chemical inputs, transport mechanisms, and degree of contamination) [145]. In general, the bioaccumulation potential of organic chemicals is linked to their lipid solubility. At present, the most accurate method for assessing the bioavailability of solid-bound organic contaminants involves animal models; however, as these methods are time-consuming and expensive, animal testing of individual compounds is impractical for large-scale screening. Therefore, new rapid methods are needed as a screening tool for evaluation bioaccumulation potential of these compounds and to provide an accurate estimate of the oral bioavailability for use in human health risk assessments.

This research focused on the mobilization of HOC from solid matrices followed by intestinal exposure, because this route is believed to be the most significant route of exposure for HOCs. The ultimate goal was to develop and evaluate a rapid, in vitro system that will be reproducible and inexpensive for predicting the oral bioavailability of

particle-associated chemicals, as one of the factors that can affect bioaccumulation potential of these chemicals.

As a result of the relationship between lipophilicity and bioaccumulation potential, considerable research has focused on determining the lipid solubility of the chemical (i.e. bioavailability) using the octanol-water partitioning coefficient (K_{ow}) as the measurement tool [145]. However, there are several problems which arise when relying on this measure alone. Firstly, the many environmental factors mentioned above are not taken into account when using a K_{ow}-based model. These factors can affect the true bioaccumulation potential of the chemical. In addition, the simple K_{ow}-based models were derived from observations and biomagnification models derived for aquatic organisms [139, 142, 245]. These models are inappropriate for assessing the bioaccumulation potential for many other organisms, particularly mammals, as they tend to underestimate the actual risk for higher organisms. Furthermore they do not take into account matrix effects which may adversely or otherwise affect risk. It is important to emphasize that the use of K_{ow}-based models is useful but inadequate to categorize substances with bioaccumulation potential. Given the fact that thousands of chemicals are listed on the PSL, and very little data beyond the K_{ow} values is available for most of them, an in vitro screening method would be a valuable addition to the arsenal of K_{ow} and animal models, as a more practicable test for such a large number of registered chemicals.

To develop a complete in vitro testing model for assessing bioaccumulation potential, it is important to examine the mechanisms driving the biomagnification processes, which include dietary absorption, various elimination processes, metabolic transformation, and growth dilution [142]. This work was focused on evaluating an in vitro model that was determined to be suitable for measuring at least two of these processes and can account for the effect of matrix binding.

The bioavailability of ingested HOCs, such as PAHs, depends on mobilization of these compounds from the surrounding matrix under physiological conditions within the gastrointestinal tract. Various in vitro models and test procedures have been described in the literature to estimate the oral bioavailability of organic pollutants. Several studies have measured the oral bioavailability of organic contaminants bound to solid matrices,

such as soil. In these systems, various contaminants bound to matrices are incubated in a low-pH solution for a period to mimic transit time in the stomach. Enzymes and organic acids are added to simulate gastrointestinal juices [12]. The pH is then increased to nearly neutral, and incubation continues to mimic the transit time in the small intestine. To determine the effect of mobilization or gastrointestinal solubilization of PAHs and PCBs from contaminated soil, Hack and Selenka [32] conducted studies using an artificial gastrointestinal model that simulated physiological conditions in two steps: stomach digestion and intestinal digestion. However, these investigators did not include in their test the exposure of the mobilized fraction to intestinal epithelium or an artificial surrogate. Although the model [32] provided valuable information, the authors may have erred in concluding that since the solubilization of HOCs in gastrointestinal juices is a dominant factor for their absorption, the mobilized amount of the contaminant can be a good estimate for the bioavailability of the screened substance, implying that the bioaccessible fraction can be translated into bioavailable fraction. If oral bioavailability is defined as the fraction of the administered dose bound to cells or reaching the systemic circulation of the organism, then the fraction that is soluble in the gastrointestinal environment and available for absorption is defined as the bioaccessible fraction [231]. In our model, we employed a sequential exposure of the contaminated matrix to gastric digestion, followed by intestinal digestion and the introduction of the mobilized fraction to cultured human enterocytes. An evaluation of the fraction sorbed to the epithelium or its surrogate allows us to distinguish between the mobilized, (bioaccessible) fraction of the contaminant, and the sorbed (bioavailable) fraction that reaches the systemic circulation.

Another study by Van de Wiele et al [246] used an in vitro gastrointestinal digestion model in the form of a Simulator of the Human Intestinal Microbial Ecosystem (SHIME) reactor. This model had five compartments, simulating stomach and small intestinal digestion, followed by an artificial colon, containing fecal bacteria. Mobilized PAHs were exposed to two genetically engineered yeast strains and the binding of these mobilized contaminants or their metabolites were evaluated. This study reported release of less than 1% of the total PAH input into each compartment, which was much lower than the mobilized fraction found in Hack and Selenka's models (20 to 60%). In the

present study, we found up to 48% of the chrysene added to forest soil was mobilized after gastrointestinal digestion and sorbed by the EVA (surrogate intestinal epithelium). However, we observed that the aqueous phase reached equilibrium very quickly (within the first two hours) and had a limited capacity for chrysene (4%), due to its hydrophobic nature. The SHIME reactor is different from other in vitro intestinal models, because it simulates the entire GIT taking into account the enzymatic process in the stomach and duodenum as well as the different characteristics of the microflora along the colon [99]; however, it does not include a sorptive epithelium. On the other hand, all physiologically significant absorption of nutrients from digestion occurs in the small intestine, the mucosal surface of which is greatly increased providing a large area for uptake. Of the total amount of aqueous phase (water) that enters the small intestine (7 L/ 24 h) only ~600 ml reaches the colon. In addition to the reduced liquid in the undigested food, the fecal matter that moves along the colon with its much smaller area for absorption of water and electrolytes than the small intestine (9% of total), has less opportunity to be sorbed and transported to the systemic circulation. That raises the question of the necessity of including the colon in in vitro models of oral bioavailability.

There are a few reports that describe attempts to evaluate in vitro the bioavailability of hydrophobic contaminants using a Caco-2 cell monolayer. Oomen et al. [122] showed that up to 54% of polychlorinated biphenyls (PCBs) were mobilized from a spiked artificial standard soil after in vitro gastro-intestinal digestion, but <10% of these organic contaminants were transported across the Caco-2 monolayers to the basolateral compartment. These authors suggested that bile salts play a central role in mobilizing PCBs and lindane from a matrix and making those contaminants bioaccessible. They found that 20-25% of the total amount of hydrophobic contaminants were sorbed by bile salt micelles: However, when we examined the effect of varying the constituents of our artificial gastro-intestinal fluid on the transport of chrysene from soil to surrogate epithelium, we found that the absence of bile salts made no difference to the uptake. The difference between our studies may be due to the fact that we used ~2 fold less bile salts than Oomen et al [122]. Normally there are 1 to 2 g of bile salts that are circulating in the intestine [98], therefore 2 g /7 L /24 h or ~0.3g/L. In other words, 0.4g/L in our model seems to be close to physiologically relevant bile salts concentrations. In contrast, we

found that the pH shift from 2.5 to 7 was the most important factor that mobilized PAHs from the matrices (soil or food). In agreement with work of Kögel-Knabner et al [247], our study showed that the mobilization process was highly dependent on the amount and ionic strength of the organic content of the matrix. However, it is important to note that in most of these studies, including ours, the soil matrix used for the study was artificially spiked under laboratory conditions rather than collected from naturally-weathered, contaminated sites. Van de Wiele et al [99, 246] used historically contaminated soils, therefore the low mobilization values in the GI fluids can be explained by possible sequestration of the contaminants. It is possible that artificial spiking introduces an artefact into the experimental setup, by using the most convenient solvent as a carrier [30, 214]. It is well acknowledged that uptake clearance and bioaccumulation factor estimates between labelled and unlabelled compounds varied by several factors (from 2 to 7) [199]. A few studies show that spiked contaminants are more bioavailable than equivalent field samples, which had a far longer time for sorption or are associated with different sedimentary phases [200]. Carmichael et al [248] reported higher desorption rates for spiked sediments, while Varanasi et al [249] showed greater accumulation of PAH in amphipods from freshly spiked sediments. These data indicate that the bioavailability of a spiked compound may not be equivalent to the same compound in environmentally contaminated sediments, but a more careful analysis would be required to form firm conclusions on this matter. We believe that radiolabeled compounds provide an advantage to those researchers who wish to study mechanisms and test assumptions because of the high sensitivity of detection, but may not be suitable as surrogates to predict the environmental fate of naturally weathered contaminants.

It is acknowledged that different matrices are known to affect bioaccessibility and thereafter bioavailability values. For example, different soils can affect the bioavailability of the contaminant [12, 194]; many authors believe that the quantity and the quality of the soil organic matter influences PAH sorption and desorption processes [79, 87, 89, 215]. In addition, Chiou et al [250] found a more pronounced sorption of PAHs to sediments than to soils and assumed that sediment organic matter is less polar. Our experiments showed that Sydney Harbour sediment had an organic content similar to soil with low percent organic matter, but rates of desorption from this sediment were similar

to that from soil with a high percent organic matter. Our system was able to show differences between behaviour of sediment and soil, which demonstrates again the utility of this in vitro model.

Because bioaccumulation data are relatively limited for chemicals currently in use, 99% of the preliminary bioaccumulation assessments rely on Quantitative Structure Activity Relationship (QSAR) and K_{ow}-based model estimates for aquatic organisms without consideration of metabolic processes. As Caco-2 cells were originally derived from a human cell line, they morphologically and biochemically resemble human intestinal epithelium, and, most importantly, possess the metabolic systems responsible for major detoxification of xenobiotics. The use of Caco-2 monolayers in our in vitro model positions our system as uniquely useful for studying the metabolism of matrix-sorbed chemicals in vitro. Furthermore, by measuring the metabolism of xenobiotics added over a range of concentrations (Michaelis-Menten equation), the kinetics of enzyme oxidation of xenobiotics could be studied. Thus, the proposed in vitro digestion model is a promising tool for estimating the bioaccumulative potential of the particle-associated metabolizable toxic compounds ingested orally.

There are two general approaches to quantify bioaccumulation in the organism: the empirical approach (experimental measurement of concentrations) and a mechanistic mass balance model in which the various uptake and loss processes are quantified. [243]. Although the experimental values measured in many empirical experiments are prone to inaccuracy due to biological variability, these data are more likely to represent "real-life" conditions and thereby allow researchers who use them as a starting point for prediction to more closely meet the aim of their model. In contrast, mass balance models require more input data regarding the chemical and the organism, such as rates of chemical uptake and clearance, feeding rates, and absorption efficiencies. The ultimate goal of this study was to use the empirical data to generate a fugacity-based model in order to describe bioavailability and bioaccumulation processes in humans. The classical fugacity approach describes an equilibrium partitioning; however, most of the time, our model describes non-equilibrium situations. Therefore we have chosen the mechanistic model which uses first order rate constants as first described by Neely [251], which is ultimately identical to the fugacity method. Rates can be expressed as transport products (Df),

where is D is fugacity-based rate constant. Transport values (D) of flow, diffusion and reaction processes can be expressed as transport products for uptake and loss processes, where fugacity applies to the same source, and mass balance equations can be generated and solved [243]. In the context of fugacity, bioavailability in our system is basically a decrease in fugacity (referred to as sorption) caused by the greater fugacity capacity in the tissue (small intestine epithelium) than the fugacity capacity of the food. The bioaccumulation process can be also explained using the fugacity concept as the ratio between the fugacity of the chemical in the food and the fugacity of the chemical in the organism. Thus, simple empirical measurements of dietary absorption can be used to screen chemicals for bioaccumulation potential.

The data presented in this thesis provides further evidence that the transport of hydrophobic chemicals between tissues or "compartments" of the body is fugacity driven. Because all the data presented from various experiments done over a period of 4 years have been converted and presented in mol/m^3, the experiments with chrysene and benzo[a]pyrene experiments are easy to compare. The fugacity theory predicts that the proportion of hydrophobic chemical that will partition to the lipids or equivalent (octanol, thin films) from the matrix will be higher for the HOC with lower K_{ow}. In each of our experiments, proportionately more chrysene (log K_{ow} =5.61) was sorbed to either surface (Caco-2 or EVA) than was BaP (log K_{ow} =6.04). Weston and Mayer [200] and Mayer et al [252] also observed the K_{ow} dependence.

The units used in many published works to express bioavailability in different organisms or models vary, leading to possible misinterpretation. Often the bioavailability of a chemical is expressed as the fraction of the total applied, which was mobilized, or sorbed. Since hydrophobic contaminants sequester almost entirely in fatty tissues it may be essential to express the values on a lipid-normalized basis. The values, if expressed on the lipid volume basis, should be comparable even if the measurements are from different tissues or different organisms. My own work illustrated this point well. In experiments where both EVA and Caco-2 cells, on the same type of coverslip are allowed to sorb PAH to near equilibrium, EVA films accumulated approximately 10 times more of chrysene per m^3 than whole Caco-2 cells. However, when the data were normalized to the lipid volume of the cells, the biological lipid bound 6-fold more chrysene per m^3 than

the equivalent volume of EVA. This can be due to structural differences of EVA and biological lipids bilayers. Lipid bilayers are amphipathic in that they have hydrophilic polar heads pointing out and the hydrophobic portion forming the core, in with various membrane protein molecules embedded. They are three major classes of membrane lipid molecules – phospholipids, cholesterol, and glycolipids and different mixtures of lipids are found in the membranes of different cell types. In contrast, ethylene-vinyl acetate is a copolymer membrane that consists of only hydrophobic substituents.

Another illustration of potential problems with the interpretation of units is as follows: when we compared two different phases from the same system as percent data or as normalized mol/standard volume data, completely different interpretations could be made. For example, the mobilized fraction of the BaP in aqueous phase (gastrointestinal fluid), which is defined as the bioaccessible fraction of the BaP, was found to be 20 to 30 % of the total BaP, and the sorbed fraction to Caco-2 cells (bioavailable fraction) achieved only up to 11% of total BaP. However, when converted to molar amount per standard volume of BaP on a volumetric basis (per m^3), the bioavailable fraction was 100-fold higher than the bioaccessible one. Therefore, in order to 'predict' bioavailability using the fugacity approach, all concentrations should be expressed in units of amount per volume making the partitioning coefficients dimensionless [243].

Our in vitro model has some limitations that may affect its validity. The use of radiolabeled compounds to follow transport throughout the system was found to provide an exquisitely sensitive method to study partitioning and it allowed us to perform a full mass balance of the system. Furthermore, the rapidity with which samples can be analysed allows the rapid accumulation of data (hundreds of samples per day). However, it is acknowledged that radioactivity cannot be used to predict environmental fate of in situ contaminants (weathered soils, contaminated foodstuffs.) Furthermore, it is not possible to apply this technique to the 23,000 chemicals outstanding in the Priority Substances List, as few will be available in a radioactive form. The use of Gas or Liquid Chromatography Mass Spectrometry (GC-MS or LC-MS) can be used as an alternative for chemical analysis. Some advantages to using GC-MS or LC-MS as the analytical tool are that it will permit the analysis of mixtures of contaminants, such as those found in environmental samples. GC-MS/LC-MS techniques not only separate the components of

the mixture, but also identify the structure of unknown compounds. They can be used, of course, with chemicals for which radioactive forms are not available.

It should be recognized that the research in this thesis was focused on development and validation of an in vitro system. Another merit of using radiolabeled compounds was that it revealed limitations of the commercially-available tissue culture systems for measuring the transport of hydrophobic chemicals. We found that the polystyrene cell supports strongly sorbed hydrophobic compounds, and that this sorption could not be blocked by any of a variety of proteins or other substances used to coat the support. Therefore, we have initiated development of a custom-made glass-based system that may provide a more suitable alternative for non-polar compounds (See Appendix for more details).

Apart from the scientific standpoint, measurements of bioaccessibility and bioavailability obtained through in vitro gastrointestinal models may be important from the regulatory or public health perspective and for human health assessment in particular. Our model also makes possible site-specific investigations for environmental risk assessments. The use of artificial digestive fluids allow for routine and extensive use and help to circumvent ethical and financial burdens, as well as the technical constraints of using laboratory animals. By estimating the fraction of contaminants available for absorption, modelled risk will develop into a more realistic and applicable resource. At this time, it is hard to say whether a generic standard could be produced, for instance relative estimates compared to the known bioavailability of BaP from a defined matrix. Perhaps not, because it is acknowledged that bioaccessibility and bioavailability of hydrophobic compounds are dependent on the type of compound and the type of matrix. The physiologically-based model combined with exposure to a cultured gastrointestinal epithelium presented in this thesis is a simple, bioavailability-predictive test. If validated, such a test could provide a rapid and inexpensive method for developing more accurate exposure estimates for use in human health risk assessments.

"Validation" is generally assumed to mean that the in vitro model is shown to correlate with results from an animal model, and that the correlation is consistent across a range of soil types and forms of contaminant. For example, there are extraction methods

which involve only gastric digestion. The European Standard for Safety of Toys has used such a method since 1994 to assess the degree of metal dissolution in a simulated gastrointestinal tract environment and to evaluate the bioaccessibility of eight metals from children's toys [231]. Another variation of an in vitro extraction, the PBET method described by Ruby [12] was found to deliver a strong correlation with two in vivo models in tests for lead. At this time, according to reports from the Solubility/Bioavailability Research Consortium (SBRC) [34], it is only a matter of time before this model will be in routine use to develop relative bioavailability estimates for use in human health risk assessment. The SBRC is a collaborative effort between scientists from academia, government, consulting firms, and industry. The main goal of this organization is to develop and validate in vitro methods for estimating the relative bioavailability of metals in contaminated soils [231].

Thus far, there is very limited information regarding the relationship between physiologically-based in vitro models and the results from in vivo studies for the bioavailability of organic compounds. Weston and Mayer [199] compared the in vitro digestive fluid extraction of sediment-bound BaP and phenanthrene with other approaches: uptake clearance, absorption efficiency, and bioaccumulation factors. Uptake clearance represents the amount of sediment that would have to be completely cleared of PAHs to provide a measurement of body burden. The absorption efficiency is measured by the comparison of PAH concentrations in the foregut and rectal sediments of worms. The authors found that the experiments with BaP yielded estimates of digestive absorption efficiency of 27% to 35% (depending on the sediment), similar to the extent of in vitro solubilization by digestive fluid from the same sediments (13-42%), which means that in their study, the bioavailable fraction was correlated with the bioaccessible fraction. However, it was also pointed out that this correlation was not significant due to the small number (4) of data points [199]. Although absorption efficiency is thought to be sediment and species specific, there was generally good agreement among the four methods on the relative bioavailability of BaP from six sandy sediments. Our in vitro results for BaP and chrysene experiments agree with in vivo data from Weston and Mayer.

It should be noted that, for metabolizable substances, such as BaP, where metabolites may have greater toxicological significance than the parent compound, it may

be useful to generate parallel models for both the parent compound and metabolites and both of them should be tested against in vivo data.

Possible applications of this model

There are two possible applications for the models (EVA and Caco-2) presented in this thesis: 1) as a screening tool to assess bioaccumulation potential for the large number of registered chemicals and 2) as an in vitro model to estimate the oral bioavailability of sorbed contaminants for human health risk assessments. The physiologically-based extraction technique (PBET) combined with exposure to cultured intestinal enterocytes or its surrogate, EVA thin film, may improve the input data used for both screening and human health risk assessments. In addition to significantly lowering costs and ethical considerations, our in vitro models allow for a systematic investigation of variables such as the manipulation of matrix and/or digestive fluid composition, which would not be feasible in vivo.

The EVA model for screening HOCs for bioaccumulation potential

The EVA model (PBET combined with exposure to EVA thin film) can provide a rapid, practical and inexpensive solution for screening a large number of HOCs for bioaccumulation potential. Personnel can be trained quickly as the model does not require special cell culture expertise. EVA is durable and can withstand long incubation periods (24-48h), which permits quick absorption kinetics resulting in chemical equilibrium. As mentioned previously, equilibrium partitioning is necessary to apply the fugacity-based model of bioavailability and, in essence, bioaccumulation processes. In the fugacity based approach, bioavailability is simply an increase in epithelial fugacity attributable to uptake into epithelial membrane (EVA thin film) caused by intrinsic capacity of the membrane ($Z_{MEMBRANE}$) being greater that fugacity capacity of the digestive fluid (the mixture of gastrointestinal fluids and sorbent, such as food or organic matter) (Z_{GIF}).

The Caco-2 model to estimate oral bioavailability adjustment factors in human health risk assessments

At present, the amount of the contaminant that is chemically extractable from a solid matrix is considered the exposure dose, i.e., the bioavailability is 100%. However, the results in this thesis clearly showed that sorption to a solid matrix can reduce the bioavailability of a contaminant. Several regulatory agencies (e.g., Health Canada,

Environment Canada, and Ontario Ministry of Environment) have recognized the need for oral bioavailability adjustment factors when estimating exposure dose, in particular for soil/sediment-borne contaminants (Health Canada Bioaccessibility Workshop Proceedings, Toronto, ON, August 30-31, 2005). How can these factors be estimated? True bioavailability can only be determined by in vivo studies (animal testing), even there interspecies extrapolations are required. To address this problem, our in vitro model using Caco-2 cells combined with physiologically-based gastrointestinal extraction technique under non-equilibrium conditions, could be employed to determine the extent of bioavailability in vitro. For example, a standard amount of contaminated matrix (e.g., 10 mg contaminated soil or sediment per insert) could be extracted in simulated gastrointestinal fluids and incubated with Caco-2 cells, and the concentrations of the contaminant in the different compartments of the system (e.g., mobilized amount into gastrointestinal fluids, as well as sorbed into cell fraction) after 5 hours of simulated gastrointestinal digestion can be measured. The use of Gas or Liquid Chromatography Mass Spectrometry (GC-MS or LC-MS) can be used for chemical analysis. Furthermore, Caco-2 system allows quantitative assessment of metabolic conversion of metabolizable compounds. GC-MS/LC-MS techniques not only separate the components of the mixture, but also will be useful to identify different metabolites of xenobiotics. The amount sorbed into the cells plus the amount present in the basal compartment would be considered as the 'bioavailable' amount. Since hydrophobic contaminants sequester almost entirely in fatty tissues it may be essential to express the values on a lipid-normalized basis. The values obtained in vitro, if expressed on the lipid volume basis, can be compared even if the measurements are from different tissues or different organisms. If the lipid-normalized bioavailable amount were divided by the amount that is chemically extractable from the same quantity of matrix, this would be considered as the percent bioavailable fraction. However, whether the bioavailable amount measured in vitro is directly related to the actual amount taken up in the human GI tract is currently unknown. Validation using a variety of relevant animal models (rodents, pig) is required before such an extrapolation is possible for human health risk assessment.

Because the physiologically-based extraction technique (PBET) was based on the anatomic and physiological characteristics of humans, it is potentially the most accurate

and practical in vitro approach for estimating bioaccessibility in humans. However, because PBET alone does not measure absorption into actual tissue, based on the results presented in this thesis it cannot be a reliable measure of bioavailability. The combination of PBET with Caco-2 cells can help to estimate the relative bioavailability of sorbed contaminants. The application of this in vitro method could yield valuable data that would reduce the uncertainty inherent in exposure dose determination, and thereby become a standard test in human health risk assessment.

APPENDIX

We initially chose to study [^{14}C]-pyrene as a model hydrophobic compound (log K_{ow}=4.88). This was because it has an excellent safety record, while being chemically similar to benzo[a]pyrene, a potent carcinogen of great concern, as it is widely dispersed in the environment. However, we found that significant amounts (60-70%) of the pyrene bound to the commercial tissue culture transport system, i.e., the polystyrene cell culture insert supports and wells, and to the polyethylene terephthalate (PET) membrane on which the cells are grown (Fig. A-1B). This high level of background binding would have invalidated the mass balance analysis that we do for each experiment. In addition, this non-specific binding would have interfered with fugacity measurements, as it would provide another compartment ('sink') for HOCs in the cell culture system. In order to overcome this problem, we screened a large number of coatings (gelatine, serum proteins, poly-l-lysine, dextran sulphate to see whether we could reduce the non-specific sorption to the polystyrene and PET inserts. None of the coatings significantly decreased the binding of pyrene (Fig. A-1A, B).

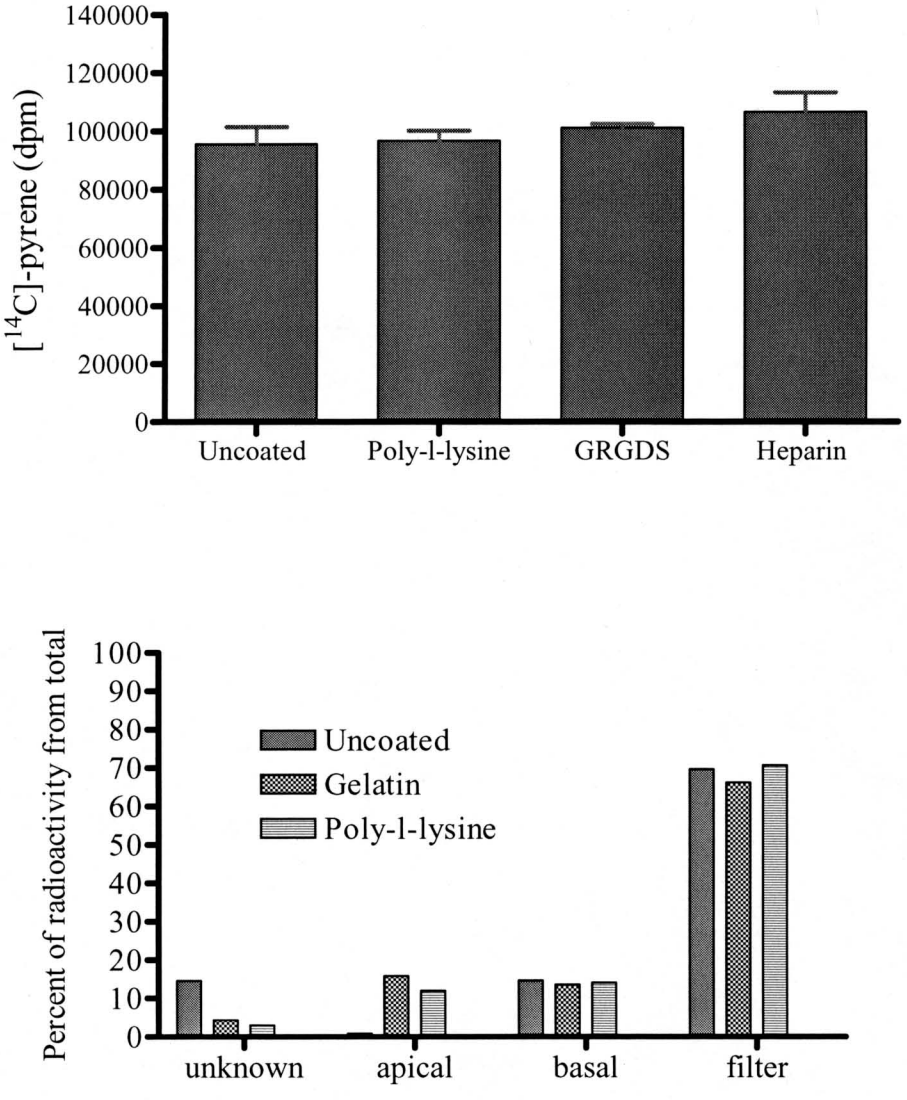

Figure A- 1. PET cell supports strongly sorb hydrophobic compounds ([^{14}C]-pyrene) even when pre-coated with polar materials.

A) Binding of [^{14}C]-pyrene to the cell culture PET membrane without pre-treatment (uncoated) and with pre-treatment with poly-L-lysine, GRGDS or heparin sulphate proteoglycan. B) Binding of [^{14}C]-pyrene to the cell culture plate and PET inserts without pre-coating (uncoated) and with pre-coating with gelatine or poly-l-lysine. Apical and basal represent the compartments above and below the PET filter. Most of the radioactivity (70% of added [^{14}C]-pyrene) bound to the PET membrane. No cells were present.

None of the commercially-available insert materials were suitable for non-polar compounds. Most of the applications of Caco-2 cells on these cell culture systems are for pharmaceutical agents and metals, which have relatively high water solubility. We then

tested the hydrophobic compound-binding properties of a glass-based system. We found low binding with BSA-coated glass fiber filters (Figure A-2).

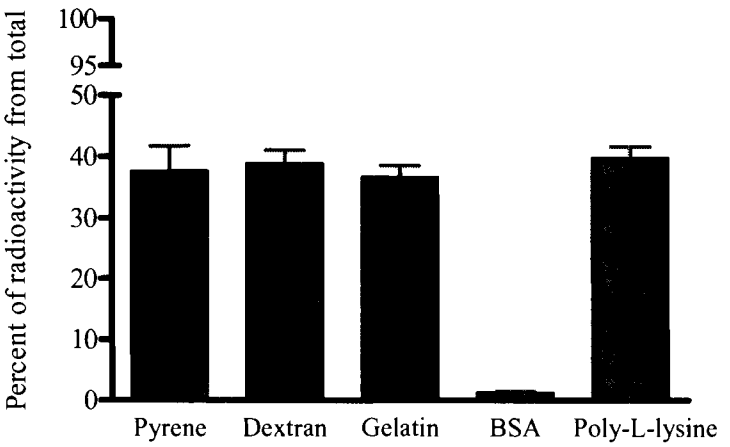

Figure A- 2. Adsorption of [^{14}C]-pyrene to glass filters in the presence of various coatings.

Filters were coated with unlabelled pyrene, dextran, gelatin, bovine serum albumin (BSA) or poly-L-lysine and dried. [^{14}C]-pyrene was added in buffer and incubated for 4 hours; the filters were washed and the radioactivity bound to filters was determined by LSC.

We determined that lower binding is seen with glass fiber filters coated with serum proteins (Fig. A-3), therefore we used BSA-coated glass fibre filters for our experiments.

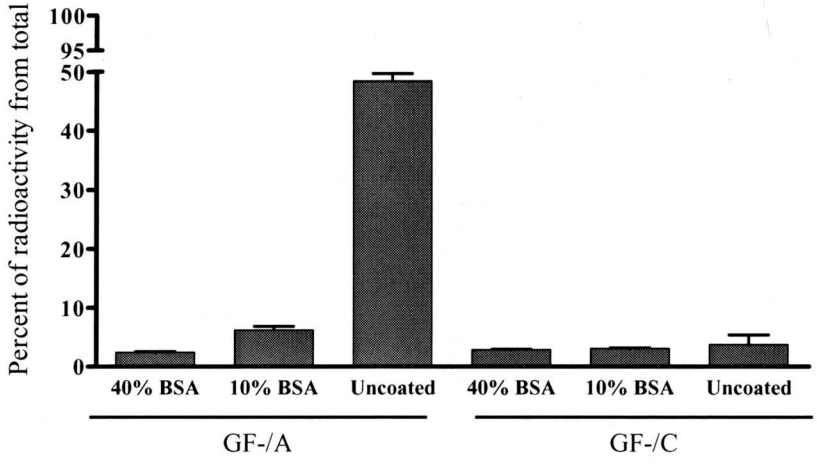

Figure A- 3. Binding of [^{14}C]- pyrene to the different Whatman glass fiber filters.

The lowest binding of [^{14}C]-pyrene was found with GF-/C filters coated with 10 and 40% of BSA. No significant difference was found between 10 and 40% of serum proteins, therefore we decided to use 10% BSA for coating glass fibre filters to be used in tissue culture.

To reduce non-specific binding to the polystyrene housing for the filters, we had a custom glass cell culture apparatus built by Scientific Glassblowing of Richmond BC. The design is shown on Figure A-4.

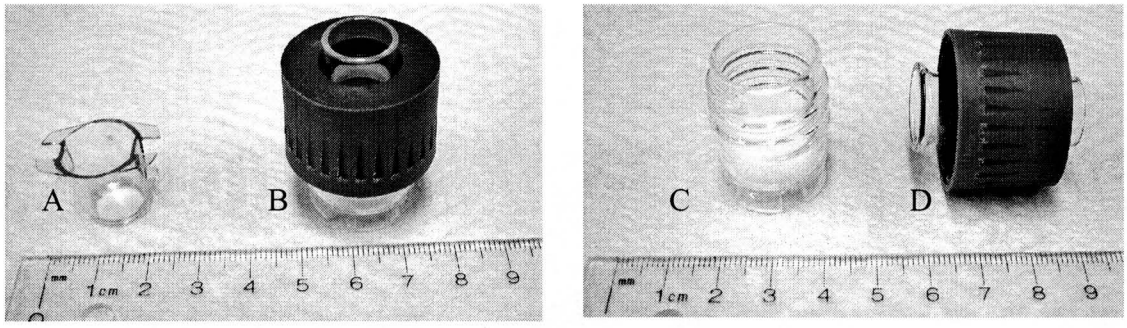

Figure A- 4. Side view of the cell culture inserts: commercially available (A) and a custom-made glass Caco-2 cell culture module (B-D).

Cells were grown on glass fiber filters which were placed on top of the glass frit (in chamber shown at left). The filter was secured by tightening the screw cap (red) to join the apical chamber (D) to the rest of the unit. An assembled unit is shown in Fig A-4 B.

We then tested the epithelial integrity of the monolayer on glass with the hydrophilic marker mannitol. We calculated the apparent permeability coefficient (P_{app}) as a measure of the integrity of the Caco-2 monolayers. This parameter has the advantage of being independent of experimental design, surface area, time of experiment, and driving concentrations, which makes it possible to compare P_{app} values obtained under quite different experimental situations [157]. To assess the integrity of the monolayers, the flux of radiolabeled hydrophilic marker molecule (mannitol) which is passively transported across the monolayer was determined for each insert [253]. The apparent permeability, P_{app} (cm/s) was calculated using transport rate slope:

$$P_{app}=k\cdot V_R/A\cdot 60 \qquad (1)$$

Where V_R is the volume (ml) of the receiver chamber and A is the surface area (cm^2) of the cell insert. The P_{app} value for [^{3}H]-mannitol in intact Caco-2 monolayers grown on PET should generally be $<1x10^{-6}$ cm/s. In general, Caco-2 cells on commercially available system (PET inserts) form well-differentiated monolayers after 21 days and remain suitable for transport experiments until day 30. Several different brands of glass fibre filters were tested for HOC binding (Whatman, Pall, Ahlstrom) and the Ahlstrom filters provided the best barrier characteristics with Caco-2 cultured on the surface. The apparent permeability of mature Caco-2 monolayers grown on BSA-coated Ahlstrom glass fiber filters or PALL glass fiber filters coated with BSA or gelatine is shown in Figure 7-5. P_{app} measured for Caco-2 cells grown on glass fibre filters have shown ranged from 5×10^{-5} cm/s (excellent) to 1.8×10^{-6} cm/s (unusable). The data in Figure 7.5 suggested that coating the glass fibre filters with gelatin prior the seeding of Caco-2 cells would have solved the problem of growing tight monolayer of cells suitable for transport studies. However, the Caco-2 cell failed to create mature monolayer in another experiments.

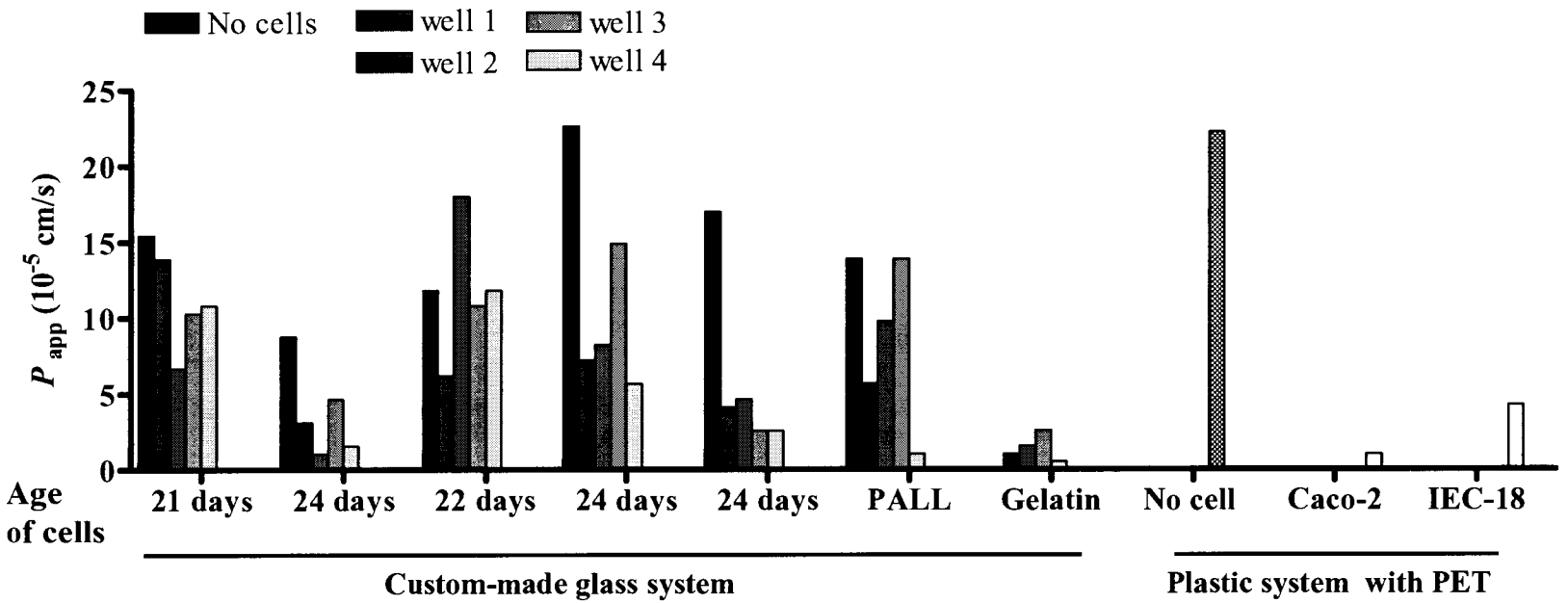

Figure A- 5. Apparent permeability of Caco-2 monolayers grown on Ahlstrom and PALL glass fiber filters.

Caco-2 cells on glass fiber filters were grown for different periods of time and assessment of monolayer integrity was performed with [^{3}H]-mannitol. P_{app} values of Caco-2 monolayers from all wells were compared to the P_{app} of Caco-2 cells and IC-18 (rat epithelium) grown the on PET system (commercially available).

Scanning electron microscopy (SEM) was used to examine the morphological properties of Caco-2 cells grown on the plastic system with PET or glass supports with glass fiber filters. If the cells are growing normally, they should form monolayers with tight junctions between connecting cells and dense microvilli at their apical surface. SEM images of Caco-2 cells grown on PET supports (Fig. A-5A) or on glass fibre filters (Fig. A-5 C-D) indicated that the cells form a tight monolayer on both supports. In both systems, microvilli cover the surfaces of the cells. In the monolayer grown on the glass fiber filter, there is a glass fiber on the surface of the cells (arrow).

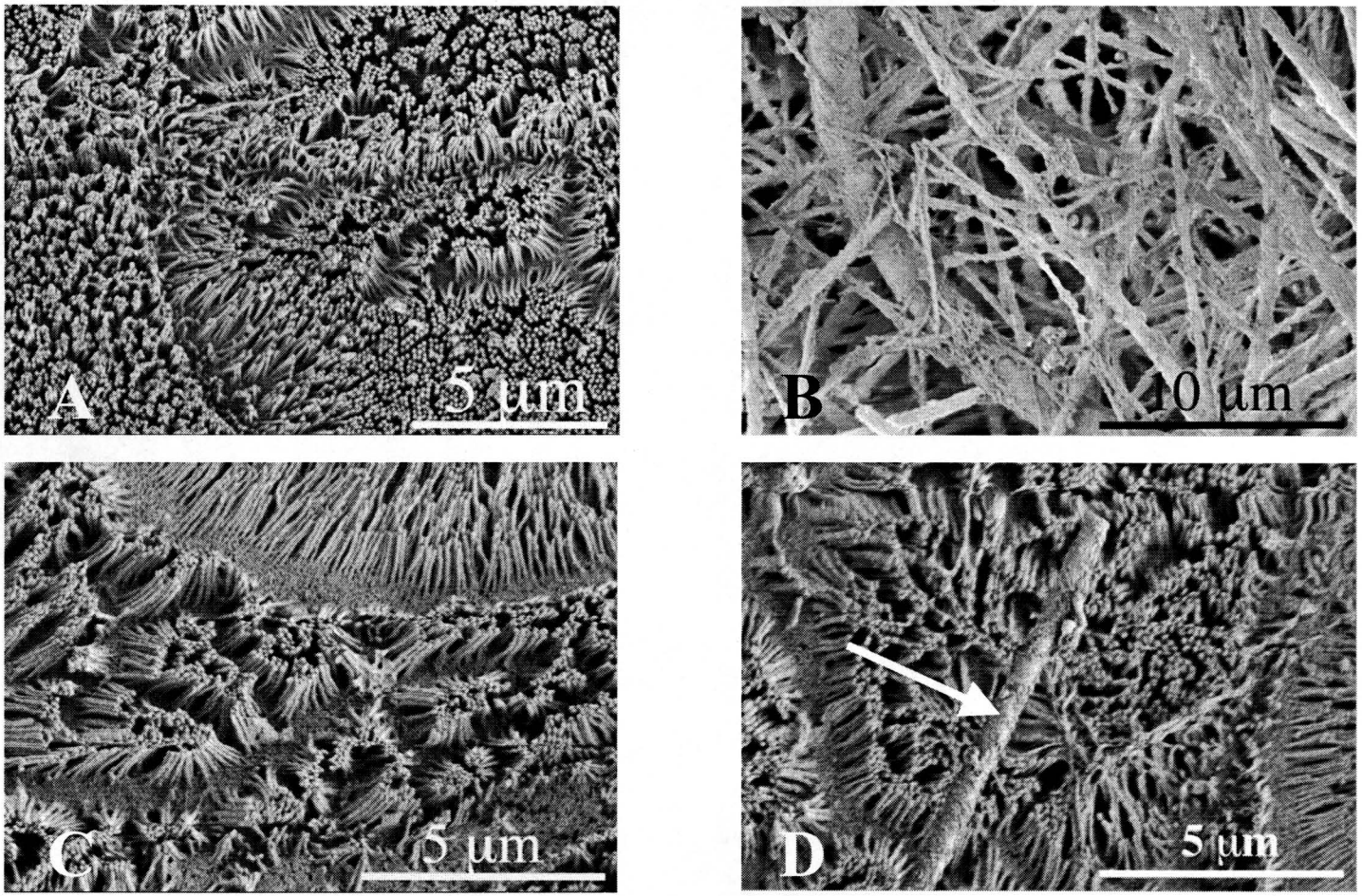

Figure A- 6. SEM images of Caco-2 cells grown on PET membrane (A) and Ahlstrom glass fiber filter without (B) and with Caco-2 cells (C-D).

Although the glass system with glass fiber filters was sometimes functional, we have noticed that glass fibres are laid down in way that can create large holes sometimes >10μm in size. Cell dimensions of Caco-2 at different growing stages can vary (cell width 6.4-13 μm) [124]. At the time of seeding, trypsinized cells shrink to even smaller dimensions and therefore can fall into holes between the glass fibres, meaning that we cannot be assured that Caco-2 cells create only one layer as desired.

Due to their high lipophilicity, HOC are poorly dissolved in aqueous phases, such as HBSS or gastrointestinal fluids. We were concerned that the HOC used in our experiments would precipitate fairly quickly, making it impossible to distinguish between the actual binding and the precipitated material. To overcome the problem we employed binding of radiolabeled compounds to a solid matrix, which reduced the non-specific binding to the plastic ware of the tissue culture system. By using this advantage of having a solid matrix in the system, we were unable to compare our results of bound chemical to a free compound.

Furthermore, filters made from glass fibres were found to have very large surface area for precipitated particles of the HOCs (e.g., benzo[a]pyrene). In addition, we wanted to simulate the real conditions of our planned experiments which was to measure bioavailability of model HOCs bound to solid matrices, the way they naturally enter our diet. Therefore, in order to move forward with the development of our model, we decided to modify it by changing a few things: 1) we looked into use of PET membrane again as this material presents a smooth surface area suitable for tissue culture; 2) we decided to eliminate the glass frit from our system, as it was slowing the aqueous flow from one chamber to another; and 3) we began to bind model HOC to a food matrix (i.e., skim milk powder).

Figure A-7 shows that it was the polystyrene supports of the tissue culture inserts, rather than PET membranes which exhibited a very high binding capacity for hydrophobic compounds. According to the manufacturer's catalogue of 12-well plates and tissue culture inserts, every piece of equipment for tissue culture has a hydrophilic coating on it. However, personal contact with a company representative revealed that tissue culture insert supports made of polystyrene are not coated and therefore remained

highly hydrophobic (Fig. A-7). Further research showed that 12-well tissue culture plates can act as additional "sink" in our experiments by binding HOC that appears in the basal compartment and changing the driving force in the transport experiments (data not shown).

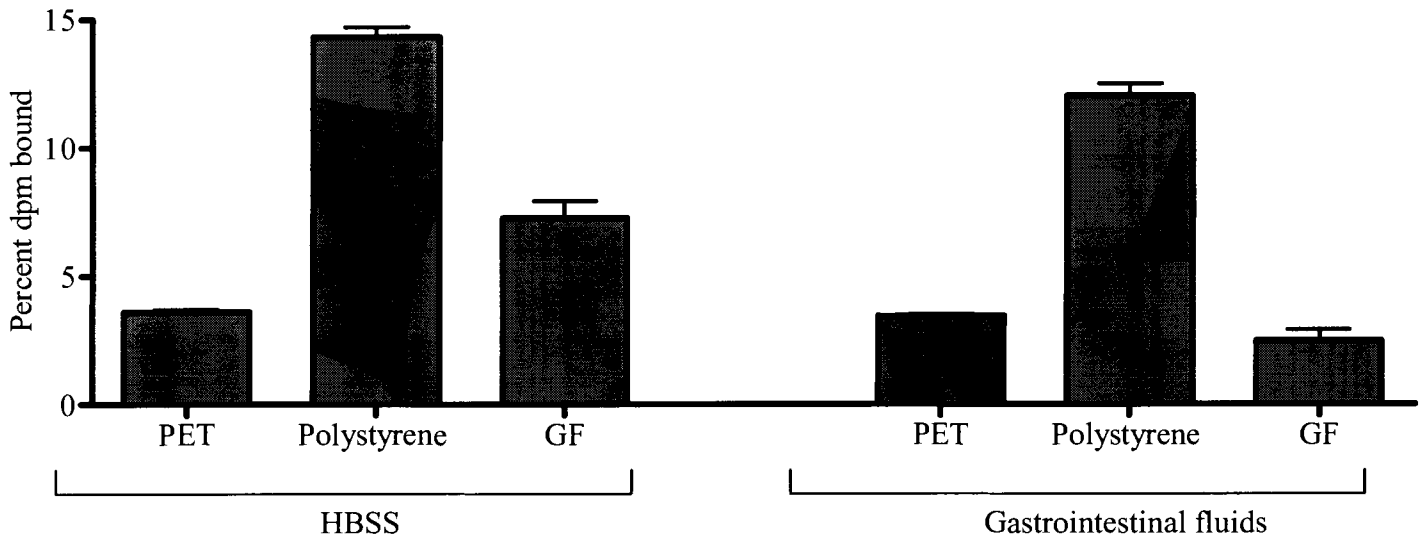

Figure A- 7. Percent of BaP bound to filters (PET or glass fibre (GF) prior to the experiment) when BaP bound to skim milk was incubated in HBSS or digestion fluids (gastrointestinal fluid).

BaP (~310,000 dpm) was added to skim milk powder and allowed to age for 7 days. Filters or supports (polystyrene) were added to beakers with either HBSS (pH 7.4) or gastrointestinal fluids after full gastrointestinal digestion of BaP-spiked skim milk as described previously in this thesis. The filters were incubated for 24 h, removed, rinsed in PBS, dried and radioactivity counted.

We then tested the ability of Caco-2 cells to establish mature monolayers on PET membranes in our custom-made glass system and tested its integrity using the hydrophilic marker mannitol (Fig.A-8).

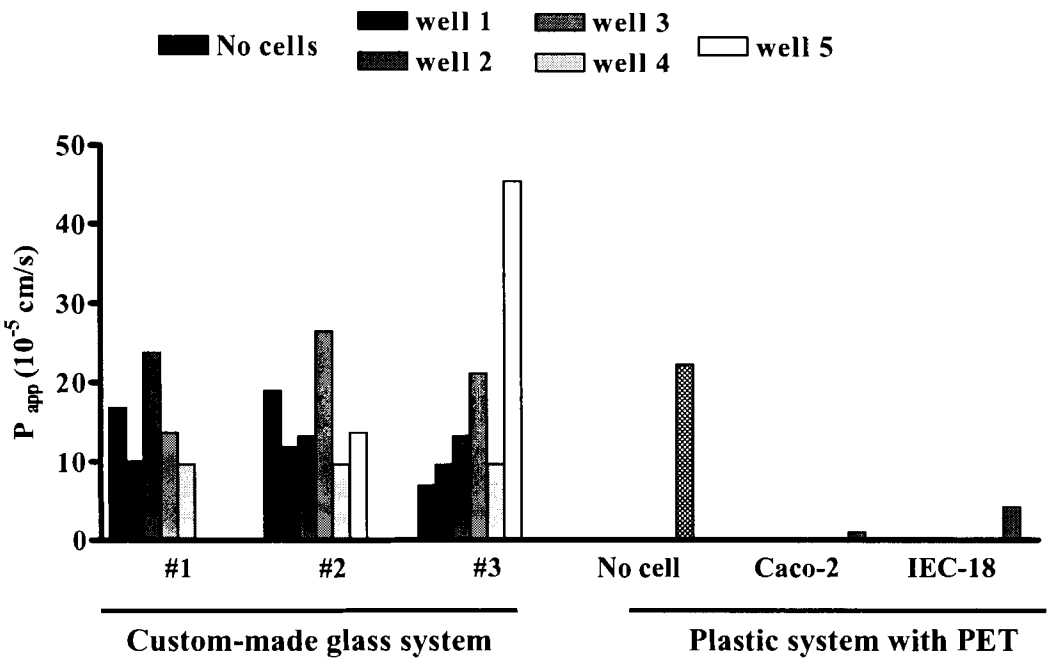

Figure A- 8. Apparent permeability of Caco-2 monolayers grown on PET filters used in custom-made glass system.

Caco-2 cells on PET filters were grown for 24 day and their P_{app} from all wells were compared to the P_{app} of Caco-2 cells and IC-18 (rat epithelium) grown the commercially available PET system.

When we determined that the polystyrene supports were more of a problem than the PET filters *per se*, it was logical to place PET membranes in glass supports, thereby eliminating most of the non-specific binding of HOC to the custom-made tissue culture support system. Unfortunately, the thin membranes could not be tightly sealed to the glass walls of the current design, and so there was leakage of apical fluids into the basal chamber, even when enough time had passed for Caco-2 cells to form monolayers with tight junctions. The leakage could have been around the monolayers or due to failure of the monolayers to seal under these conditions. Either event could be traced to failure due to the "architecture" of the glass supports.

All further attempts to halt the leakage of the apical fluid into the basal compartment have failed. I would therefore like to propose that a future model take into account the following design parameters:

1) The membrane must seal to the sides of the support in such a way that liquids cannot bypass for from one compartment to another except through the pores of the filter (without Caco-2 cells)

2) The physical structure of the apical compartment must permit Caco-2 cells to create a properly sealed monolayer that will limit the passage of hydrophilic marker [^{3}H]-mannitol to the paracellular route only and will reduce the apparent permeability of the marker to values received with Caco-2 cells grown on commercially available tissue culture system

3) The system should be suitable for mass production in a relatively inexpensive format.

REFERENCES

[1] Voigt K. 1990. Registering and analyzing data on detection of chemicals in the environment. *Chemosphere* 21:1429-1434.

[2] Mucke W. 1986. Approach for identification of hazardous environmental chemicals in food. *Toxicol Environ Chem* 13:129-140.

[3] Canadian Environmental Protection Act, 1999 (1999, c. 33) An Act respecting pollution prevention and the protection of the environment and human health in order to contribute to sustainable development. 1999.

[4] Ramesh A, Walker SA, Hood DB, Guillen MD, Schneider K, Weyand EH. 2004. Bioavailability and risk assessment of orally ingested polycyclic aromatic hydrocarbons. *Int J Toxicol* 23:301-333.

[5] Pignatello JJ, Xing B. 1996. Mechanisms of slow sorption of organic chemicals to natural particles. *Environ Sci Technol* 30:1-11.

[6] Pinto LJ, Moore MM. 2000. Release of polycyclic aromatic hydrocarbons from contaminated soils by surfactant and remediation of this effluent by Penicillium spp. *Environ Toxicol Chem* 19:1741-1748.

[7] Liste HH, Alexander M. 2002. Butanol extraction to predict bioavailability of PAHs in soil. *Chemosphere* 46:1011-1017.

[8] Mackay D. 2001. *Multimedia environmental models: the fugacity approach.* Lewis Publishers

[9] Alexander R, Alexander M. 1999. Genotoxicity of two polycyclic aromatic hydrocarbons declines as they age in soil. *Environ Toxicol Chem* 18:1140-1143.

[10] Duggan C, Gannon J, Walker WA. 2002. Protective nutrients and functional foods for the gastrointestinal tract. *Am J Clin Nutr* 75:789-808.

[11] Alexander M. 1995. How toxic are toxic chemicals in soil? *Environ Sci Technol* 29:2713-2717.

[12] Ruby M. 1996. Estimation of lead and arsenic bioavailability using a physiologically based extraction test. *Environ Sci Technol* 30:422-430.

[13] Patton JS, Stone B, Papa C, Abramowitz R, Yalkowsky S. 1984. Solubility of fatty acids and other hydrophobic molecules in liquid trioleoyglycerol. *J Lipid Research* 25:189-197.

[14] Mayer P, Vaes WH, Hermens JL. 2000. Absorption of hydrophobic compounds into the poly(dimethylsiloxane) coating of solid-phase microextraction fibers: high partition coefficients and fluorescence microscopy images. *Anal Chem* 72:459-464.

[15] Arnot JA, Gobas FAPC. 2004. A food web bioaccumulation model for organic chemicals in aquatic ecosystems. *Environ Toxicol Chem* 23:2343-2355.

[16] Gobas FAPC, MacLean LG. 2003. Sediment-water distribution of organic contaminants in aquatic ecosystems: the role of organic carbon mineralization. *Environ Sci Technol* 37:735-741.

[17] Eickhoff CV, He SX, Gobas FAPC, Law FC. 2003. Determination of polycyclic aromatic hydrocarbons in dungeness crabs (Cancer magister) near an aluminum smelter in Kitimat Arm, British Columbia, Canada. *Environ Toxicol Chem* 22:50-58.

[18] Gobas FAPC, Lahittete JM, Garofalo G, Shiu WY, Mackay D. 1988. A novel method for measuring membrane-water partition coefficients of hydrophobic organic chemicals: comparison with 1-octanol-water partitioning. *J Pharm Sci* 77:265-272.

[19] Pruijn FB, Sturman JR, Liyanage HD, Hicks KO, Hay MP, Wilson WR. 2005. Extravascular transport of drugs in tumor tissue: effect of lipophilicity on diffusion of tirapazamine analogues in multicellular layer cultures. *J Med Chem* 48:1079-1087.

[20] Reta M, Giacomelli L, Santo M, Cattana R, Silber JJ, Ochoa C, Rodriguez M, Chana A. 2003. Determination of lipophilic descriptors of antihelmintic 6,7-diaryl-pteridine derivatives useful for bioactivity predictions. *Biomed Chromatogr* 17:365-372.

[21] Verkade HJ, Tso P. 2001.Biophysics of intestinal Luminal Lipids. In: Mansbach II CM, Tso P, Kuksis A, editors. *Intestinal Lipid Metabolism*. Kluwer Academic / Plenum Publishers, New York. pp. 1-19.

[22] Chiou CT, Schmedding DW, Block JH. 1981. Correlation of water solubility with octanol-water partition coefficient. *J Pharm Sci* 70:1176-1177.

[23] Vetter RD, Carey MC, Patton JS. 1985. Coassimilation of dietary fat and benzo(a)pyrene in the small intestine: an absorption model using the killifish. *J Lipid Res* 26:428-434.

[24] Van Veld PA, Patton JS, Lee RF. 1988. Effect of preexposure to dietary benzo[a]pyrene (BP) on the first-pass metabolism of BP by th intestine of Toadfish (*Obsanus tau*): in vivo studies usinf portal vein-catheterized fish. *Toxicol Appl Pharmacol* 92:255-265.

[25] Kraaij R, Mayer P, Busser FJ, van het Bolscher M, Seinen W, Tolls J, Belfroid AC. 2003. Measured pore-water concentrations make equilibrium partitioning work--a data analysis. *Environ Sci Technol* 37:268-274.

[26] Tang J, Liste HH, Alexander M. 2002. Chemical assays of availability to earthworms of polycyclic aromatic hydrocarbons in soil. *Chemosphere* 48:35-42.

[27] Cornelissen G, Rigterink H, ten Hulscher DE, Vrind BA, van Noort PC. 2001. A simple Tenax extraction method to determine the availability of sediment-sorbed organic compounds. *Environ Toxicol Chem* 20:706-711.

[28] Sabaliunas D, Sodergren A. 1996. Uptake of organochlorine pesticides by solvent-filled cellulose and polyethylene membranes. *Ecotoxicol Environ Saf* 35:150-155.

[29] Sodergren A. 1987. Solvent-filled dialysis membranes simulate uptake of pollutants by aquatic organisms. *Environ Sci Technol* 21:855-859.

[30] Alexander M. 2000. Aging, bioavailability, and overestimation of risk from environmental pollutants. *Environ Sci Technol* 34:4259-4265.

[31] Notari RE. 1971. *Biopharmaceutics and pharmacokinetics : an introduction.* M. Dekker, New York.

[32] Hack A, Selenka F. 1996. Mobilization of PAH and PCB from contaminated soil using a digestive tract model. *Toxicol Lett* 88:199-210.

[33] Holman HY, Goth-Goldstein R, Aston D, Yun M, Kengsoontra J. 2002. Evaluation of gastrointestinal solubilization of petroleum hydrocarbon residues in soil using an in vitro physiologically based model. *Environ Sci Technol* 36:1281-1286.

[34] Ruby M. 2004. Bioavailability of soil-borne chemicals: Abiotic assessment tools. *Hum Ecol Risk Assess* 10:647-656.

[35] Semple K, Morriss A, Paton G. 2003. Bioavailability of hydrophobic organic contaminants in soils: fundamental concepts and techniques for analysis. *European Journal of Soil Science* 54:809-818.

[36] International Agency for Research on Cancer (IARC). 1983.Polynuclear aromatic compounds, Part 1, Chemical, environmental and experimental data. In: *IARC Monographs on the Evaluation of Carcinogenic Risk of Chemicals to Humans*, vol.32. Lyon, IARC. pp. 1-453.

[37] Jacob J. 1996. The significance of polycyclic aromatic hydrocarbons as environmental carcinogens. *Pure & Appl Chern* 6:301-308.

[38] Verhaar HJ, Solbe J, Speksnijder J, van Leeuwen CJ, Hermens JL. 2000. Classifying environmental pollutants: Part 3. External validation of the classification system. *Chemosphere* 40:875-883.

[39] Cerniglia CE, Kelly DW, Freeman JP, Miller DW. 1986. Microbial metabolism of pyrene. *Chem Biol Interact* 57:203-216.

[40] Pucknat AW. 1981. *Health impacts of polynuclear aromatic hydrocarbons.* Noyes Data Corporation, Park Ridge, New Jersey, U.S.A.

[41] Santodonato J. 1997. Review of the estrogenic and antiestrogenic activity of polycyclic aromatic hydrocarbons: relationship to carcinogenicity. *Chemosphere* 34:835-848.

[42] Armstrong RN. 1987. Enzyme-catalyzed detoxication reactions: mechanisms and stereochemistry. *CRC Crit Rev Biochem* 22:39-88.

[43] Jacob J, Grimmer G. 1996. Metabolism and excretion of polycyclic aromatic hydrocarbons in rat and in human. *Cent Eur J Public Health* 4 Suppl:33-39.

[44] Omura T, Sato R, Cooper DY, Rosenthal O, Estabrook RW. 1965. Function of cytochrome P-450 of microsomes. *Fed Proc* 24:1181-1189.

[45] Buening MK, Wislocki PG, Levin W, Yagi H, Thakker DR, Akagi H, Koreeda M, Jerina DM, Conney AH. 1978. Tumorigenicity of the optical enantiomers of the diastereomeric benzo[a]pyrene 7,8-diol-9,10-epoxides in newborn mice: exceptional activity of (+)-7beta,8alpha-dihydroxy-9alpha,10alpha-epoxy-7,8,9,10-tetrahydrobenzo[a]pyrene. *Proc Natl Acad Sci U S A* 75:5358-5361.

[46] O'Brien PJ, Hales BF, Josephy PD, Castonguay A, Yamazoe Y, Guengerich FP. 1996. Chemical carcinogenesis, mutagenesis, and teratogenesis. *Can J Physiol Pharmacol* 74:565-571.

[47] Koob M, Dekant W. 1991. Bioactivation of xenobiotics by formation of toxic glutathione conjugates. *Chem Biol Interact* 77:107-136.

[48] Okamoto H, Yoshida D. 1981. Metabolic formation of pyrenequinones as enhancing agents of mutagenicity in Salmonella. *Cancer Lett* 11:215-220.

[49] Barr WH, Riegelman S. 1970. Intestinal drug absorption and metabolism. I. Comparison of methods and models to study physiological factors of in vitro and in vivo intestinal absorption. *J Pharm Sci* 59:154-163.

[50] George CF. 1981. Drug metabolism by the gastrointestinal mucosa. *Clin Pharmacokinet* 6:259-274.

[51] Foth H, Kahl R, Kahl GF. 1988. Pharmacokinetics of low doses of benzo[a]pyrene in the rat. *Food Chem Toxicol* 26:45-51.

[52] Stavric B, Klassen R. 1994. Dietary effects on the uptake of benzo[a]pyrene. *Food Chem Toxicol* 32:727-734.

[53] Waldman JM, Lioy PJ, Greenberg A, Butler JP. 1991. Analysis of human exposure to benzo(a)pyrene via inhalation and food ingestion in the Total Human Environmental Exposure Study (THEES). *J Expo Anal Environ Epidemiol* 1:193-225.

[54] Lioy PJ, Greenberg A. 1990. Factors associated with human exposures to polycyclic aromatic hydrocarbons. *Toxicol Ind Health* 6:209-223.

[55] Phillips DH. 1999. Polycyclic aromatic hydrocarbons in the diet. *Mutat Res* 443:139-147.

[56] Larsson BK, Sahlberg GP, Eriksson AT, Busk LA. 1983. Polycyclic aromatic hydrocarbons in grilled food. *J Agric Food Chem* 31:867-873.

[57] Guillen MD, Sopelana P, Partearroyo MA. 1997. Food as a source of polycyclic aromatic carcinogens. *Rev Environ Health* 12:133-146.

[58] Wickstrom K, Pyysalo H, Plaami-Heikkila S, Tuominen J. 1986. Polycyclic aromatic compounds (PAC) in leaf lettuce. *Z Lebensm Unters Forsch* 183:182-185.

[59] Grova N, Feidt C, Crepineau C, Laurent C, Lafargue PE, Hachimi A, Rychen G. 2002. Detection of polycyclic aromatic hydrocarbon levels in milk collected near potential contamination sources. *J Agric Food Chem* 50:4640-4642.

[60] Cavret S, Feidt C, Le Roux Y, Laurent F. 2005. Study of mammary epithelial role in polycyclic aromatic hydrocarbons transfer to milk. *J Dairy Sci* 88:67-70.

[61] Yabiku HY, Martins MS, Takahashi MY. 1993. Levels of benzo[a]pyrene and other polycyclic aromatic hydrocarbons in liquid smoke flavour and some smoked foods. *Food Addit Contam* 10:399-405.

[62] Fontana RJ, Lown KS, Paine MF, Fortlage L, Santella RM, Felton JS, Knize MG, Greenberg A, Watkins PB. 1999. Effects of a chargrilled meat diet on expression of CYP3A, CYP1A, and P-glycoprotein levels in healthy volunteers. *Gastroenterology* 117:89-98.

[63] Guillen MD, Sopelana P. 2004. Occurrence of polycyclic aromatic hydrocarbons in smoked cheese. *J Dairy Sci* 87:556-564.

[64] Guillen MD, Sopelana P, Palencia G. 2004. Polycyclic aromatic hydrocarbons and olive pomace oil. *J Agric Food Chem* 52:2123-2132.

[65] Ferguson LR. 2002. Natural and human-made mutagens and carcinogens in the human diet. *Toxicology* 181-182:79-82.

[66] Jones KC, Grimmer G, Jacob J, Johnston AE. 1989. Changes in the polynuclear aromatic hydrocarbon content of wheat grain and pasture grassland over the last century from one site in the U.K. *Sci Total Environ* 78:117-130.

[67] Sera N, Morita K, Nagasoe M, Tokieda H, Kitaura T, Tokiwa H. 2005. Binding effect of polychlorinated compounds and environmental carcinogens on rice bran fiber. *J Nutr Biochem* 16:50-58.

[68] Husain A, Naeemi E, Dashti B, al-Omirah H, al-Zenki S. 1997. Polycyclic aromatic hydrocarbons in food products originating from locally reared animals in Kuwait. *Food Addit Contam* 14:295-299.

[69] Guillen MD, Sopelana P. 2004. Load of polycyclic aromatic hydrocarbons in edible vegetable oils: importance of alkylated derivatives. *J Food Prot* 67:1904-1913.

[70] Li S, Pan D, Wang G. 1994. Analysis of polycyclic aromatic hydrocarbons in cooking oil fumes. *Arch Environ Health* 49:119-122.

[71] Schauer JJ, Kleeman MJ, Cass GR, Simoneit BR. 2002. Measurement of emissions from air pollution sources. 4. C1-C27 organic compounds from cooking with seed oils. *Environ Sci Technol* 36:567-575.

[72] Menichini E, Bocca A, Merli F, Ianni D, Monfredini F. 1991. Polycyclic aromatic hydrocarbons in olive oils on the Italian market. *Food Addit Contam* 8:363-369.

[73] Vassilaros DL, Stoker PW, Booth GM, Lee ML. 1982. Capillary gas chromatographic determination of polycyclic aromatic compounds in vertebrate fish tissue. *Anal Chem* 54:106-112.

[74] Devier MH, Augagneur S, Budzinski H, Le Menach K, Mora P, Narbonne JF, Garrigues P. 2005. One-year monitoring survey of organic compounds (PAHs, PCBs, TBT), heavy metals and biomarkers in blue mussels from the Arcachon Bay, France. *J Environ Monit* 7:224-240.

[75] Sanders M. 1995. Distribution of polycyclic aromatic hydrocarbons in oyster (Crassostrea virginica) and surface sediment from two estuaries in South Carolina. *Arch Environ Contam Toxicol* 28:397-405.

[76] Lemiere S, Cossu-Leguille C, Bispo A, Jourdain MJ, Lanhers MC, Burnel D, Vasseur P. 2005. DNA damage measured by the single-cell gel electrophoresis (Comet) assay in mammals fed with mussels contaminated by the 'Erika' oil-spill. *Mutat Res* 581:11-21.

[77] Houessou JK, Benac C, Delteil C, Camel V. 2005. Determination of polycyclic aromatic hydrocarbons in coffee brew using solid-phase extraction. *J Agric Food Chem* 53:871-879.

[78] Kuratsune M, Hueper WC. 1960. Polycyclic aromatic hydrocarbons in roasted coffee. *J Natl Cancer Inst* 24:463-469.

[79] Tao S, Cui YH, Xu FL, Li BG, Cao J, Liu WX, Schmitt G, Wang XJ, Shen WR, Qing BP, Sun R. 2004. Polycyclic aromatic hydrocarbons (PAHs) in agricultural soil and vegetables from Tianjin. *Sci Total Environ* 320:11-24.

[80] Zhong W, Wang M. 2002. Some polycyclic aromatic hydrocarbons in vegetables from northern China. *J Environ Sci Health A Tox Hazard Subst Environ Eng* 37:287-296.

[81] Dennis MJ, Massey RC, Cripps G, Venn I, Howarth N, Lee G. 1991. Factors affecting the polycyclic aromatic hydrocarbon content of cereals, fats and other food products. *Food Addit Contam* 8:517-530.

[82] Kazerouni N, Sinha R, Hsu CH, Greenberg A, Rothman N. 2001. Analysis of 200 food items for benzo[a]pyrene and estimation of its intake in an epidemiologic study. *Food Chem Toxicol* 39:423-436.

[83] Falco G, Domingo JL, Llobet JM, Teixido A, Casas C, Muller L. 2003. Polycyclic aromatic hydrocarbons in foods: human exposure through the diet in Catalonia, Spain. *J Food Prot* 66:2325-2331.

[84] Blumer M. 1961. Benzyprenes in soil. *Science* 134:474-475.

[85] Edwards NT. 1983. Polycyclic aromatic hydrocarbons (PAHs) in the terrestrial environment - a review. *J Environ, Qual* 12:427-441.

[86] Prevedouros K, Brorstrom-Lunden E, C JH, Jones KC, Lee RG, Sweetman AJ. 2004. Seasonal and long-term trends in atmospheric PAH concentrations: evidence and implications. *Environ Pollut* 128:17-27.

[87] Wilcke W. 2000. Polycyclic aromatic hydrocarbons (PAHs) in soil - a review. *J Plant Nutr Soil Sci* 163:229-248.

[88] Chiou CT, Sheng G, Manes M. 2001. A partition-limited model for the plant uptake of organic contaminants from soil and water. *Environ Sci Technol* 35:1437-1444.

[89] Piatt JJ, Brusseau ML. 1998. Rate-limited sorption of hydrophobic organic compounds by soil with well characterized organic matter. *Environ Sci Technol* 32:1604-1608.

[90] Hatzinger PB, Alexander M. 1995. Effect of aging of chemicals in soils on their biodegradability and extractability. *Environ Sci Technol* 29:537-545.

[91] Nam K, Alexander M. 1998. Role of nanoporosity and hydrophobicity in sequestration and bioavailability tests with model solids. *Environ Sci Technol* 32:71-74.

[92] Bosma TNP, Middeldorp PJM, Schraa G, Zehnder AJB. 1997. Mass transfer limitaion of biotransformation:quantifying bioavailability. *Environ Sci Technol* 31:1248-1252.

[93] Dec J, Haider K, Bollag JM. 2003. Release of substituents from phenolic compounds during oxidative coupling reactions. *Chemosphere* 52:549-556.

[94] Crank J. 1975. *The mathematics of diffusion*. Oxford, Clarendon Press, Oxford, United Kingdom.

[95] Calabrese EJ, Stanek EJ, James RC, Roberts SM. 1997. Soil ingestion: a concern for acute toxicity in children. *Environ Health Perspect* 105:1354-1358.

[96] Wilson NK, Chuang JC, Lyu C. 2001. Levels of persistent organic pollutants in several child day care centers. *J Expo Anal Environ Epidemiol* 11:449-458.

[97] Oomen AG, Mayer P, Tolls J. 2000. Nonequilibrium solid-phase microextraction for determination of the freely dissolved concentration of hydrophobic organic compounds: matrix effects and limitations. *Anal Chem* 72:2802-2808.

[98] Johnson LR, editor. 1997. Gastrointestinal Physiology. Mosby.St. Louis, Missouri:

[99] Van de Wiele T, Verstraete W, Siciliano SD. 2004. Polycyclic aromatic hydrocarbons release from a soil matrix in the in vitro gastrointestinal tract. *J Environ Qual* 33:1343-1353.

[100] Gorelick FS, Jamieson JD. 1994.The pancreatic Acinar Cell:Structure-Functional Relationship. In: Johnson LR, editor. *Physiology of the Gastrointestinal Tract*, vol.2. Raven Press, New York. pp. 1353-1377.

[101] Walsh JH. 1994.Gastrointestinal Hormones. In: Johnson LR, editor. *Physiology of the Gastrointestinal Tract*, vol.1. Raven Press, New York. pp. 1-128.

[102] Madara JL. 1998. Regulation of the movement of solutes across tight junctions. *Annu Rev Physiol* 60:143-159.

[103] Hillgren KM, Kato A, Borchardt RT. 1995. In vitro systems for studying intestinal drug absorption. *Med Res Rev* 15:83-109.

[104] Forstner JF, Forstner GG. 1994.Gastrointestinal mucus. In: Johnson LR, editor. *Physiology of the Gastrointestinal Tract*, vol.2. Raven Press, New York. pp. 1255-1283.

[105] Wils P, Warnery A, Phung-Ba V, Scherman D. 1994. Differentiated intestinal epithelial cell lines as in vitro models for predicting the intestinal absorption of drugs. *Cell Biol Toxicol* 10:393-397.

[106] Madara JL, Trier JS. 1994.The Functional Morphology of the Mucosa of the Small Intestine. In: Johnson LR, editor. *Physiology of the Gastrointestinal Tract.* 3rd, vol.2. Raven Press, New York. pp. 1577-1622.

[107] Tso P. 1994.Intestinal Lipid Absorption. In: Johnson LR, editor. *Physiology of the Gastrointestinal Tract.* 3rd, vol.2. Raven Press, New York. pp. 1867-1907.

[108] Seetharam B. 1994.Gastrointestinal Absorption and Transport of Cobalamin (Vitamin B12). In: Johnson LR, editor. *Physiology of the Gastrointestinal Tract.* 3rd, vol.2. Raven Press, New York. pp. 1997-2026.

[109] Mansbach CM. 2001.Triacylglycerol movement in enterocytes. In: Kuksis A, editor. *Intestinal lipid metabolism.* Klumer Academic/Plenum Publishers, New York. pp. 215-229.

[110] Thomson AB, Keelan M, Garg ML, Clandinin MT. 1989. Intestinal aspects of lipid absorption: in review. *Can J Physiol Pharmacol* 67:179-191.

[111] Dulfer W, Govers HA, Groten JP. 1998. Kinetics and conductivity parameters of uptake and transport of polychlorinated biphenyls in the Caco-2 intestinal cell line model. *Environ Toxicol Chem* 17:493-501.

[112] Gobas FAPC, Opperhuizen A, Hutzinger O. 1986. Bioconcentration of hydrophobic chemicals in fish - relationship with membrane permeation. *Environ Toxicol Chem* 5:637-646.

[113] Flynn GL, Yalkowsky SH. 1972. Correlation and prediction of mass transport across membranes. I. Influence of alkyl chain length on flux-determining properties of barrier and diffusant. *J Pharm Sci* 61:838-852.

[114] Sijm DTHM, Van der Linde A. 1995. Size-dependent bioconcentration kinetics of hydrophobic organic-chemicals in fish based on diffusive mass-transfer and allometric relationships. *Environ Sci Technol* 29:2769-2777.

[115] Buesen R, Mock M, Nau H, Seidel A, Jacob J, Lampen A. 2003. Human intestinal Caco-2 cells display active transport of benzo[a]pyrene metabolites. *Chem Biol Interact* 142:201-221.

[116] Goodwin JT, Conradi RA, Ho NF, Burton PS. 2001. Physicochemical determinants of passive membrane permeability: role of solute hydrogen-bonding potential and volume. *J Med Chem* 44:3721-3729.

[117] Sambruy Y, Ferruzza S, Ranaldi G, De Angelis I. 2001. Intestinal cell culture models: applications in toxicology and pharmacology. *Cell Biol Toxicol* 17:301-317.

[118] Quaroni A, Isselbacher KJ. 1981. Cytotoxic effects and metabolism of benzo[a]pyrene and 7,12-dimethylbenz[a]anthracene in duodenal and ileal epithelial cell cultures. *J Natl Cancer Inst* 67:1353-1362.

[119] Versantvoort CHM, Ondrewater RCA, Duizer E, Van de Sandt JJM, Gilde AJ, Groten JP. 2002. Monolayers of IEC-18 cells as an in vitro model for screening the passive transcellular and paracellular transport across the intestinal barrier: comparison of active and passive transport with the human colon carcinoma Caco-2 cell line. *Environ Toxicol Pharmacol* 11:335-344.

[120] Artursson P, Borchardt RT. 1997. Intestinal drug absorption and metabolism in cell cultures: Caco-2 and beyond. *Pharm Res* 14:1655-1658.

[121] Duizer E, Gilde AJ, Versantvoort CH, Groten JP. 1999. Effects of cadmium chloride on the paracellular barrier function of intestinal epithelial cell lines. *Toxicol Appl Pharmacol* 155:117-126.

[122] Oomen AG, Tolls J, Kruidenier M, Bosgra SS, Sips AJ, Groten JP. 2001. Availability of polychlorinated biphenyls (PCBs) and lindane for uptake by intestinal Caco-2 cells. *Environ Health Perspect* 109:731-737.

[123] Cavret S, Feidt C. 2005. Intestinal metabolism of PAH: in vitro demonstration and study of its impact on PAH transfer through the intestinal epithelium. *Environ Res* 98:22-32.

[124] Hidalgo IJ, Raub TJ, Borchardt RT. 1989. Characterization of the human colon carcinoma cell line (Caco-2) as a model system for intestinal epithelial permeability. *Gastroenterology* 96:736-749.

[125] Hauri HP, Sterchi EE, Bienz D, Fransen JA, Marxer A. 1985. Expression and intracellular transport of microvillus membrane hydrolases in human intestinal epithelial cells. *J Cell Biol* 101:838-851.

[126] Howell S, Kenny AJ, Turner AJ. 1992. A survey of membrane peptidases in two human colonic cell lines, Caco-2 and HT-29. *Biochem J* 284 (Pt 2):595-601.

[127] Matsumoto H, Erickson RH, Gum JR, Yoshioka M, Gum E, Kim YS. 1990. Biosynthesis of alkaline phosphatase during differentiation of the human colon cancer cell line Caco-2. *Gastroenterology* 98:1199-1207.

[128] Mitic LL, Anderson JM. 1998. Molecular architecture of tight junctions. *Annu Rev Physiol* 60:121-142.

[129] Karlsson J, Artursson P. 1992. A new diffusion chamber system for the determination of drug permeability coefficients across the human intestinal epithelium that are independent of the unstirred water layer. *Biochim Biophys Acta* 1111:204-210.

[130] Dix CJ, Hassan IF, Obray HY, Shah R, Wilson G. 1990. The transport of vitamin B12 through polarized monolayers of Caco-2 cells. *Gastroenterology* 98:1272-1279.

[131] Hidalgo IJ, Borchardt RT. 1990. Transport of bile acids in a human intestinal epithelial cell line, Caco-2. *Biochim Biophys Acta* 1035:97-103.

[132] Lampen A, Bader A, Bestmann T, Winkler M, Witte L, Borlak JT. 1998. Catalytic activities, protein- and mRNA-expression of cytochrome P450 isoenzymes in intestinal cell lines. *Xenobiotica* 28:429-441.

[133] Stein J, Schroder O, Bonk M, Oremek G, Lorenz M, Caspary WF. 1996. Induction of glutathione-S-transferase-pi by short-chain fatty acids in the intestinal cell line Caco-2. *Eur J Clin Invest* 26:84-87.

[134] Galijatovic A, Otake Y, Walle UK, Walle T. 1999. Extensive metabolism of the flavonoid chrysin by human Caco-2 and Hep G2 cells. *Xenobiotica* 29:1241-1256.

[135] Boulenc X, Bourrie M, Fabre I, Roque C, Joyeux H, Berger Y, Fabre G. 1992. Regulation of cytochrome P450IA1 gene expression in a human intestinal cell line, Caco-2. *J Pharmacol Exp Ther* 263:1471-1478.

[136] Field FJ, Albright E, Mathur SN. 1988. Regulation of triglyceride-rich lipoprotein secretion by fatty acids in Caco-2 cells. *J Lipid Res* 29:1427-1437.

[137] Mackay D, Paterson S. 1981. Calculating fugacity. *Environ Sci Technol* 15:1006-1014.

[138] DiToro DM, Zarba CS, Hansen DJ, Berry WJ, Swartz RC, Cowan CE, Pavlour SP, Allen HE, Thomas NA, R. PP. 1991. Technical basis for establishing sediment quality criteria for nonionic organic chemicals using equilibrium partitioning. *Environ Toxicol Chem* 10:1541-1583.

[139] Gobas FAPC, Zhang X, Wells R. 1993. Gastrointestinal magnification: The mechanism of biomagnification and food chain accumulation of organic chemicals. *Environ Sci Technol* 27:2855-2863.

[140] Gobas FAPC, Muir DCG, Mackay D. 1988. Dynamics of dietary bioaccumulation and fecal elimination of hydrophobic organic chemicals in fish. *Chemosphere* 17:943-962.

[141] Dulfer WJ, Groten JP, Govers HA. 1996. Effect of fatty acids and the aqueous diffusion barrier on the uptake and transport of polychlorinated biphenyls in Caco-2 cells. *J Lipid Res* 37:950-961.

[142] Kelly BC, Gobas FAPC, McLachlan MS. 2004. Intestinal absorption and biomagnification of organic contaminants in fish, wildlife, and humans. *Environ Toxicol Chem* 23:2324-2336.

[143] Schlummer M, Moser GA, McLachlan MS. 1998. Digestive tract absorption of PCDD/Fs, PCBs, and HCB in humans: mass balances and mechanistic considerations. *Toxicol Appl Pharmacol* 152:128-137.

[144] Moser GA, McLachlan MS. 2001. The influence of dietary concentration on the absorption and excretion of persistent lipophilic organic pollutants in the human intestinal tract. *Chemosphere* 45:201-211.

[145] Gobas FAPC, Wilcockson JB, R. R, G. H. 1999. Mechanism of biomagnification in fish under laboratory and field conditions. *Environ Sci Technol* 33:133-141.

[146] Cushman DJ, Driver KS, Ball SD. 2001. Risk assessment for environmental contamination: an overview of the fundamentals and application of risk assessment at contamianted sites. *Can J Civ Eng* 28:155-162.

[147] United States Environmental Protection Agency. 1989.Risk assessment guidance for Superfund. In: *Human health evaluation manual (Part A); Interim Final.*, vol.1. United States Environmental Protection Agency, Office of Emergency and Remedial Response., Washington, D.C.

[148] Ruby M. 1993. Development of an in-vitro screening test to evaluate the in-vivo bioaccessibility of ingested mine-waste lead. *Environ Sci Technol* 27:2870-2877.

[149] Williams GM, Kroes R, Munro IC. 2000. Safety evaluation and risk assessment of the herbicide Roundup and its active ingredient, glyphosate, for humans. *Regulatory Toxicology and Pharmacology* 31:117-165.

[150] Ghassemi M, Quinlivan S, Dellarco M. 1982. Environmental effects of new herbicides for vegetation control in forestry. *Environment International* 7:389-402.

[151] Sprankle P, Meggit WF, Penner D. 1975. Absorption action and translocation of glyphosate. *Weed Science* 23:235-240.

[152] Eberbach PL. 1999. Influence of incubation temperature on the behavior of triethylamine-extractable glyphosate (N-phosphonomethylglycine) in four soils. *J Agric Food Chem* 47:2459-2467.

[153] Malkomes HP. 2000. Comparison of the effects of differently formulated herbicides on soil microbial activities - a review. *Zeitschrift Fur Pflanzenkrankheiten Und Pflanzenschutz-Journal of Plant Diseases and Protection*:781-789.

[154] Brewster DW, Warren J, Hopkins WE, 2nd. 1991. Metabolism of glyphosate in Sprague-Dawley rats: tissue distribution, identification, and quantitation of glyphosate-derived materials following a single oral dose. *Fundam Appl Toxicol* 17:43-51.

[155] NTP. 1992. Technical Report on Toxicity Studies of Glyphosate (CAS No. 1071-83-6) Administered in Doses Feed to F344/N rats and B6C3F$_1$ mice.NIH Publication 92-3135. Technical Report. U.S. Department of Health and Human Services, Research Triangle Park, NC.

[156] Duizer E, van der Wulp C, Versantvoort CH, Groten JP. 1998. Absorption enhancement, structural changes in tight junctions and cytotoxicity caused by palmitoyl carnitine in Caco-2 and IEC-18 cells. *J Pharmacol Exp Ther* 287:395-402.

[157] Artursson P, Karlsson J, Ocklind G, Schipper N. 1996.Studying Transport Processes in Absorptive Epithelia. In: Shaw AJ, editor. *Epithelial cell culture : a practical approach*. 1st. IRL Press at Oxford University Press, Oxford. pp. 111-133.

[158] Duizer E, Penninks AH, Stenhuis WH, Groten JP. 1997. Comparison of permeability characteristics of the human colonic Caco-2 and rat small intestinal IEC-18 cell lines. *Journal of Controlled Release* 49:39-49.

[159] Versantvoort CHM, Ondrewater RCA, Duizer E, Van de Sandt JJM, Gilde AJ, Groten JP. 2002. Monolayers of IEC-18 cells as an in vitro model for screening the passive transcellular and paracellular transport across the intestinal barrier: comparison of active and passive transport with the human colon carcinoma Caco-2 cell line. *Environmental Toxicology and Pharmacology* 11:335-344.

[160] Sawada Y, Nagai Y, Ueyama M, Yamamoto I. 1988. Probable toxicity of surface-active agent in commercial herbicide containing glyphosate. *Lancet* 1:299-299.

[161] Talbot AR, Shiaw MH, Huang JS, Yang SF, Goo TS, Wang SH, Chen CL, Sanford TR. 1991. Acute poisoning with a glyphosate-surfactant herbicide ('Roundup'): a review of 93 cases. *Hum Exp Toxicol* 10:1-8.

[162] Adam A, Marzuki A, Rahman HA, Aziz MA. The oral and intratracheal toxicities of Roundup and its components to rats. Vet Hum Toxicol, 1997. pp. 147-151.

[163] Bolognesi C. Genotoxic activity of glyphosate and its technical formulation roundup. J Agric Food Chem, 1997. pp. 1957-1962.

[164] Delie F, Rubas W. 1997. A human colonic cell line shaping similarities with enterocytes as a model to examine oral absorption: Advantages and limitations of the Caco-2 model. *Critical Reviews in Therapeutic Drug Carrier Systems* 14:221-286.

[165] Grasset E, Pinto M, Dussaulx E, Zweibaum A, Desjeux JF. 1984. Epithelial properties of human colonic carcinoma cell line Caco-2: electrical parameters. *Am J Physiol* 247:C260-267.

[166] Harris DS, Slot JW, Geuze HJ, James DE. 1992. Polarized distribution of glucose transporter isoforms in Caco-2 cells. *Proc Natl Acad Sci U S A* 89:7556-7560.

[167] Duizer E, Penninks AH, Stenhuis WH, Groten JP. 1997. Comparison of permeability characteristics of the human colonic Caco-2 and rat small intestinal IEC-18 cell lines. *J Control Release* 49:39-49.

[168] Snipes RL. Intestinal absorptive surface in mammals of different sizes. *Adv Anat Embryol Cell Biol*, 1997. pp. III-VIII, 1-90.

[169] Farshori P, Kachar B. Redistribution and phosphorylation of occludin during opening and resealing of tight junctions in cultured epithelial cells. *J Membr Biol*, 1999. pp. 147-156.

[170] Madara JL. Regulation of the movement of solutes across tight junctions. *Annu Rev Physiol*, 1998. pp. 143-159.

[171] Balda M. Assembly of the tight junction: the role of diacylglycerol. *J Cell Biol*, 1993. pp. 293-302.

[172] Richard JF, Mainguy G, Gibert M, Marvaud JC, Stiles BG, Popoff MR. Transcytosis of iota-toxin across polarized CaCo-2 cells. *Mol Microbiol*, 2002. pp. 907-917.

[173] Okada T, Narai A, Matsunaga S, Fusetani N, Shimizu M. Assessment of the marine toxins by monitoring the integrity of human intestinal Caco-2 cell monolayers. *Toxicol In Vitro*, 2000. pp. 219-226.

[174] Waymouth C. Osmolality of mammalian blood and of media for culture of mammalian cells. *In Vitro*, 1970. pp. 109-127.

[175] Parnaud G, Corpet DE, Gamet-Payrastre L. Cytostatic effect of polyethylene glycol on human colonic adenocarcinoma cells. *Int J Cancer,* 2001. pp. 63-69.

[176] Stanek EJ, Calabrese EJ. 1995. Daily estimates of soil ingestion in children. *Environ Health Perspect* 103:276-285.

[177] Paustenbach D, Bruce GM, Chrostowsky P. 1997. Current views on the oral bioavailability of inorganic mercury in soil: Implications for health risk assessments. *Risk Anal* 17:533-544.

[178] Calabrese E, Stanek E, James R, Roberts S. 1997. Soil ingestion: a concern for acute toxicity in children. *Environ Health Perspect* 105:1354-1358.

[179] Kelsey JW, Alexander M. 1997. Declining bioavailability and inappropriate estimation of risk of persistent compounds. *Environ Toxicol Chem* 16:582-585.

[180] Freeman GB, Dill JA, Johnson JD, Kurtz PJ, Parham F, Matthews HB. 1996. Comparative absorption of lead from contaminated soil and lead salts by weanling Fischer 344 rats. *Fundam Appl Toxicol* 33:109-119.

[181] Norris DA, Puri N, Sinko PJ. 1998. The effect of physical barriers and properties on the oral absorption of particulates. *Adv Drug Deliv Rev* 34:135-154.

[182] Tang J, Alexander M. 1999. Mild extractability and bioavailability of polycyclic aromatic hydrocarbons in soil. *Environ Toxicol Chem* 18:2711-2714.

[183] Ramos E, Meijer SN, Vaes WHJ, Verhaar HJM, Hermens JLM. 1998. Using solid-phase microextraction to determine partition coefficients to humic acids and bioavailable concentrations of hydrophobic chemicals. *Environ Sci Technol* 32:3430-3435.

[184] Pignatello J. 1990. Slowly reversible sorption of aliphatic halocarbons in soils. 1. Formation of residual fractions. *Environ Toxicol Chem* 9:1107-1115.

[185] Cornelissen G. 1998. Rapidly desorbing fractions of PAHs in contaminated sediments as a predictor of the extent of bioremediation. *Environ Sci Technol* 32:966-970.

[186] Ma W, van Kleunen A, Immerzeel J, de Maagd PGJ. 1998. Bioaccumulation of polycyclic aromatic hydrocarbons by earthworms: Assessment of equilibrium partitioning theory in in situ studies and water experiments. *Environ Toxicol Chem* 17:1730-1737.

[187] Mayer P, Vaes WH, Hermens JL. 2000. Sensing dissolved sediment porewater concentrations of persistent and bioaccumulative pollutants using disposable solid-phase microextraction fibers. *Environ Sci Technol* 34:5177-5183.

[188] Wilcockson JB, Gobas FAPC. 2001. Thin-film solid-phase extraction to measure fugacities of organic chemicals with low volatility in biological samples. *Environ Sci Technol* 35:1425-1431.

[189] Rotard W, Christmann W, Knoth W, Mailahn W. 1995. Bestimmung der resorptionsverfügbaren PCDD/PCDF aus Kieselrot. *Umweltwissenschaften und Schadstoff-Forschung - Z Umweltchem Okotox* 7:3-9.

[190] Minekus M, Marteau P, Havenaar R, Huis in't Veld JHJ. 1995. A multicompartmental dynamic computer-controlled model simulating the stomach and small intestine. *Altern Lab Anim* 23:197-209.

[191] Wilcockson JB, Gobas FA. 2001. Thin-film solid-phase extraction to measure fugacities of organic chemicals with low volatility in biological samples. *Environ Sci Technol* 35:1425-1431.

[192] Gobas F, Zhang X, Wells R. 1993. Gastrointestinal magnification: The mechanism of biomagnification and food-chain accumulation of organic chemicals. *Environ Sci Technol* 27:2855-2863.

[193] Gobas F, Wilcockson J, Russell R, Haffner G. 1999. Mechanism of biomagnification in fish under laboratory and field conditions. *Environ Sci Technol* 33:133-141.

[194] Hamel SC, Buckley B, Lioy PJ. 1998. Bioaccessibility of metals in soils for different liquid to solid ratios in synthetic gastric fluid. *Environ Sci Technol* 32:358-362.

[195] Ruby MV, Davis AO, Link TE, Chaney RL, Freeman GB, Bergstrom PD. 1993. Development of an in-vitro screening test to evaluate the in-vivo bioaccessibility of ingested mine-waste lead. *Environ Sci Technol* 27:2870-2877.

[196] Bligh E, Dyer W. 1959. A rapid method of lipid extraction and purification. *Can J Biochem Physiol* 35:911-917.

[197] Reeves WR, McDonald TJ, Bordelon NR, George SE, Donnelly KC. 2001. Impacts of aging on in vivo and in vitro measurements of soil-bound polycyclic aromatic hydrocarbon availability. *Environ Sci Technol* 35:1637-1643.

[198] Xing B, Pignatello JJ. 1997. Dual-model sorption of low-polarity compounds in glassy poly(vinyl chloride) and soil organic matter. *Environ Sci Technol* 31:792-799.

[199] Weston DP, Mayer LM. 1998. Comparison of in vitro digestive fluid extraction and traditional in vivo approaches as measures of polycyclic aromatic hydrocarbon bioavailability from sediments. *Environ Toxicol Chem* 17:830-840.

[200] Weston DP, Mayer LM. 1998. In vitro digestive fluid extraction as measure of the bioavailability of sediment-associated polycyclic aromatic hydrocarbons: source

of variation and implications for partitioning models. *Environ Toxicol Chem* 17:820-829.

[201] Yang Y, Ratte D, Smets BF, Pignatello JJ, Grasso D. 2001. Mobilization of soil organic matter by complexing agents and implications for polycyclic aromatic hydrocarbon desorption. *Chemosphere* 43:1013-1021.

[202] Garbarini DR, Lion LW. 1986. Influence of the nature of soil organics on the sorption of toluene and trechloroethylene. *Environ Sci Technol* 20:1263-1269.

[203] Weber LP, Lanno RP. 2001. Effect of bile salts, lipid, and humic acids on absorption of benzo[a]pyrene by isolated channel catfish (Ictalurus punctatus) intestine segments. *Environ Toxicol Chem* 20:1117-1124.

[204] Engebretson R, Von Wandruszka R. 1994. Microorganization in dissolved humic acids. *Environ Sci Technol* 28:1934-1941.

[205] Chung N, Alexander M. 2002. Effect of soil properties on bioavailability and extractability of phenanthrene and atrazine sequestered in soil. *Chemosphere* 48:109-115.

[206] Abrahams P. 2002. Soils: their implications to human health. *Sci Total Environ* 291:1-32.

[207] Buesen R, Mock M, Nau H, Seidel A, Jacob J, Lampen A. Human intestinal Caco-2 cells display active transport of benzo[a]pyrene metabolites. Chem Biol Interact, 2003. pp. 201-221.

[208] Minhas JK, Vasiluk L, Pinto LJ, Gobas FAPC, Moore MM. 2005. Mobilization of chrysene from soil in a model digestive system. *Environ Toxicol Chem* in press.

[209] Rodriguez RR, Basta NT, Casteel SW, Pace LW. 1999. An in vitro gastrointestinal method to estimate bioavailable arsenic in contained soils and solid media. *Environmental Science & Technology* 33:642-649.

[210] Launen L, Pinto L, Wiebe C, Kiehlmann E, Moore M. 1995. The oxidation of pyrene and benzo[a]pyrene by nonbasidiomycete soil fungi. *Can J Microbiol* 41:477-488.

[211] Nelson D, Sommers L. 1996.Total carbon, organic carbon, and organic matter. In: Bartels J, editor. *Methods of soil analysis*. Second, vol.3rd. American Society of Agronomy : Soil Science Society of America, Madison, Wisconsin. pp. 961-1010.

[212] Ben-Dor E, Banin A. 1989. Determination of organic matter content in arid-zone soils using a simple loss-on-ignition methos. *Communications in Soil Science and Plant Analysis* 20:1675-1696.

[213] Vasiluk L, Pinto LJ, Moore MM. 2005. Oral bioavailability of glyphosate: studies using two intestinal cell lines. *Environ Toxicol Chem* 24:153-160.

[214] Alexander M. 2000. Aging, bioavailability, and overestimation of risk from environmental pollutants. *Environ Sci Technol* 34:4259-4265.

[215] Sun H, Tateda M, Ike M, Fujita M. 2003. Short- and long-term sorption/desorption of polycyclic aromatic hydrocarbons onto arti.cial solids: effects of particle and pore sizes and organic matters. *Water Res* 37:2960–2968.

[216] Lee K. 2002. TSRI#93 - Environmental effects and remediation of contamiants in Sydney Harbour, Nova Scotia. Technical Report. Maurice Lamontagne Institute, Mont-Joli, Quebec.

[217] Peress J. 2003. Estimate Evaporative Lossess from Spills. *Chem Engin Progress* 99.

[218] Northcott GL, Jones KC. 2000. Spiking hydrophobic organic compounds into soil and sediment: A review and critique of adopted procedures. *Environ Toxicol Chem* 19:2418-2430.

[219] Sun H, Li JG. 2005. Availability of pyrene in unaged and aged soils to earthworm uptake, butanol extraction and SFE. *Water Air Soil Poll* 166:353-365.

[220] Malagelada JR, Robertson JS, Brown ML, Remington M, Duenes JA, Thomforde GM, Carryer PW. 1984. Intestinal transit of solid and liquid components of a meal in health. *Gastroenterology* 87:1255-1263.

[221] Kaus LC, Gillespie WR, Hussain AS, Amidon GL. 1999. The effect of in vivo dissolution, gastric emptying rate, and intestinal transit time on the peak concentration and area-under-the-curve of drugs with different gastrointestinal permeabilities. *Pharm Res* 16:272-280.

[222] Lijinsky W, Shubik P. 1964. Benzo(a)Pyrene and Other Polynuclear Hydrocarbons in Charcoal-Broiled Meat. *Science* 145:53-55.

[223] Hattemer-Frey HA, Travis CC. 1991. Benzo-a-pyrene: environmental partitioning and human exposure. *Toxicol Ind Health* 7:141-157.

[224] Gaylor DW, Culp SJ, Goldstein LS, Beland FA. 2000. Cancer risk estimation for mixtures of coal tars and benzo(a)pyrene. *Risk Anal* 20:81-85.

[225] Bauer E, Guo Z, Ueng YF, Bell LC, Zeldin D, Guengerich FP. 1995. Oxidation of benzo[a]pyrene by recombinant human cytochrome P450 enzymes. *Chem Res Toxicol* 8:136-142.

[226] Vakharia DD, Liu N, Pause R, Fasco M, Bessette E, Zhang QY, Kaminsky LS. 2001. Polycyclic aromatic hydrocarbon/metal mixtures: effect on PAH induction of CYP1A1 in human HEPG2 cells. *Drug Metab Dispos* 29:999-1006.

[227] Shimada T, Sugie A, Shindo M, Nakajima T, Azuma E, Hashimoto M, Inoue K. 2003. Tissue-specific induction of cytochromes P450 1A1 and 1B1 by polycyclic aromatic hydrocarbons and polychlorinated biphenyls in engineered C57BL/6J mice of arylhydrocarbon receptor gene. *Toxicol Appl Pharmacol* 187:1-10.

[228] Savas U, Bhattacharyya KK, Christou M, Alexander DL, Jefcoate CR. 1994. Mouse cytochrome P-450EF, representative of a new 1B subfamily of cytochrome P-450s. Cloning, sequence determination, and tissue expression. *J Biol Chem* 269:14905-14911.

[229] Culp SJ, Gaylor DW, Sheldon WG, Goldstein LS, Beland FA. 1998. A comparison of the tumors induced by coal tar and benzo[a]pyrene in a 2-year bioassay. *Carcinogenesis* 19:117-124.

[230] Weyand EH, Chen YC, Wu Y, Koganti A, Dunsford HA, Rodriguez LV. 1995. Differences in the tumorigenic activity of a pure hydrocarbon and a complex mixture following ingestion - benzo[a]pyrene vs manufactured-gas plant residue. *Chem Res Toxicol* 8:949-954.

[231] Ruby MV, Schoof R, Brattin W, Goldade M, Post G, Harnois M, Carpenter M, Edwards D, Cragin D, Chappell W. 1999. Advances in evaluating the oral bioavailability of inorganics in soil for use in human health risk assessment. *Environ Sci Technol* 33:3697-3705.

[232] Isozaki T, Tamura H. 2001. Epigallocatechin gallate (EGCG) inhibits the sulfation of 1-naphthol in a human colon carcinoma cell line, Caco-2. *Biol Pharm Bull* 24:1076-1078.

[233] Jodoin J, Demeule M, Beliveau R. 2002. Inhibition of the multidrug resistance P-glycoprotein activity by green tea polyphenols. *Biochim Biophys Acta* 1542:149-159.

[234] Lampen A, Ebert B, Stumkat L, Jacob J, Seidel A. 2004. Induction of gene expression of xenobiotic metabolism enzymes and ABC-transport proteins by PAH and a reconstituted PAH mixture in human Caco-2 cells. *Biochim Biophys Acta* 1681:38-46.

[235] Ebert B, Seidel A, Lampen A. 2005. Induction of phase-1 metabolizing enzymes by oltipraz, flavone and indole-3-carbinol enhance the formation and transport of benzo[a]pyrene sulfate conjugates in intestinal Caco-2 cells. *Toxicol Lett* 158:140-151.

[236] Galijatovic A, Otake Y, Walle UK, Walle T. 2001. Induction of UDP-glucuronosyltransferase UGT1A1 by the flavonoid chrysin in Caco-2 cells--potential role in carcinogen bioinactivation. *Pharm Res* 18:374-379.

[237] Traber MG, Kayden HJ, Rindler MJ. 1987. Polarized secretion of newly synthesized lipoproteins by the Caco-2 human intestinal cell line. *J Lipid Res* 28:1350-1363.

[238] Trotter PJ, Ho SY, Storch J. 1996. Fatty acid uptake by Caco-2 human intestinal cells. *J Lipid Res* 37:336-346.

[239] Hidalgo IJ, Raub TJ, Borchardt RT. Characterization of the human colon carcinoma cell line (Caco-2) as a model system for intestinal epithelial permeability. Gastroenterology, 1989. pp. 736-749.

[240] Miggiano GA, Gagliardi L. 2005. [Diet, nutrition and bone health]. *Clin Ter* 156:47-56.

[241] Stremmel W, Lotz G, Strohmeyer G, Berk PD. 1985. Identification, isolation, and partial characterization of a fatty acid binding protein from rat jejunal microvillous membranes. *J Clin Invest* 75:1068-1076.

[242] Trotter PJ, Storch J. 1991. Fatty acid uptake and metabolism in a human intestinal cell line (Caco-2): comparison of apical and basolateral incubation. *J Lipid Res* 32:293-304.

[243] Mackay D, Fraser A. 2000. Kenneth Mellanby Review Award. Bioaccumulation of persistent organic chemicals: mechanisms and models. *Environ Pollut* 110:375-391.

[244] Seibert H, Morchel S, Gulden M. 2002. Factors influencing nominal effective concentrations of chemical compounds in vitro: medium protein concentration. *Toxicol In Vitro* 16:289-297.

[245] Gobas FAPC, Zhang X, Wells R. 1993. Gastro-intestinal magnification: The mechanism of biomagnification and food-chain accumulation of organic chemicals. *Environ Sci Technol* 27:2855-2863.

[246] Van de Wiele T, Verstraete W, Siciliano S. 2002. PAH exposure risk assessment: combining digestion models and bioassays. *Med Fac Landbouww Univ Gent* 67:153-156.

[247] Kogel-Knabner I, Totsche KU, Raber BJ. 2000. Desorption of polycyclic aromatic hydrocarbons from soil in the presence of dissolved organic matter: Effect of solution composition and aging. *J Environ Qual* 29:906-916.

[248] Carmichael LM, Christman RF, Pfaender FK. 1997. Desorption and mineralization kinetics of phenanthrene and chrysene in contaminanted soils. *Environ Sci Technol* 31:126-132.

[249] Varanasi U, Reichert WL, Stein JE, Brown DW, Sanborn HR. 1985. Bioavailability and biotransformation of aromatic hydrocarbons in benthic organisms exposed to sediment from an u7rban estuary. *Environ Sci Technol* 19:836-841.

[250] Chiou CT, McGroddy SE, Kile DE. 1998. Partition characteristics of polycyclic aromatic hydrocarbons on soil and sediment. *Environ Sci Technol* 32:264-269.

[251] Neely BW, Branson DR, Blau GE. 1974. Partitioning coefficient to measure bioconcentration potential of organic chemicals in fish. *Environ Sci Technol* 8:1113-1115.

[252] Mayer LM, Chen Z, Findlay RH, Fang J, Sampson S, Self RFL, Jumars PA, Quetel C, Donard OFX. 1996. Bioavailability of sedimentary contaminants subjects to deposit-feeder digestion. *Environ Sci Technol* 30:2641-2645.

[253] Wu SJ, Robinson JR. 1999. Transcellular and lipophilic complex-enhanced intestinal absorption of human growth hormone. *Pharm Res* 16:1266-1272.